Influence of hydrological model structures on extreme high flow simulations in the Meuse basin

Niels van den Brink
April, 2018

Deltares
Enabling Delta Life

UNIVERSITY OF TWENTE.

Picture: www.ardennes.com

Influence of hydrological model structures on extreme high flow simulations in the Meuse basin

Master thesis Water Engineering & Management
University of Twente
Faculty of Engineering Technology
Civil Engineering & Management

Author: Cornelis Johannes Ruben (Niels) van den Brink

Status: Final
Date: 19-4-2018
Place: Hilversum
University: University of Twente
External Location: Deltares, hydrology department

Graduation committee:

University of Twente, Department of Water Engineering and Management
Prof. Dr.J.C.J. Kwadijk
Dr. ir. M.J. Booij

Deltares, Hydrology department:
ir. L. Bouaziz
ir. M. Hegnauer

Summary

Already multiple studies have been performed with the use of synthetic weather data. These studies aim to determine extreme high discharge waves that have not yet been observed. The synthetic weather series are generated over a long period, within these long periods extreme conditions will occur. These synthetic weather series are used as input by hydrological models to simulate long discharge series, during extreme precipitation events the hydrological should simulate extreme high discharge waves. These studies have in common that only a single hydrological model is used for simulating the long discharge series. Therefore, it is unclear how another hydrological model might simulate these discharge waves associated with large return periods. Blazkova & Beven, (2002) already mentions that simulations performed by other models can show completely different results. This thesis is an explorative study, which will analyse the influence of different hydrological model structures on discharges that are simulated with the use of synthetic data series. The synthetic data that will be used for this study is developed by the KNMI and creates daily weather in the Meuse basin for a period of 50000 years. The analysis of the discharge simulations is delimited to daily annual maximum discharge values, which helps with filter the amount of data that is generated. Combining the notions stated above the following research objective can be formulated: *Too study the effect of different hydrological model structures on their capability to reproduce statistical characteristics of extreme high flow events of the Meuse river basin using synthetic weather series.*

In this thesis discharges are simulated for the Meuse basin at Monsin which is located in Liege. The discharges are simulated with the use of 14 sub-basins, which are connected to each other via a routing system. Annual maximum discharge simulations of different hydrological models for individual sub-basins and the whole Meuse basin are compared to each other. However, in order to analyse the influence of the model structure it is important to limit the influence of other factors on the discharge simulations. Therefore, an experiment is designed in which the difference in simulations is only caused by the difference in the model structure. First of all the used hydrological model have similar characteristics. This means that the used hydrological models, which are the GR4J, HyMOD, and HBV model, can use the same data but also have a similar conceptualised model structures. This makes it easier to identify how model structure differences influence the discharge simulations.

Secondly, the preparation of the hydrological models in the calibration process is done the same for every hydrological model. The value of an aggregated objective function that combines multiple aspects of the hydr is optimized using an optimization algorithm. The use of an optimization algorithm reduces the influence of the modeller during the calibration process. As a result the best parameter values are found using a more objective method. The calibration is performed for nine upstream sub-basins (Lorraine Sud, Chiers, Semois, Viroin, Lesse, Ourthe, Ambleve, Vesdre, Mehaigne), four sub-basins that are located downstream (Lorraine Nord, Stenay-Chooz, Chooz-Namur, Namur-Monsin), and one sub-basins is calibrated combined with an upstream basin due to lack of observed discharge data (Sambre). The calibration of downstream sub-basins required input from at least one of the upstream sub-basins.

Finally, the routing of the discharge is simulated in the same way for every hydrological model. Upstream sub-basin discharges are added to downstream sub-basin discharges in order to simulate the total discharge of the Meuse. The routing is simulated by applying a lag on the upstream sub-basin discharge. This lag is kept constant and the same for every hydrological model. This ensures that the routing does not influence simulation differences of the hydrological models. The value for the lag is based on previous studies of the Meuse basin.

The hydrological models are first used for a simulation of two 15 year historical periods (for most sub-basins, for some sub-basins discharge data within these periods is missing). The first 15 year period (1-1-1968/1-1-1983) is used for the calibration of the model. Whereas the second 15 year is used for the validation of the hydrological models (1983/1998). The results are presented in the form of objective function values for each sub-basin. The GR4J and HBV show the best performance in simulating the historical discharge series. Also these two hydrological models show similar performances for the calibration and validation periods. This indicates that the these two hydrological have robust performances with the optimized parameter values. The HyMOD model performs worse compared to the GR4J and HBV model for upstream sub-basins. The performance improves for the downstream discharge simulations.

The results for the simulations using synthetic data are determined with the use of statistical analysis. For the statistical analysis a couple of upstream and downstream are selected from the 14 sub-basins (Chiers, Semous, Lesse, Ourthe, Mehaigne, Stenay-Chooz, Namur-Monsin). First of all the equality of population annual maximum means/variances of the used hydrological models was assessed between: historical data simulations/observations, synthetic data simulations/historical data simulations, and synthetic data simulations/observations. The population means/variances were unequal for synthetic data simulations/observations for the HyMOD model in most upstream basins. Which are in line with the performance results. After this analysis Gumbel plots are presented that show the annual maximum discharges of the observations and synthetic data simulations. In these Gumbel plots the GR4J and HBV synthetic data simulations in upstream sub-basins are almost equal for more common annual maximum discharge values. However, in most upstream sub-basins the GR4J model starts to show higher annual maximum discharge values compared to the HBV model for rare events (associated return periods larger than 10 years). The GR4J and HBV, synthetic data simulations of the annual maximum discharge at Monsin are similar, even for the largest return periods

Due to the similarity of the simulations it cannot be determined whether the HBV model or the GR4J model shows a better performance in simulating discharges of the Meuse. Furthermore these similarities continue for synthetic data simulations. However, on a sub-basin level different hydrological model structure have a large influence on synthetic data simulations when looking at discharges associated with large return periods. This means that similar performance does not automatically result in similar synthetic data simulations of the larger more uncommon discharge values. The combination of discharges from multiple sub-basins can lead to an reduction of the effect that was seen for separate sub-basins. This results in similar synthetic data annual maximum discharge simulations of the GR4J and HBV model at Monsin for all return periods. Although the paths might be different the result is encouraging, indicating that these synthetic data simulations are in the right direction.

Preface

This thesis is the result of months of research and is the final step that is required to receive my Civil Engineering and Management degree at the University of Twente. While writing this thesis I learned a lot about hydrology, programming and myself. These acquired skills are without a doubt useful for the phase that inevitably comes after studying. I am proud of the end result and hope that this research provides possible new directions for research regarding the GRADE instrument.

I want to thank Martijn Booij not only for the help he provided during the master thesis but also for helping me find a master subject that suited my interests. While writing the thesis he provided excellent support and gave great advice. I want to thank Jaap Kwadijk for providing an opportunity to write my thesis at Deltares. Besides, this he made sure that I didn't lose myself into less relevant details and keep the bigger picture mind. For all the GRADE related questions I could turn to Mark Hegnauer. I want to thank him for answering all these questions and for suggesting which directions I could take during the research process. Finally I want to thank Laurene Bouaziz. I could always turn to her when I was stuck or needed someone to share my ideas with. She helped me to create a better understanding of different hydrological models and the hydrological processes in the Meuse basin. However, most of all I want to thank all my supervisors for being able to put up with me.

Niels van den Brink

Hilversum, 19 April 2018

Content

Summary 3

Preface 5

1. Introduction 10

1.1 Synthetic weather generator coupled with hydrological models 10

1.2 Case study: Meuse 11

1.3 Research objective 13

1.4 Research questions 13

1.5 Report outline 14

2. Sub-basins and datasets of the Meuse basin 15

2.1 The GRADE instrument 15

2.1.1 Synthetic data generation for the Meuse 16

2.1.2 Sub-basins of the Meuse 17

2.2 Historical data sets for the Meuse 18

2.2.1 Historical weather data series 18

2.2.2 Discharge data series 20

3. Method 21

3.1 Hydrological model preparation 21

3.2 Hydrological models 21

3.2.1 Hydrological models categorization 21

3.2.2 Hydrological model structures 22

3.2.3 Discharge simulations of the Meuse at Monsin 31

3.3 Hydrological model calibration 32

3.3.1 Objective functions 33

3.3.2 Optimization Algorithm 34

3.3.3 Termination criteria/Calibration data 36

3.4 Hydrological model Validation 36

3.5 Statistical analysis 37

3.5.1 Sub-basins selection for statistical analysis 37

3.5.2 Comparing the mean 37

3.5.3 Comparing the variance 37

3.5.4 Gumbel plot 38

3.5.5 Comparing Synthetic data simulations with observations 38
3.6 Model structure effect on high flow discharges 39
3.6.1 Hydrograph analysis 39
3.6.2 Floodwave contribution 39
4. Results 40
4.1 Hydrological model discharge simulation performance (Historical) 40
4.2 Synthetic data analysis 44
4.2.1 Equality of mean test 45
4.2.2 Equality of variance test 46
4.2.3 Gumbel plots 47
4.2.4 Scatter plots 49
4.3 Model structure analysis (historical) 51
4.3.1 Linear storages 51
4.3.2 Unit hydrographs 52
4.3.3 Snow module 52
4.3.4 Upstream basin contribution 53
5. Discussion 55
6. Conclusion and Recommendations 57
6.1 Performance of the hydrological models 57
6.2 Annual maximum discharge simulations using synthetic data 57
6.3 Final conclusion 58
6.4 Recommendations 58
References 59
Appendix A. The GRADE instrument 62
A.1 Stochastic weather generator 62
A.1.1 Generating Potential evapotranspiration 62
A.2.1 Resampling process 63
A.2 GRADE instrument discharge simulations at Borgharen 66
A.1.2 HBV and SOBEK model implementations 66
A.3 GRADE instrument results 67
A.1.3 HBV model performance 67
A.2.3 Final GRADE result 67

Appendix B. 69
B.1 Weather data 69
Long daily weather series 70
B.2 Discharge 71
B.3 Calibration data 72
B.4 Validation data 72
Appendix C. Floodwave hydrographs 73
C.1 Summer Flood wave of 1980 73
C.2 Floodwave of 1984 75
C.3 Floodwave with large snowmelt contribution of 1988 77
C.4 Floodwave of 1993 79
C.5 Floodwave of 1995 81
Appendix D. Leaking catchments 83
Appendix E. Parameter values 84

1. Introduction

1.1 Synthetic weather generator coupled with hydrological models

Floods are causing large amounts of material damage and casualties worldwide. Each year a large and damaging flood occurs. In 2011 and 2012 severe floods occurred in , Madagascar, Mozambique, Namibia, Niger, Nigeria, South Africa and Uganda in Africa; Argentina, Brazil, Columbia, Haiti, Mexico and the United States in the Americas; and Bangladesh, Cambodia, China, India, North Korea, Pakistan, the Philippines, Russia, Thailand and South Korea in Asia. Each of these flood event caused at least 50 casualties, in the Philippines and Colombia the number of casualties even exceeded the 1000 (Kundzewicz et al., 2014). These floods caused high structural damages especially in the developing countries. Furthermore there are indications that in the recent decades that population and assets exposed to floods have increased more rapidly compared to the overall population and economic growth (Kundzewicz et al., 2014). Preventing floods will remain a relevant research subject due to the extensive damage that is caused by flooding, and also the recent increase in flood risk exposure.

Flood defence systems are often designed by stating that it should be able to handle an extreme discharge event with a certain return period (Apel et al., 2004). In order to determine the discharges and the associated return periods a flood frequency analysis can be performed. Traditional methods for performing the flood frequency analysis include the estimation of a series of flood peak magnitudes that are fitted to a suitable probability distribution function, or use the definition of an extreme design storm as input for a rainfall-runoff model (Blazkova & Beven, 2004). When using the probability distribution function for the flood frequency analysis discharge observations are required, which are not always available and have a limited time length (Kundzewicz et al., 2014). The reproduction of events that have a return period that is less or equal than the observation period is generally good. However, there is a difference between the values that are found for discharges with a return period that goes beyond the time length of the observed discharges (Arnaud & Lavabre, 2002). The reason for this is that the discharges that are a result of extrapolation depend on the probability distribution that is fitted to the cumulative frequency distribution of the observed discharges. The main drawback of the second method is that it is difficult to estimate the probability of an extreme design storm and the effect runoff coefficient. Also, the conditions before the extreme design storm are usually not taken into account (Blazkova & Beven, 2004).

Weather generators can be used to bypass the limited length of discharge observations and the difficulty of estimating the probability of an extreme storm event. Several studies indicate using a weather generator to create input for a hydrological model in order to estimate low probability flood frequencies (Arnaud & Lavabre, 2002; Blazkova & Beven, 2002; Blazkova & Beven, 2004; Falter et al., 2015; Hegnauer et al, 2014; Kuchment & Gelfan, 2011). Within these studies the approaches of determining low probability flood frequencies are different. However, all of the studies acknowledge the use of this method as an improved way of dealing with design problems such as dam/bridge/levee construction, flood risk assessment and water management issues.

The studies that use synthetic data as hydrological model input have another important aspect in common. All these studies only use a single hydrological model for the simulations (Arnaud & Lavabre, 2002; Blazkova & Beven, 2002; Blazkova & Beven, 2004; Falter et al., 2015; Hegnauer et al, 2014; Kuchment & Gelfan, 2011). However, it is important to note that the outcome of these studies is dependent on which models are used (Blazkova & Beven, 2002). Since, only a single hydrological model is used for the analysis in the studies mentioned above it is unclear how different hydrological models might have an effect on the results. This study aims to explore the influence of hydrological models on discharge simulations that use synthetic data.

1.2 Case study: Meuse

One of the synthetic data sources mentioned above is the stochastic weather generator developed by The Royal Netherlands Meteorological Institute (KNMI). This generator creates long synthetic weather series for the Rhine and Meuse basin, the two largest rivers that flow into the Netherlands (Hegnauer et al., 2014). With the use of the synthetic data long discharge series are determined and are used for flood defense purposes. For this study the synthetic data generated for the Meuse basin will be used in a case study. Synthetic weather data is not generated for the Dutch part of the Meuse. Therefore, the focus will be on the Belgium and French part of the Meuse.

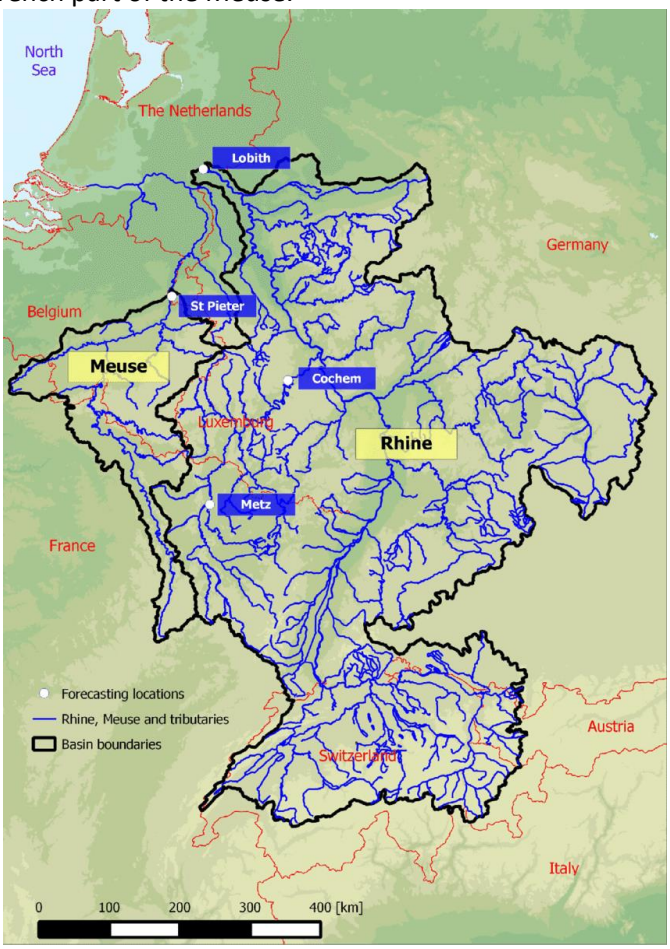

figure 1-1, Meuse and Rhine basins, (Verkade et al., 2017)

The Meuse is smaller compared to the Rhine basin as is depicted in figure 1-1. The source of the Meuse is located in northern France and flows through the south eastern part of Belgium before it enters the Netherlands near St Pieter. The Meuse can be categorized as a rain fed river which means that the discharge highly fluctuates between seasons. The Meuse basin is complex due to the amount of human interventions, heterogeneity of the basin, and the fast reaction of the basin to precipitation (Berger & Mugie, 1994). The Meuse basin can be divided into three main sections. The most upstream area from the source to the mouth of the Chiers can be described as a calm section due to the slim, stretched form and the low gradient of the basin. The middle section of the Meuse is from the mouth of the Chiers until the Dutch border. The Ardennes, located in this middle section, have a high elevation compared to the rest of the Meuse basin (figure 1-2). As a result the Ardennes receive the most amount of precipitation over the year. In combination with the impervious rocky soil, the Ardennes have a large contribution to high discharge waves and low contribution to low flow discharges. The width of the river in this section is small since it cuts through rocky soil (Berger & Mugie, 1994). A more detailed map of the Meuse basin is presented in figure 1-2, important tributaries for the upstream and middle sections of the Meuse are depicted in this figure as well (Chiers, Semois, Viroin, Lesse, Sambre, Ourthe, Ambleve, Vesdre).

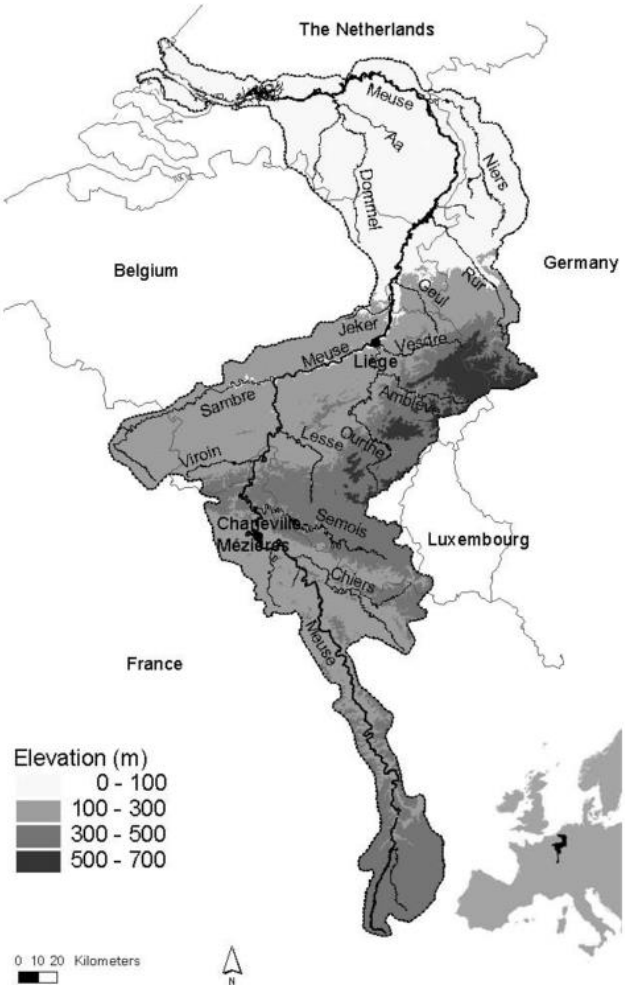

figure 1-2, Meuse basin elevation map, (de Wit et al., 2007)

1.3 Research objective

While using one model can provide good simulations when compared to the observations, it is not clear if the hydrological model is simulating the hydrological behaviour of a catchment correctly. For instance the hydrological model can overestimate the actual evapotranspiration resulting in correct discharge simulations. Though in reality, the amount of discharge is reduced via another process. Hydrological model (inter-)comparison studies can be used to determine which hydrological model structures best represent the hydrological behaviour of a catchment (de Boer-Euser et al., 2016). Aside from knowledge about the hydrological basins, the results of simulations depends on which hydrological model is chosen for the simulations (Blazkova & Beven, 2002). In order to evaluate the influence of model structures on the synthetic data simulations some form of model inter-comparison is required.

The multiple studies using synthetic data series are mainly used for the estimation of discharge waves that have low occurrence rate. In most cases these values are beyond any values that have been observed. Therefore, this study was also focus on the simulation of high flow discharges. In order to analyse the higher discharge values generated with synthetic data and the absence of observation data, statistical methods are applied. With the use of annual maximum discharge values, extreme value statistics such as Gumbel plots can be used for the analysis. Combining the goal of determining the influence of model structures on synthetic data simulations for the Meuse basin and the notions stated above the following research objective can be formulated:

To study the effect of different hydrological model structures on their capability to reproduce statistical characteristics of annual maximum discharges of the Meuse river basin using synthetic weather series.

1.4 Research questions

The research objective is split into two different research questions. Research question one will focus on the preparation of the hydrological models before the synthetic data simulations and will use historical data. Research question two is similar to the research objective and will focus on comparing the synthetic data simulations. Reason for splitting the research objective is that the preparation of the hydrological models is a large part of this study. The results and conclusions will be described with the use of these research questions. Further details on the method is described in chapter three.

1. Which hydrological model shows the best performance in simulating discharges of the Meuse river basin?

Before hydrological model simulations using a weather generator can be performed it is required to prepare the hydrological models for simulations of the Meuse basin. This is done using historical discharge and weather data. During the preparation it becomes clear which hydrological model has the best capability of mimicking certain aspects of the observed discharge. This can be translated as hydrological model performance. It is important to answer this questions since a good model performance strengthens the notion that the hydrological model is correctly simulating the hydrological behaviour of a catchment. When a hydrological model correctly simulates the hydrological behaviour the chances of correctly simulating annual maximum discharge with a small chance of occurrence (synthetic data) increases. In order to answer this question multiple aspects of the observed discharge series will be used.

2. What is the effect of different hydrological model structures on the annual maximum discharge simulations that use data of a synthetic weather generator as input.

After the preparation of the different hydrological models the synthetic data can be used to simulate daily discharges for 50000 years. During this simulation extreme discharge events occur (low and high flows), however most of the time the discharges are similar to the historically observed discharges. As stated before this study will focus on the annual maximum discharges, since this is also the main application of the synthetic data studies. Since annual maximum discharges are used, yearly return periods for these peaks can be determined. These annual maximum discharge values of the different sources will be compared to each other using statistical methods. This will determine whether the synthetic data simulations are similar to the observed annual maximum discharges.

1.5 Report outline

This report will be structured in the following way.

Chapter 2 GRADE instrument and data description
In this section a description of the GRADE instrument is given. This description will mostly focus on how the weather generator creates long weather series and how the HBV model is designed in order to simulate discharges for the entire Meuse. Additionally the used data sets that are used for the GRADE instrument are described. This includes the preparations that were necessary before the data could be used and which data sets are used directly for this thesis.

Chapter 3 Methods
This chapter will include a description of all different processes that were necessary to acquire the results for this thesis. This will include the hydrological model selection, hydrological model structure, calibration process, validation process, analysis of the hydrological model performance and statistical tests for comparing the annual maximum discharges.

Chapter 4 Results
In chapter 4 the results are described. This will be done in the same order as the research questions mentioned above. The calibration and validation results are included in the first research question since these results will be the first step in assessing the performance of the hydrological models. The results will be mostly presented in figures and tables with a description explaining the content of the figures/tables.

Chapter 5 Discussion
The first section of the discussion will focus on possible explanations for the results that were found. Stating the potential, limitations, generalizations and implications of this study

Chapter 6 Conclusion + Recommendation
The final chapter will state the answer for each research question separately. Based on these answers a final conclusion will be presented. After this recommendations will be made for policy making and further research.

2. Sub-basins and datasets of the Meuse basin

2.1 The GRADE instrument

The Generator of Rainfall and Discharge Extremes (GRADE) is developed by Deltares and the Royal Netherlands Meteorological Institute (KNMI). This instrument is created in order to simulate long discharge series. This series present a discharge value for each day over a period of 50000 years. The GRADE instrument consists of three different components: the weather generator, the HBV hydrological model and the hydrodynamic SOBEK model. Mainly the synthetic data created by the weather generator is used for this thesis. However, the historical data sets and a similar hydrological model are used for this study as well. The weather generator creates continuous daily weather series, which are used as input for the hydrological model. The discharges are routed using the hydrodynamic SOBEK model. The result of these simulations is a 50000 year daily discharge series. These series contain randomly generated extreme events that can occur over such a long time-period. An overview of the GRADE instrument is presented in Figure 2-1.

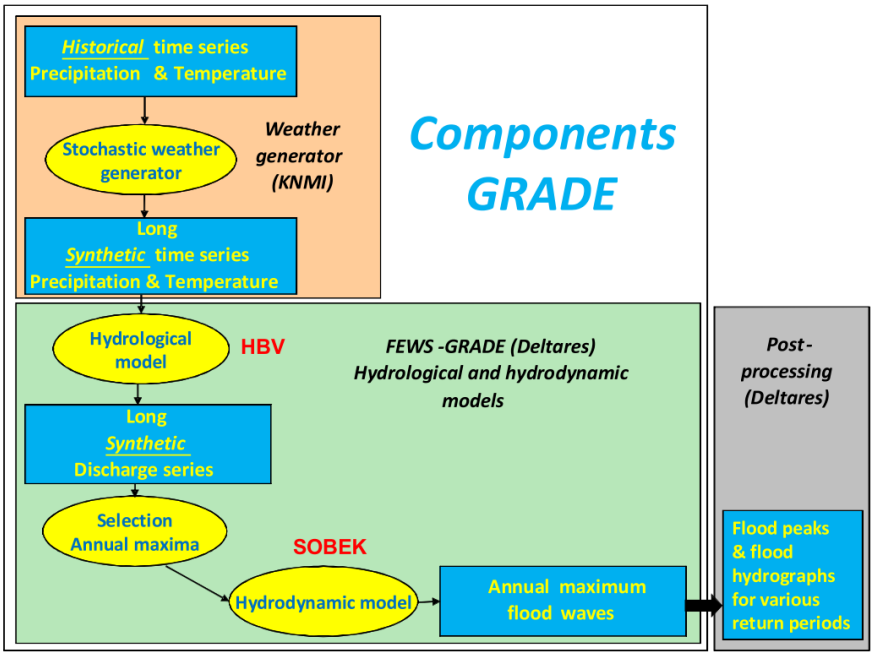

Figure 2-1 Systematic view of the GRADE components (Hegnauer et al., 2014)

2.1.1 Synthetic data generation for the Meuse

The stochastic weather generator creates synthetic data based on historically observed daily weather. For multiple Meuse sub-basins areally averaged records are available. These records are used to create new series of daily weather for each sub-basin. By resampling the records these new weather series are created and repeated for a period of 50000 years. Some restrictions are implemented in the resampling such that seasonal weather is taken into account. In other words weather on a day in December cannot be followed by weather from a day in June. During these long time-series extreme events occur. This happens when multiple days with heavy precipitation are resampled, resulting in a larger multiple day precipitation value. An example of this is depicted in figure 2-2, where a larger maximum four day amount is the result of resampling daily precipitation. Thus, by using this technique only multiple day extremes are created within the synthetic weather series. A more detailed description of the resampling and the use of the historical data is described in Appendix A.A.1.

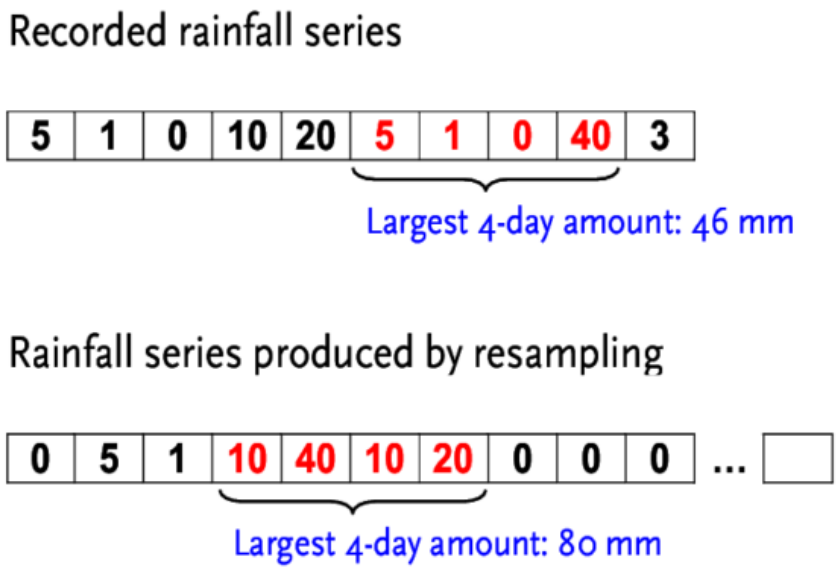

figure 2-2, Resampling of the historical recorded rainfall series results in a different "largest 4 day amount" (Hegnauer et al., 2014).

2.1.2 Sub-basins of the Meuse

As is mentioned before the Meuse basin is divided in multiple sub-basins. Lorraine Sud is the first sub-basin and represents the Meuse basin from the source to St Mihiel. The other upstream sub-basins represent tributaries of the Meuse (Chiers, Semois, Viroin, Lesse, Sambre, Ourthe, Ambleve, Vesdre, Mehaigne). The remaining downstream sub-basins represent different sections around the main river (Lorraine Nord, Stenay-Chooz, Chooz-Namur, Namur-Monsin). The different sub-basins are presented in figure 2-3. The Jeker is not used for this study since it confluences with the main river after Monsin. A detailed description of the schematization that is used for Meuse discharge simulations at Monsin are presented in the next chapter (3.2.4).

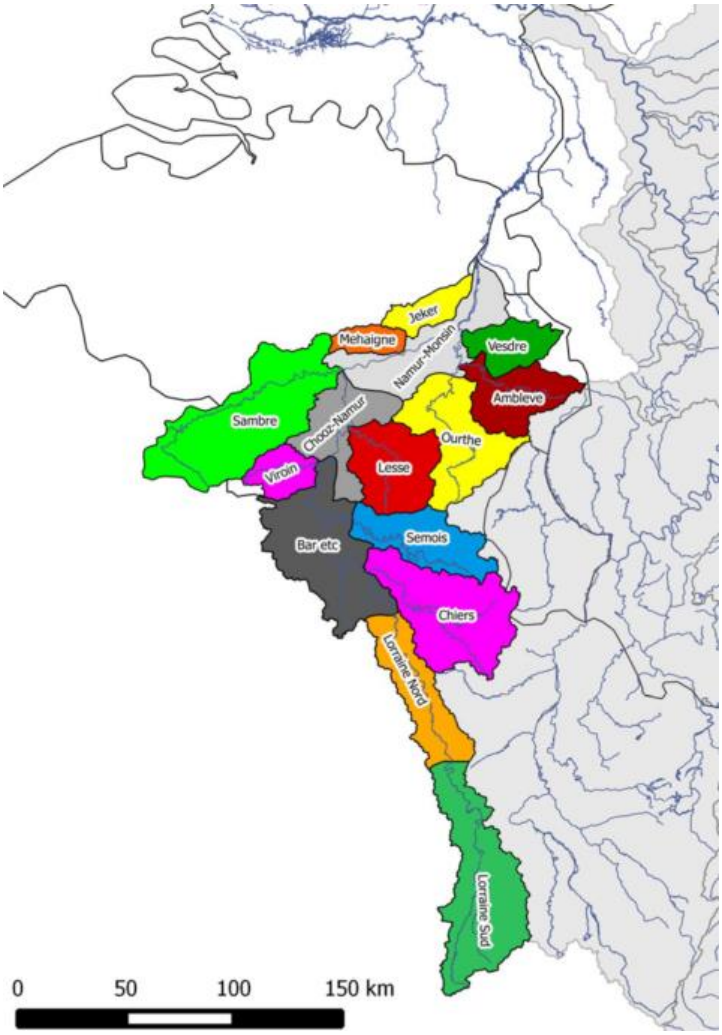

figure 2-3, Sub-basins of the Meuse (Hegnauer et al., 2014)

2.2 Historical data sets for the Meuse

2.2.1 Historical weather data series

For this thesis areally averaged historical daily weather data series are used for discharge simulations of the 14 sub-basins that were mentioned in the previous section. The weather data extended over a 31 year period, between 1-1-1967/31-12-1998. The weather consists of temperature, precipitation and actual precipitation data series. The method of areally averaging the weather data differentiated between the French and Belgium part of the Meuse. For the French part precipitation station data is available, whereas for the Belgian part area-averaged basin data (precipitation, potential evapotranspiration) is available for multiple sub-basins. The available data is divided in two time periods table 2-1. The first period is used for the calibration (preparation of the hydrological model) and the second period is used for the validation (assessing hydrological model robustness). The next chapter will go into detail about the used calibration method. A description of the source can be found in Appendix B.

table 2-1, Weather data for the calibration and validation period. The data includes daily precipitation, temperature and potential evapotranspiration series, The first year of both periods is used as run-up period for the hydrological models

Weather data sub-basin	Calibration	Validation
1. Lorraine Sud	01-01-1967 , 01-01-1983	01-01-1982 , 01-01-1998
2. Chiers	01-01-1967 , 01-01-1983	01-01-1982 , 01-01-1998
3. Lorraine Nord	01-01-1967 , 01-01-1983	01-01-1982 , 01-01-1998
4. Stenay-Chooz	01-01-1967 , 01-01-1983	01-01-1982 , 01-01-1998
5. Semois	01-01-1967 , 01-01-1983	01-01-1982 , 01-01-1998
6. Viroin	01-01-1967 , 01-01-1983	01-01-1982 , 01-01-1998
7. Chooz - Namur	01-01-1967 , 01-01-1983	01-01-1982 , 01-01-1998
8. Lesse	01-01-1967 , 01-01-1983	01-01-1982 , 01-01-1998
9. Sambre	01-01-1967 , 01-01-1983	01-01-1982 , 01-01-1998
10. Ourthe	01-01-1967 , 01-01-1983	01-01-1982 , 01-01-1998
11. Ambleve	01-01-1967 , 01-01-1983	01-01-1982 , 01-01-1998
12. Vesdre	01-01-1967 , 01-01-1983	01-01-1982 , 01-01-1998
13. Mehaigne	01-01-1967 , 01-01-1983	01-01-1982 , 01-01-1998
14. Namur - Monsin	01-01-1967 , 01-01-1983	01-01-1982 , 01-01-1998

Precipitation

For the French section of the Meuse basin precipitation has been derived from 55-63 precipitation stations. Some of the precipitation stations in the French part of the Meuse basin are added/terminated, therefore the number of precipitation stations varies between 55-63. The Royal Meteorological Institute of Belgium (RMIB) has provided precipitation data, which is already areally averaged, for 31 sub-basins (Leander & Buishand, 2011). These sub-basins are often smaller compared to the sub-basins that are used by the hydrological model.

From the total of 14 sub-basins, 3 sub-basins are located in France (Stenay-Chooz, Lorraine Nord and Lorraine Sud) 10 in Belgium (Ambleve, Chooz-Namur, Lesse, Mehaigne, Namur-Monsin, Ourthe, Semois, Vesdre, Virion) and 2 in France and Belgium (Sambre, Chiers)(figure 2-3). The daily rainfall for the sub-basins located in France and the France part of the Sambre are determined by using inverse squared distance interpolation on a 2.5 km x 2.5 km grid (Hegnauer et al., 2014). For the interpolation only the stations 50 km from the grid point of interest were used (Leander & Buishand, 2011) . For the Belgian sub-basins and the Belgian part of the Sambre the sub-basin precipitation is determined with the use of the areally averaged data that is available for the 31 (smaller) sub-basins.

Temperature

Temperature records from eleven different temperature measurement stations are used. The stations are located in France (3), Belgium (6), Germany (1), Netherlands (1) (Leander & Buishand, 2011). The temperature for the 15 sub-basins is also determined by using interpolation, the temperature for each sub-basin was estimated by interpolating the daily temperature data from eleven stations using inverse square distance interpolation (Leander & Buishand, 2011).

Potential evapotranspiration

Potential evapotranspiration observations are only available in the form of area averaged daily potential evapotranspiration of 31 Belgian Meuse sub-basins. Meaning that potential evapotranspiration was not available for the French section (Hegnauer et al., 2014). Potential evapotranspiration for each of the 15 sub-basins is entirely based on the 31 Belgian sub-basin data. According to the metadata of an historical weather dataset, the potential evapotranspiration for the first 4 sub-basins (Lorraine Sud, Chiers, Lorraine Nord, Stenay-Chooz), which happen to be mostly located in France, have been estimated by averaging the daily potential evapotranspiration values. Furthermore the potential evapotranspiration for some of the sub-basins have been based on from another basin and slightly changed with the help of a transformation factor. For the Belgian section long-term monthly average potential evapotranspiration (which is required for the weather generator) is derived from the area averaged daily potential evapotranspiration of the 31 Belgian sub-basins. While the average monthly potential evapotranspiration of the Belgian sub-basins is used for determining the long-term monthly average potential evapotranspiration of the French section.

2.2.2 Discharge data series

The observed daily discharge data series that are used for this research is mostly in line with the data set described by Kramer et al (2008). Multiple discharge datasets were available at the same observation location. However there were differences between the datasets as has been highlighted by Kramer et al (2008). In order to clarify which dataset has been used for this thesis, Table B-2 is presented in Appendix A and contains the period of the daily discharge dataset per sub-basin, location of observation and source. The periods of the observed discharge datasets mostly vary between 1968 and 1998. This is not the case for the discharge series at Monsin though, where observations are available from 1911 – 2015. Eight observations are from the Meuse tributaries (Chiers, Semois, Viroin, Lesse, Ourthe, Ambleve, Vesdre, Mehaigne), which are taken from the final observation station before the tributary enters the Meuse. Three observation stations are directly located from the main river (St-Mihiel, Stenay, Chooz). The "observations" at Monsin are not directly observed Monsin, but are constructed based on observations at Kanne and St-Pieter. These observations are added in order to determine the discharge of the whole Meuse, which separates into two different flows at Monsin. For two sub-basins (Sambre, Chooz-Namur) are no observed discharge data series available. The table presented below shows the used data for the calibration and validation periods. The long discharge series at Monsin are used for the analysis of synthetic data.

table 2-2, Discharge data for the calibration and validation period.

Discharge data sub-basin	Calibration	Validation
1. Lorraine Sud	01-01-1969 , 01-01-1983	01-01-1983 , 01-01-1998
2. Chiers	01-01-1968 , 01-01-1983	01-01-1985 , 01-01-1998
3. Lorraine Nord	01-01-1968 , 01-01-1983	01-01-1983 , 01-01-1998
4. Stenay-Chooz	01-01-1968 , 01-01-1983	01-01-1983 , 01-01-1998
5. Semois	01-01-1968 , 01-01-1983	01-01-1983 , 01-01-1998
6. Viroin	01-01-1974 , 01-01-1983	01-01-1983 , 01-01-1998
7. Chooz - Namur	-	-
8. Lesse	01-01-1968 , 01-01-1983	01-01-1983 , 01-01-1998
9. Sambre	-	-
10. Ourthe	01-01-1968 , 01-01-1983	01-01-1983 , 01-01-1998
11. Ambleve	01-01-1968 , 01-01-1983	01-01-1983 , 01-01-1998
12. Vesdre	01-01-1968 , 01-01-1983	01-01-1983 , 01-01-1998
13. Mehaigne	01-01-1969 , 01-01-1983	01-01-1983 , 01-01-1998
14. Namur - Monsin	01-01-1968 , 01-01-1983	01-01-1983 , 01-01-1998

3. Method

3.1 Hydrological model preparation

One of the most important part of this research is to isolate the influence of hydrological model structures on the discharge simulation. This was the main aspect that had to be kept in mind when preparing the hydrological models for the simulation of the Meuse basin. Thus, an experiment has been designed where only the hydrological model structure varies. First of all hydrological models have been selected with similar ideas and conceptualisations. This means that the same data can be used in all the hydrological models. Furthermore, it makes it easier to identify which model structure components influence the, in this case, annual maximum discharge simulations. Secondly the routing that connects the sub-basins for the discharge of the Meuse basin at Monsin is kept constant for all hydrological models. This means that the time that it takes for discharge to reach the next sub-basin does not change and cannot influence discharge simulation differences. Finally, the calibration of the hydrological models is performed with the use of an aggregated objective function, which takes multiple hydrograph aspects into account. This aggregated objective function is optimized by changing the model parameters with an optimization algorithm. The influence of human decision making on the calibration process is reduced and ensures that the hydrological models are calibrated in a similar fashion.

3.2 Hydrological models

3.2.1 Hydrological models categorization

Only hydrological models with similar characteristics as the HBV model are used in this study. These characteristics are based on the classification system by Wheater et al., (1993) as mentioned in Pechlivanidis et al., (2011). All the different characteristics are presented in table 3-1 and are used to categorize different hydrological models. Using hydrological models with similar characteristics increases the chance of identifying model conceptualisations that are responsible for differences in simulations. Besides this, the weather data that will be used as input for the hydrological models in this study (historical weather data, and synthetic data) is areally averaged. Distributed hydrological models cannot use this data since these hydrological models require grid based data. Therefore the hydrological model should be semi-distributed or lumped in order to be able to use the weather data as input. The hydrological models that are selected for the comparison are the HBV model, the GR4J, and HyMOD hydrological models. Instead of using more hydrological models for separate sub-basins the focus will lie on simulating the entire Meuse river basin with each model.

table 3-1, Hydrological model characteristics Wheater et al.,(1993) as mentioned in Pechlivanidis et al., (2011)

Model structure	Model Distribution	Model results	Model time-scale	Model space scale
Metric models	Lumped	Deterministic	Continuous simulation	Small (< 100 km^2)
Conceptual models	Distributed	Stochastic	Event based	Medium (100-1000 km^2)
Physics based models	Semi-distributed			Large (1000 km^2 >)
Hybrid models				

3.2.2 Hydrological model structures

Aside from determining how much hydrological model structures can influence annual maximum discharge simulations it will be important to know how high flow discharges are generated. By analysing the model structures differences between these structures can be found and can increase the understanding of which hydrological process is important for the Meuse for generating high flow discharges. Therefore it is important to describe the hydrological model structures in detail. At the the of this chapter the main differences between the model structures are explained. Sometimes the state of a storage from a previous timestep is required. In order to illustrate the timestep the storages can sometimes be denoted by *(i)*, indicating the current timestep. During some of the model calculations the states of some storages will change in the same timestep. The number after *(,)* denotes the number of storage state updates.

GR4J model

The GR4J model stands for : 'modèle du Génie Rural à 4 paramètres Journalier' and is developed by Perrin et al., (2003). The GR4J hydrological has conceptual model structures but they are determined based on empirical findings from many different (French) sub-basins and should be considered as an empirical model. The GR4J model is a modified version of the GR3J model. The GR4J model uses daily potential evapotranspiration and precipitation as input. The input is not changed or corrected before it is used to determine the daily discharge. The GR4J model does not contain a snow module. This should only have a minor influence due to the small snow percentage that is used in the HBV model. The absence of a snow module results in a reduction of used parameters. Furthermore the other components in the GR4J model are only controlled by four parameters (figure 3-1).

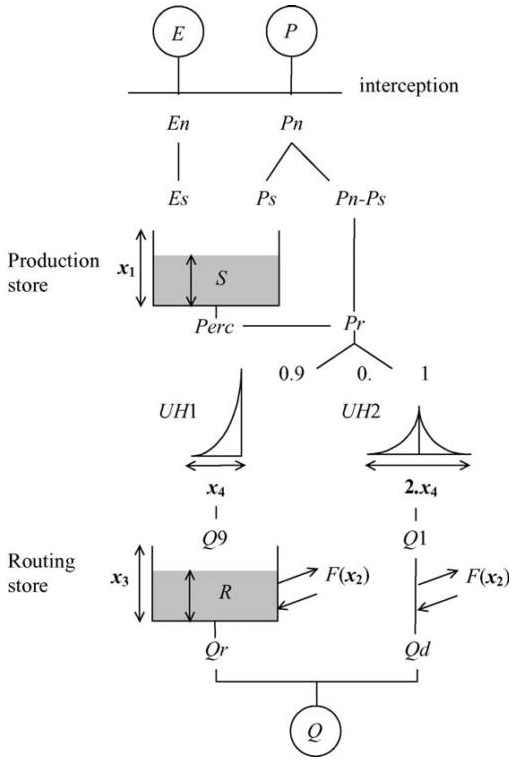

figure 3-1, GR4J Diagram (Perrin et al., 2003), *parameters:* x_1, x_2, x_3, x_4

Soil Routine

The first step of the GR4J model is to assess whether there is net evaporation or net precipitation during a day. When the input precipitation is larger than the input potential evapotranspiration the net rainfall *(P_n)* is calculated. Net potential evaporation capacity *(E_n)* is calculated when the potential evapotranspiration is larger than the precipitation. In the event that there is net rainfall a part of this rain *(P_s)* will enter production store *(S).* This is based on the outcome of equation 3-1. When there exist a net potential evapotranspiration the actual evapotranspiration is determined with equation 3-2 and this portion will leave the production store*(S).* The value of *S* can never exceed x_1, thus the value of x_1 represents the production store limit. A section of the volume that is contained in the production store will enter other containers via percolation *(Perc)* and is found using equation 3-3 After the value of the percolation is calculated the water will leave the production store. The remainder of the net rainfall and percolation *(P_r)* will be transferred to the next section of the GR4J model (equation 3-4).

equation 3-1

$$P_s = \frac{x_1\left(1-\left(\frac{S}{x_1}\right)^2\right)\tanh\left(\frac{P_n}{x_1}\right)}{1+\frac{S}{x_1}\tanh\left(\frac{P_n}{x_1}\right)}$$

equation 3-2

$$E_s = \frac{S\left(2-\frac{S}{x_1}\right)\tanh\left(\frac{E_n}{x_1}\right)}{1+\left(1-\frac{S}{x_1}\right)\tanh\left(\frac{E_n}{x_1}\right)}$$

equation 3-3

$$Perc = S\left\{1-\left[1+\left(\frac{4}{9}\frac{S}{x_1}\right)^4\right]^{-\frac{1}{4}}\right\}$$

equation 3-4

$$P_r = P_n - P_s + Perc$$

equation 3-5 , equation 3-6

$$S_{(i,1)} = S_{(i-1,2)} + P_n - E_n \qquad S_{(i,2)} = S_{(i,1)} - Perc$$

Routing Store

The P_r that is calculated on a certain day will be split into two flow components. The first flow component *(Q9)* will contain 90% of P_r and will be routed using unit hydrograph 1 *(UH1)*, while the second flow component *(Q1)* will contain remaining 10% of P_r and will be routed with unit hydrograph 2 (*UH2).* These unit hydrographs will spread the P_r from a certain day over several days and are based on the parameter x_4 which governs over how many days P_r is spread . The groundwater exchange term *(F)* is computed using x_2 and influences R and *Q1* (equation 3-7). The routing store *(R)* is updated by adding *Q9* and *F* (which can be either negative or positive). *R* cannot exceed one day ahead maximum capacity of the routing store *(x_3).* The outflow of the routing store *(Q_r)* is calculated based on *R* (equation 3-8), which will be also be used to update *R* by subtracting Q_r from *R* equation 3-9. *Q1* is changed by adding *F* as well and becoming Q_d. When F is negative and is larger than *Q1,* Q_d becomes zero (equation 3-10). The total streamflow *(Q)* is the sum of Q_r and Q_d (equation 3-11).

equation 3-7

$$F = x_2 \left(\frac{R_{(i-1,2)}}{x_3}\right)^{\frac{7}{2}}$$

equation 3-8

$$Q_r = R_{(i,1)} \left\{1 - \left[1 + \left(\frac{R}{x_3}\right)^4\right]^{-\frac{1}{4}}\right\}$$

equation 3-9

$$R_{(i,1)} = max\left(0;\ R_{(i-1,2)} + F + Q9\right), \quad R_{(i,2)} = R_{(i,1)} - Q_r$$

equation 3-10

$$Q_d = \max(0; Q1 + F)$$

equation 3-11

$$Q_{total} = Q_d + Q_r$$

Model code

The GR4J model is coded using the Python language. However there was no reliable Matlab code for the GR4J from an official scientific source. On the website of the GR4J model developers, GR4J models were available in R and in excel (Irstea., 2017). Due to the lack of experience with R it was decided to compare the output from the Python version of the GR4J model with the output from the excel version of the GR4J model. Due to different number rounding in the excel version and Python version, the outputs of the model versions do not match perfectly. The average difference between the outputs is in the order of 'E-14'.

The HyMOD model

The actual word HyMOD is never mentioned in the paper containing the description of the model (Wagener et al., 2001). However every other paper mentioning the HyMOD model is referencing to this paper. HyMOD simply stands for hydrological model and is a simple model with typical conceptual components according to Wagener et al., (2001). Like the GR4J model the HyMOD model does not contain a snow module, reducing the number of required parameters. Furthermore the precipitation and the potential evapotranspiration are not changed by the HyMOD model. The HyMOD model has five parameters, which need to be calibrated figure 3-2.

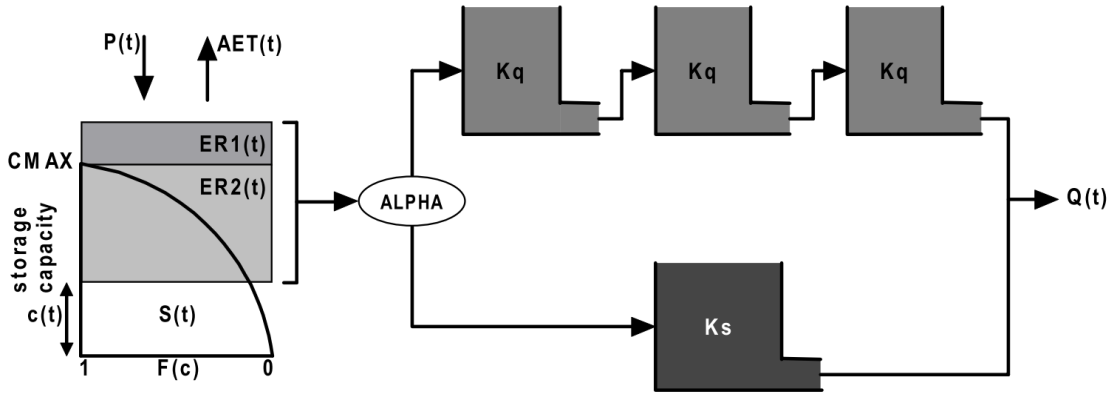

figure 3-2, the HyMOD model, (Wagener et al., 2001)*, parameters CMAX, BEXP, ALPHA, Kq, Ks*

Soil Routine

The HyMOD model computes two kinds of effective rainfall (*ER1* and *ER2*). In this model the storage capacity *(C)* does not have to be equal to soil moisture state *(S)*. In order to illustrate spatial soil variety within the catchment a curve is introduced governed by two parameters, the degree of spatial variability of the soil moisture capacity within the catchment *(BEXP)* and the *CMAX.* Based on this curve the value of *C* can be determined using the *(S)* from the previous timestep (equation 3-13). ER1 depends on the (Soil moisture) storage capacity *C* and the precipitation *(P)*. When the precipitation combined with *C* exceeds the maximum storage capacity (*CMAX*) the water will be transitioned into run-off *(ER1)* (equation 3-12). With the *(C)* and the precipitation that might be stored in the soil *(P-ER1)* the soil state *(S)* can be updated (equation 3-14). Using these values for ER2 are determined (equation 3-15). Based on the value of *S* and the potential evapotranspiration *(PET)* the actual evapotranspiration *(AET)* can be calculated (equation 3-16). Which in turn is used to update the soil moisture state *(S)* (equation 3-17).

equation 3-13

$$C = CMAX\left(1-\left(1-\left((BEXP+1)*\frac{S_{(i-1,2)}}{CMAX}\right)^{\frac{1}{BEXP+1}}\right)\right)$$

equation 3-12

$$ER1 = max(0; P - CMAX + C)$$

equation 3-14

$$S_{(i,1)} = \frac{CMAX}{BEXP+1}\left(1-\left(1-min(1;\ \frac{C+P-ER1}{CMAX})\right)^{BEXP+1}\right)$$

equation 3-15

$$ER2 = max\left(0; P - ER1 - \left(S_{(i,1)} - S_{(i-1,2)}\right)\right)$$

equation 3-16

$$AET = PET\left(1 - \frac{\frac{CMAX}{BEXP+1} - S_{(i,1)}}{\frac{CMAX}{BEXP+1}}\right)$$

equation 3-17

$$S_{(i,2)} = S_{(i,1)} - AET$$

Routing routine

The sum of *ER1* and *ER2* is distributed by parameter *ALPHA* and is directed to three linear reservoirs (*Rf)* with residence time *(Kq)* or a single linear reservoir (*Rs)* with residence time (*Ks)*(equation 3-18). The linear reservoirs are governed with similar equations, the *(j)* indicates one of the three fast linear reservoirs (equation 3-19, equation 3-20). This distribution will be further revered to as Inflow *(I)*. The outflow *(O)* from the first fast linear reservoir enters the second fast linear reservoir, while the outflow from the second fast linear reservoir enter the last fast linear reservoir. The outflow of the linear reservoirs are controlled by similar equations as well (equation 3-21, equation 3-22). The outflow from the last fast linear reservoir and quick reservoir form the total discharge (equation 3-23).

equation 3-18

$$I_{fast_1} = ALPHA \cdot (ER1 + ER2), \quad I_{slow} = (1 - ALPHA) \cdot (ER1 + ER2)$$

equation 3-19

$$Rf_{(i,j)} = Rf_{(i-1,j)}(1 - Kq) + I_{fast_j}(1 - Kq)$$

equation 3-20

$$Rs_{(i)} = Rs_{(i-1)}(1 - Ks) + I_{slow}(1 - Ks)$$

equation 3-21

$$O_{fast_j} = \frac{Kq}{1 - Kq} \cdot Rf_{(i,j)}$$

equation 3-22

$$O_{slow} = \frac{Kq}{1 - Kq} \cdot Rs_{(i)}$$

equation 3-23

$$Q_{total} = O_{fast_3} + O_{slow}$$

Hydrological model code

The hydrological model code was originally coded using Matlab and was found in one of the Matlab packages designed by J, Vrugt. In a study he has used the HyMOD model alongside the co-authors of the original paper describing the HyMOD model (Vrugt et al., 2002; Wagener et al., 2001) . Based on this Matlab script the code was rewritten using Python. The results from both scripts were identical when using the exact same parameters and input data.

The HBV model

In chapter two the Hydrologiska Byråns Vattenbalansavdelning (HBV) model has already been introduced. The HBV hydrological model that is used in this thesis is mostly based on the description given by Lindström et al., (1997). The HBV model uses many different parameters and constants. According to Lindström et al., (1997) twelve parameters are usually calibrated. A schematization of the model structure is presented in figure 3-3. table 3-2 presents the values of all the parameters that are used for the HBV model.

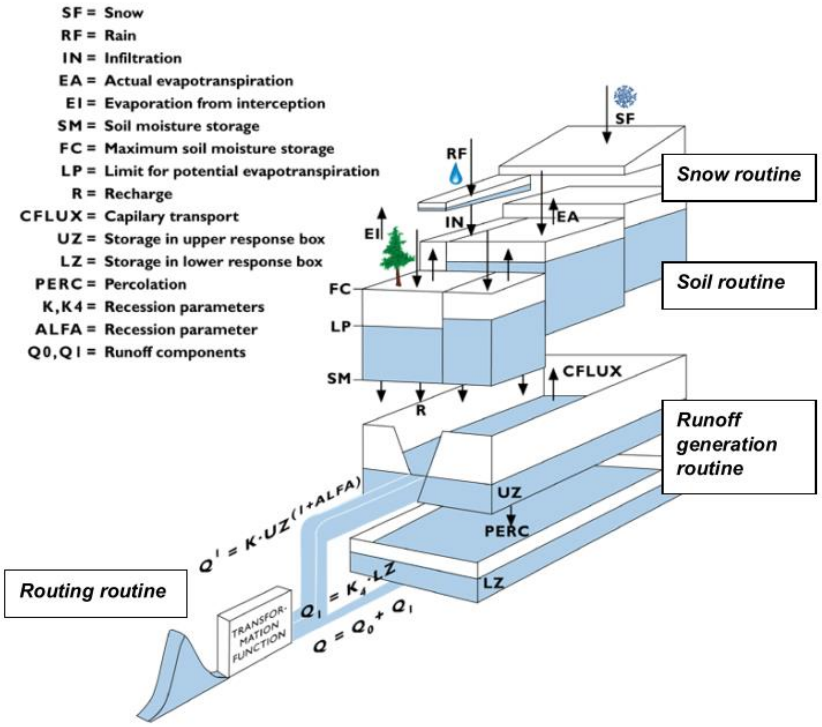

figure 3-3, Schematization of the HBV model structure (Hegnauer et al., 2014) *based on* (Lindström et al., 1997) *(CFLUX is described here as capillary transport , this is CF in* Lindström et al., (1997)*, while CFLUX is the maximum value of CF*

Snow module

The snow module of the HBV module can be complicated by stating values of a lot of different parameters. In this case most of the parameters that control the snow module have their basic value, Which simplifies the snow module. In this case the precipitation *(P)* can either come down as either snow or rain. When the temperature *(T)* is below zero the precipitation is snow otherwise its rain (equation 3-24). The snow module also keeps track of the total snow accumulation after multiple days with snow *(SP)*. When the temperature start to rise the snow melts *(SM)*. The rate of the *SM* depends on the snowmelt factor *(cfmax,* input temperature, and value of the *SP* (equation 3-25). The *SM* could infiltrate *(inf)* into the soil alongside the rain. However the value of *SP* has a certain water holding capacity *(WHC)* meaning that the melt water does not infiltrate immediately and is contained within the snow. Additionally, this water could refreeze further influencing the infiltration (equation 3-25). The refreeze rate is controlled by *T,* and how much melt water resides in the snow *(MW)* (equation 3-27). With the *SM, RF, Snow,* and current *SP* state the *SP* value for the next day is be calculated (equation 3-28). The next value of *MW* depends on *inf*, rain, *RF,* and current *MW* value, and is calculated using equation 3-29. When there is no snow melt or snow pack the rain will fully account for the infiltration.

equation 3-24
$$P = Snow, \quad \text{when } T < 0, \quad P = Rain, \quad \text{when } T > 0$$

equation 3-25
$$SM = \min\left(SP_i;\ \max(0;\ cfmax \cdot T)\right)$$

equation 3-26
$$inf = (Rain + SM - RF - WHC \cdot SP_i)$$

equation 3-27
$$RF = \min\left(MW_i;\ \max(0;\ -T)\right)$$

equation 3-28
$$SP_{i+1} = max(0;\ SP_i + snow + RF - SM)$$

equation 3-29
$$MW_{i+1} = \max(0;\ MW_i + Rain - RF - inf)$$

Soil routine

The water enters the soil via infiltration, which is already determined by the snow module. The amount of water that will flow to the upper zone *(UZ)* via the soil *(IF)* is controlled by the maximum soil moisture content *(FC),* current soil moisture content *(SMC)* and the soil routine parameter *(BETA)* using equation 3-30. However, when the soil is saturated the excess water from the infiltration will flow directly *(DF)* into the *UZ* (equation 3-31). The actual evapotranspiration, like the flow from the soil moisture, also depends on the soil moisture content. Using the potential evapotranspiration limit *(LP)* and the potential evapotranspiration input data *(PET)* the *AET* is calculated (equation 3-32). The HBV model also takes capillary flow *(CF)* into account which depends on the soil moisture content and is controlled further by the parameter *Cflux* (equation 3-33). The soil moisture for the following day will be determined with equation 3-34.

equation 3-30
$$IF = \max\left(0;\ (inf - DF)\frac{S_i}{FC}\right)^{BETA}$$

equation 3-31
$$DF = \max(0;\ inf + S_i - FC)$$

equation 3-32
$$AET = \min\left(PET; \frac{PET \cdot S_i}{LP \cdot FC}\right)$$

equation 3-33

$$CF = \min\left(UZ_i;\ Cflux\left(\frac{FC - S_i}{FC}\right)\right)$$

equation 3-34

$$S_{i+1} = \min\left(FC;\ \max(0;\ S_i + inf - IF - DF - AET + CF)\right)$$

Run off generation

The excess water from the infiltration and the flow from the soil moisture will enter the upper zone. A portion of this container will become run-off *(Q_0)* using two parameters (kf and ALPHA), the latter controls the non-linearity of this container (equation 3-35). A small portion of this container will percolate to the groundwater. The percolation is equal to the percolation parameter *(PERC).* Run-off generated from the groundwater *(Q_1)* is only controlled by one parameter *(ks)* and depends on the groundwater content (equation 3-36).The two run-offs combined form the total daily discharge. The state of the upper zone for the next day is calculated with equation 3-37, whereas the state of the lower zone (groundwater, LZ) is calculated using equation 3-38. Combining Q_0 and Q_1 gives the total discharge *(Q_{total})* (equation 3-39).

equation 3-35

$$Q_0 = \min(UZ_i;\ kf \cdot UZ^{1+ALPHA})$$

equation 3-36

$$Q_1 = ks \cdot LZ$$

equation 3-37

$$UZ_{i+1} = \max\left(0;\ UZ_i - Q_0 + \max(0;\ IF + DF - Perc) - \min(UZ_i; CF)\right)$$

equation 3-38

$$LZ_{i+1} = \max\left(0;\ LZ_i - Q_1 + \min(Perc;\ IF + DF)\right)$$

equation 3-39

$$Q_{total} = Q_0 + Q_1$$

*table 3-2, HBV model parameters that are used, *the sensitivity analysis will be discussed in detail in the calibration method*

HBV model parameter					
Input				**Soil**	
P	Precipitation			FC	Maximum soil moisture content
T	Temperature			LP	Limit for potential evapotranspiration
ET	potential evapotranspiration			BETA	Parameter in soil routine
				CFLUX	Maximum value of CF
Snow module					
TT	threshold temperature	0		**Response**	
WHC	Water holding capacity	0.1		Kf	Recession coefficient upper storage
CFMAX	snow melt	3.5		ALFA	Response upper storage parameter
CFR	refreezing	0.05		PERC	Percolation from upper to lower storage
				Ks	Recession coefficient lower storage
	always kept constant				
	Calibrated when most sensitive				

Model Code

The HBV model is coded using Python and is based on a Matlab script, which was present at the University of Twente. The Python script output has been compared to the Matlab script output in order to assess whether the python script model was functioning properly. The Python script output was the same compared to the Matlab script output.

3.2.3 Hydrological model differences/similarities

This paragraph is included in order to highlight important differences and similarities between hydrological models. Besides this, assumptions of the hydrological models that are not always stated in the hydrological model descriptions. will be described in this paragraph as well.

Weather interception

The HBV and GR4J model both have a form of weather interception, while the HyMOD model does not have a form of weather interception. For the HBV model the interception is included in the form of a snow module in which is determined if the precipitation falls as either snow or rain based on the temperature. The interception module of the GR4J model is used in a different matter. In this section the net precipitation/evapotranspiration is determined. This is done by subtracting the precipitation with the potential evapotranspiration when the precipitation is larger than the potential evapotranspiration and vice versa if the potential evapotranspiration is larger than the precipitation. Thus the GR4J model assumes that the actual transpiration is equal to the potential evapotranspiration if the precipitation is larger than the potential evapotranspiration.

Hydrological model storages

Each hydrological model uses a different number of storages. Most of these storages however are used to represent similar processes. For example each hydrological model uses a storage to symbolize soil moisture and has at least one routing store. Still, the water content of these storages are usually not controlled with the same equations or limitations. For the soil moisture storage each model uses one parameter to limit the amount of water that can be stored by the soil moisture. This value can vary a lot between hydrological models, even for the same sub-basin. The remaining water storage of the HBV and HyMOD model do not have a limit. This means that each sub-basin can contain unlimited amount of water. The GR4J model only uses two storages that both have a limit, which are controlled by two parameters (Perrin et al., 2003). This means that each sub-basin has a water storage limit and that this limit can be adjusted during the calibration process.

Discharge generation

The discharge is mostly generated using routing stores, the only exception is 10% of the water that will be used for the discharge generation (P_r) in the GR4J model. This water becomes discharge with a unit hydrograph induced delay. The use of a unit hydrographs enables the GR4J model to control how quickly the sub-basin reacts to precipitation. This is less apparent in the other hydrological models where the response to precipitation is more controlled by “residence time” parameters. Another difference is the clear separation of base flow in the HyMOD and HBV models. The base flow discharge of the HBV and HyMOD model is generated based on content of the storages that represent groundwater. Both of these storages have in common that the discharge increases linearly with the content of the storage. For the GR4J model it is less apparent what the different flows represent.

3.2.4 Discharge simulations of the Meuse at Monsin

In order to use the synthetic data from the weather generator, without modifying the data, it is necessary to use the same Meuse sub-basins and time step that were used by the HBV model in the GRADE instrument. Therefore all the hydrological models will use daily a time step and 14 sub-basins will be used to simulate the discharge of the Meuse basin at Monsin (The Jeker confluences with the Meuse after Monsin). The discharges from the separate sub-basins have to be transformed into a single discharge value that represents the total discharge of the river Meuse. To achieve this, the discharges of separate sub-basins have been summed with an induced lag. The induced lag simulates the travel time of the discharge from a certain sub-basin to reach Monsin.

The travel time for most sub-basins have been based on research by Berger & Mugie (1994). However, the mentioned travel time is the time that it takes for the discharge to reach Borgharen. The travel times for most sub-basins to Borgharen are in the range of hours, thus using a full day as lag would result in an estimation that is to rough. In order to prevent this, the daily discharges with lag and without lag (sometimes two days and one day lag if the lag is longer than a day) have been multiplied by a fraction. These fractioned daily discharges simulate the hourly lag (table 3-3). Although the travel time in Berger & Mugie, (1994) could have been modified in order to better suit the travel time to Monsin it was decided to keep the travel time of Borgharen. This is due to the hourly travel time that is already approximated in the daily time step. Furthermore, modifications of the travel time would have been based on assumptions of the travel time of the Meuse between Monsin and Borgharen. A schematization of the Meuse that is used to link the sub-basins together is provided in figure 3-4.

table 3-3, The lag that will be used to simulate the travel time of the discharges too reach Monsin. The lag at Stenay and Chooz are used as intermediary steps where the discharges from upstream sub-basins accumulate. These intermediary steps are necessary steps for the calibration and will be discussed in paragraph 2 of this chapter.

basin numbers	Stenay	hours	days	applied lag (days)
1	St-Mihiel, Stenay	17.35	0.72	0.7
	Chooz	**hours**	**days**	**applied lag (days)**
2	Carignan ,Chooz	32	1.33	1.35
1 , 3	Stenay ,Chooz	32	1.33	1.35
5	Membre ,Chooz	8	0.33	0.35
6	Treignes ,Chooz	4	0.17	0.15
	Monsin	**hours**	**days**	**applied lag (days)**
1 , 2, 3, 4, 5, 6	Chooz, Borgharen	16	0.67	0.65
8	Gendron,Borgharen	13	0.54	0.55
7 ,9	Namur-Salzinne,Borgharen	7	0.29	0.3
10	Tabreux,Borgharen	7	0.29	0.3
11	Martinrive,Borgharen	7	0.29	0.3
12	Chaudfontaine,Borgharen	5	0.21	0.2
13	Statte,Borgharen	4.97	0.21	0.2
14	Namur - Monsin, Borgharen	0	0	0
Directly from Berger & Mugie, 1994				
Estimated based on Berger & Mugie, 1994				
Assumed lag				

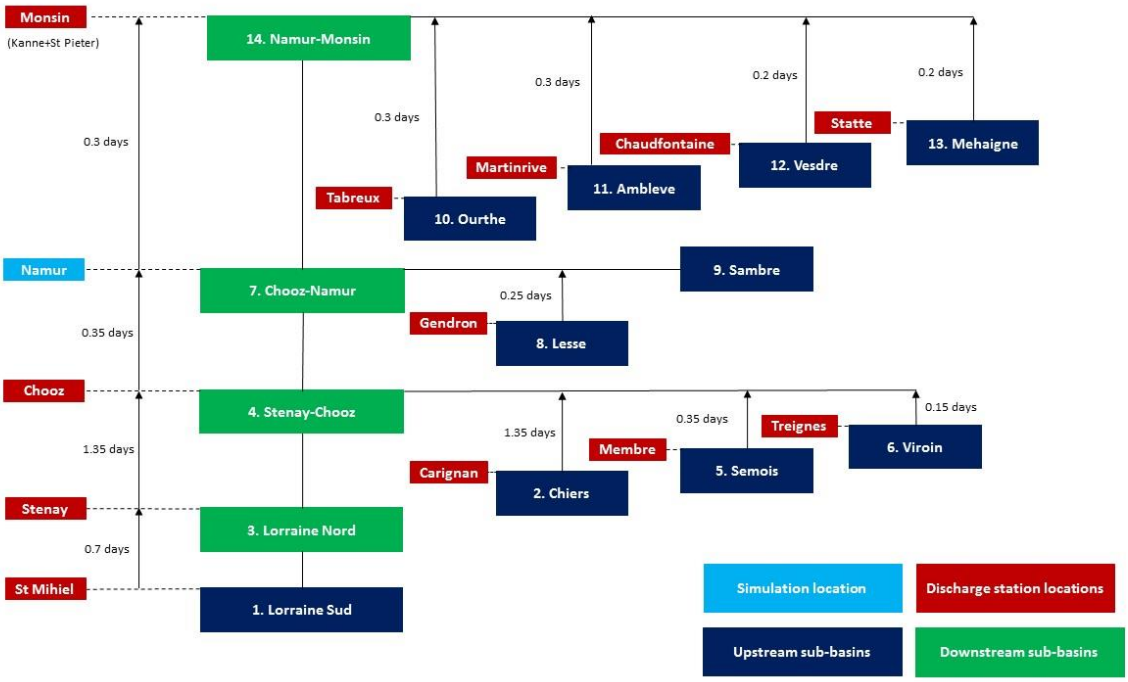

figure 3-4, Applied schematization of the Meuse for the simulation of discharges. This schematization is used for all hydrological models. Namur is only used as an output location for sub-basin 7 and 9. No discharge records where available at this location. The discharge "observations" at Monsin are the result of the summation of the observations at Kanne and St Pieter

3.3 Hydrological model calibration

Before a conceptual hydrological model can simulate the hydrological behaviour of a catchment, parameters need to be estimated. These parameters are estimated by calibrating the hydrological model against an observed discharge time series (Pechlivanidis et al., 2011). Model calibration in hydrology can be defined as the process of selecting suitable values of model parameters such that the simulations of the hydrological model approaches the hydrological behaviour of a catchment (Madsen, 2000; Sorooshian & Gupta, 1995 in: Booij & Krol, 2010 and Pechlivanidis et al., 2011). The same calibration method is used for all the hydrological models

As was mentioned before the calibration will be automated using an optimization algorithm, limiting influence of human descision making on the calibration process. This will ensure that the calibration process will be consistent and objective (Pechlivanidis et al., 2011). Four major elements can be identified in a typical automatic parameter estimation process: the selected objective function, the optimization algorithm, the termination criteria, and the calibration data. In this case, the automatic calibration process is used to find the values of the hydrological model parameters that will optimize the objective functions (Pechlivanidis et al., 2011). The hydrological models will be calibrated using data from the period 1967-1983 (1967-1968 used as run-up year). The source and preparation of the data is already described in chapter 2

3.3.1 Objective functions

An objective function is a numerical measure of the difference between the hydrological model discharge output and the observed catchment output (Pechlivanidis et al., 2011). A single objective function is often biased on an individual aspect of the hydrograph (Pechlivanidis et al., 2011). Four calibration objectives of the hydrograph are formulated by Madsen, (2000).

1. A good agreement between the average simulated and observed catchment runoff volume (i.e. a good water balance).

2. A good overall agreement of the shape of the hydrograph.

3. A good agreement of the peak flows with respect to timing, rate and volume.

4. A good agreement for low flows.

Each calibration objective focusses on a certain aspect of the hydrograph and should be represented by a single objective function. Usually there are trade-offs between these different calibration objectives. This means that a parameter set which is optimal for a calibration objective is less optimal for another (Madsen, 2000; Pechlivanidis et al., 2011). As mentioned before the GRADE instrument simulates daily discharges over a period of 50000 years, with the main goal to find the most extreme high flows (Hegnauer et al., 2014). Since this will be also the case for this research project the calibration process should focus on the peak flows while the general shape of the hydrograph remains similar to the observed hydrograph. Thus calibration objectives 1, 2 and 3 will be used in the calibration process.

The objective functions that will represent calibration objective 1, 2 and 3 are similar to the study performed by Booij & Krol (2010). For calibration objective 1 the relative volume error (RVE, equation 3-40) will be used, while for calibration objective 2 the Nash Sutcliffe coefficient (NS, equation 3-41) will be used. The Relative Mean Error in 10-year and 100 year return values (RMERV, equation 3-42) that will be used for calibration objective 3 . Booij & Krol, (2010) stated that the disadvantage of using the RMERV is that it is assumed that the annual maximum discharges are Gumbel distributed. The optimum values for the RVE and RMERV are 0, and can fluctuate between -∞ and ∞. The optimum value for the NS is 1 and can fluctuate between 1 and -∞. The RMERV equation presented here has been modified in two ways. The 100 year return period is replaced by the 25 year return period. Furthermore the absolute values are used from the results that consider different return periods. This is done in order to prevent any compensation which would also result in an optimum value of 0.

equation 3-40

$$RVE = \frac{\sum_{i=1}^{N}\left[Q_{sim,i} - Q_{obs,i}\right]}{\sum_{i=1}^{N} Q_{obs,i}}$$

equation 3-41

$$NS = 1 - \frac{\sum_{i=1}^{N}\left[Q_{sim,i} - Q_{obs,i}\right]^2}{\sum_{i=1}^{N}\left[Q_{obs,i} - \bar{Q}_{obs}\right]^2}$$

equation 3-42
$$RMERV = \frac{\left|\frac{RV_{sim}(y_1) - RV_{obs}(y_1)}{RV_{obs}(y_1)}\right| + \left|\frac{RV_{sim}(y_2) - RV_{obs}(y_2)}{RV_{obs}(y_2)}\right|}{2}, y_1 = 10\,, y_1 = 25$$

Where: $Q_{sim,i}$ is the simulated discharge at time i, $Q_{obs,i}$ is the observed discharge at time i, RV_{sim} is the simulated return value using Gumbel, RV_{obs} is the observed return value using Gumbel. y_1 and y_2 denote the return period that is associated with the return value.

In order to perform the calibration these objective functions have been combined in a single objective function. This combined function is often revered to as an aggregated function. The objective functions have to be combined since the optimization process that is used for the calibration of the hydrological model can only optimize a single objective function. The aggregated objective function has a form that is similar to the aggregated objective function that is suggested by Akhtar et al, (2009) and has the following form (equation 3-43).

equation 3-43
$$Y = \frac{NS}{1 + |RVE|}$$

The NS and RVE are given by equation 3-40 and equation 3-41 respectively. The optimum value for this objective function is one and ranges between one and -∞. The use of the absolute value of the RVE is important since negative values can lower the '1' in the function. This results in a higher aggregated objective function score thus valuing negative RVE values over positive RVE values. equation 3-43 has been modified by adding the RMERV function (equation 3-42) and results in equation 3-44. It is not required to use the absolute value since the result of the used RMERV equation is already absolute.

equation 3-44
$$Y_{mod} = \frac{NS}{1 + |RVE| + RMERV}$$

3.3.2 Optimization Algorithm

The optimization algorithm that will be used in this research is the shuffled complex evolution (SCE-UA) algorithm, which can be considered as a global search method (Duan et al., 1992). The SCE-UA method ensures that the starting values of the parameters do not influence the outcome of the optimization, thus resulting in a global optimum value. The SCE-UA method can only be used for optimizing a single objective function. The use of an aggregated objective function like equation 3-44 makes it possible to optimize the parameters based on multiple calibration objectives using the SCE-UA method.

SCE-UA set up

The SCE-UA optimization is performed by using a Python package (Houska et al., 2015). Before this optimization algorithm can be used in the calibration process it has to be set-up correctly. This set-up can be translated to the termination criteria that are mentioned before (Pechlivanidis et al., 2011). The following decisions have to be made in order properly set-up the SCE-UA algorithm: (1.) Selecting the numerical measure that will be optimized (Y_{mod} ,equation 3-44), (2.) Selecting the hydrological model parameters that will be calibrated (3.) Determine the parameter ranges of the hydrological model parameters that will be calibrated, (4.) Selecting the maximum number of iterations and (5.) Choosing the proper algorithm parameters, which influence the performance of the SCE-UA algorithm. The selected parameter ranges are based on prior research for which these hydrological models have been used (table 3-4). By selecting large ranges for the parameters, the optimisation algorithm can find the global optimum from a large parameter space, while making no prior assumptions about the hydrological behaviour of the sub-basin.

For this thesis, four parameters for the GR4J model, five parameters for the HyMOD model and eight parameters for the HBV model need to be calibrated. However the calibration of eight parameters could be much more time consuming compared to the calibration of four/ five parameters. Furthermore, by decreasing the number of parameters that will be calibrated, the over-parametrization and parameter dependence risk will be reduced (Brauer, Teuling, F. Torfs, & Uijlenhoet, 2014). By performing a sensitivity analysis for each sub-basin, five parameters will be selected for the calibration process of the HBV model (table 3-5). Some parameters in the HBV model do not have a default value, in this case the sensitivity analysis is also used to estimate a constant value for that parameter if said parameter will not be calibrated.

table 3-4, parameter ranges used for the calibration, GR4j: (Tian et al., 2014), HyMOD: (Herman et al. , 2013), HBV 2: (Harlin & Liden, 2000), 3 (Booij & Krol, 2010) 1: It is stated that x4 cannot become lower than 0.5 and is therefore adjusted (Perrin et al., 2003).

GR4J	Range	HBV	Range
x1 (mm)	10, 2000	FC (mm) [2]	100, 800
x2 (mm)	-8 , 6	Beta (-) [2]	1 , 6
x3 (mm)	10, 500	LP (-) [3]	0.2 , 1
x4 (d)[1]	0.5, 4	Alpha (-) [2]	0 , 3
		Kf (d^{-1}) [3]	0.005, 0.1
HyMOD	**Range**	Ks ($mm*d^{-1}$)[3]	0.005, 0.1
cmax (mm)	10 , 2000	Cflux ($mm*d^{-1}$) [3]	0.01, 2.5
b_exp (-)	0 , 7	Perc ($mm*d^{-1}$) [2,3]	0.01 , 5
Alpha (-)	0 , 1		
Ks (d^{-1})	0 , 0.15		
Kq (d^{-1})	0.15 , 1		

The SCE-UA algorithm uses a certain set of parameters that influence the overall performance of the optimization algorithm. For the optimization of objective function Y_{mod} the SCE-UA global optimization algorithm will use a maximum of 10000 iterations. The minimum number of complexes should at least be the same as the number of calibrated parameters. The number of complexes for the SCE-UA algorithm will be set to six for each hydrological model. This number is larger than the amount of parameters used in the calibration process and will be kept constant for each hydrological model. The rest of the parameters have been set to the default values as is suggested by Duan et al (1994).

table 3-5, The HBV model parameters that will be calibrated for each sub-basin. [1,2,3] Denote for which sub-basins the same parameters will be calibrated

HBV model parameters			
1. Lorraine sud [1]	1, 2, 3, 4, 5	8. Lesse [2]	1, 3, 4, 5, 8
2. Chiers [2]	1, 3, 4, 5, 8	10. Ourthe [1]	1, 2, 3, 4, 5
3. Lorraine nord	1, 2, 3, 4, 8	11. Ambleve [1]	1, 2, 3, 4, 5
4. Bar etc [2]	1, 3, 4, 5, 8	12. Vesdre [1]	1, 2, 3, 4, 5
5. Semois [1]	1, 2, 3, 4, 5	13. Mehaigne [3]	1, 2, 4, 5, 8
6. Viroin [2]	1, 3, 4, 5, 8	14. Namur - Monsin [3]	1, 2, 4, 5, 8
FC = 1 , Beta = 2, LP = 3, Alpha = 4, Kf= 5, Ks = 6, Cflux = 7, Perc = 8			

3.3.3 Termination criteria/Calibration data

The calibration process will stop if the improvement of the aggregated objective function by changing the hydrological model parameters is no longer sufficient. The improvement is no longer sufficient when the aggregated objective function only improves with a very small number (in the order of 0,0001). In chapter two it was already shortly mentioned which data would be used for the calibration and validation process. The hydrological models will be calibrated using data from the period 1967-1983 (1967-1968 used as run-up year). If the available discharge data is limited the calibration period is shortened accordingly and includes a run-up year that predates the earliest available discharge data by a year. For the Sambre and the Namur-Monsin sub-basins no discharge data is available. Therefore these sub-basins will be calibrated alongside the most downstream sub-basin (Monsin)

3.4 Hydrological model Validation

After the hydrological model is calibrated, the model needs to be validated in order to assess the model performance. This is done by using a portion of the observed discharge that has not been used in the calibration process (Pechlivanidis et al., 2011). The validation reveals the hydrological models robustness, how well hydrological behaviour is simulated and whether some calibrated parameters have any biases (Pechlivanidis et al., 2011). Usually it is found that the hydrological performance is better during the calibration period compared to the validation period. For the sub-basins that have an available discharge data set the remainder of the available historical data is used. This is 1983-1998 for all sub-basins excluding Sambre and Namur-Monsin. Days with missing discharge values are filtered and not used for calculating the objective function values (Chiers). The aggregated objective function (equation 3-44) that is used for the hydrological model calibration will also be used for the hydrological model validation.

3.5 Synthetic data analysis

The focus will lie on the high flow simulations and observations. For this reason the maximum discharges of each hydrological year of the simulations and observations are selected. The analysis will be performed using these yearly maximum discharges. With the use of statistical tests the annual maximum discharge distributions of the synthetic data simulations, historical simulations and observations can be compared.

3.5.1 Sub-basins selection for statistical analysis

The test described above will be performed for multiple sub-basins and for each hydrological model. The first notion was to mainly focus on analysing the discharges at congregating sections of the Meuse (Chooz and Monsin). Simulated discharges at Monsin can be compared to the results of the original GRADE instrument, while the simulated discharges at Chooz give an intermediate result of the simulations. However, the discharge input of multiple sub-basins makes it more difficult to identify which model structure components are causing differences in the high discharge simulations of the hydrological models. For this reason it is also interesting to perform the analysis on multiple upstream sub-basins. Only a limited number of sub-basins will be selected to be analysed in order to save time. The Ourthe, Lesse and Semois are already used in an earlier inter-comparison study (de Boer-Euser et al., 2016). The results might be similar to the results of the inter-comparison study making these sub-basins good candidates for analysis. In order to incorporate an upstream sub-basin that is not located in the Ardennes the Chiers will be used for the analysis as well. Additional sub-basins might be selected if the results of a sub-basin for the calibration and validation prove to be interesting.

3.5.2 Comparing the mean

The mean of the annual maximum discharges of the WG simulation, historical simulations and observations are compared using the Two-independent samples T-test. An advantage of this T-Test is that it does not have to be assumed that the variances of the samples are the same. A disadvantage of this test is that the test is sensitive to normality of the data. However, the T-distribution approaches the normal distribution when the size of a sample is around 30 (Davis, 2002). The observed annual maximum discharge sample has the smallest size which is usually 31. Thus the Two-independent samples T-test can be used for this analysis. The null-hypothesis for this test is that the two population means are equal.

3.5.3 Comparing the variance

For the comparison of the variances of the WG simulation, historical simulation and observation annual maximum discharges the Brown-Forsythe test is used. This has the following null-hypothesis: The variances of the populations are equal. This test is a different version of the more commonly used Levene's test. The difference is that the Brown-Forsythe test uses the median instead of the mean. Furthermore the Brown-Forsythe test does not require that the samples have a normal distribution. This makes the number of samples less relevant.

3.5.4 Gumbel plot

After the variance and means comparisons that are used to compare the different simulations of the same hydrological model, Gumbel plots are presented. These graphs will be used compare the synthetic data annual maximum discharge simulations of the different hydrological models with each other. Gumbel plots are a way to present annual maximum discharge values with an associated return period. In order to create a Gumbel plot the synthetic data annual maximum discharge simulations and observations are sorted from highest to lowest. Ranks are assigned to each of the sorted values beginning with 1 until the lowest value has an assigned rank. The first step in determining the plotting positions on the X-axis is to transform the rank values using the Gringorten equation (equation 3-45).

equation 3-45

$$P(X) = 1 - F(X) = \frac{r - 0.44}{N + 0.12}$$

Where *P(X)* is the probability of exceedance*, F(X)* is the opposite of *P(X)*, *r* is the rank, and *N* is the number of used values. These probability of exceedance can be transformed into a reduced variate, and a return period (equation 3-46, equation 3-47).The reduced variate is used for the X-axis plotting positions.

equation 3-46

$$y = -\ln\left(-\ln(1 - P(X))\right)$$

equation 3-47

$$T(X) = \frac{1}{P(X)}$$

Where *y* is the reduced variate, and $T(X)$ is return period in years. The synthetic data annual maximum discharge simulations and observations values are plotted against the associated reduced variates, resulting in a Gumbel plot.

3.5.5 Comparing Synthetic data simulations with observations

The Gumbel plots provide a method for comparing the simulations using synthetic data of the different hydrological models. Although the annual maximum discharge observations are presented in these graphs as well, it is still difficult to compare the synthetic data simulations with the observations. The reason for this is that the number of annual maximum discharge observations is much lower compared to the number of annual maximum discharge simulations using synthetic data. Therefore a method is designed in order to perform the comparison. First of all the simulation values are selected that have similar associated reduced variates (*y*) compared to the reduced variates associated with the observed values. Thus the sample size of the annual maximum discharge observations and synthetic data simulations will be the same. After the selection procedure the observations are plotted against the simulations with similar reduced variates. The resulting scatter plot reveals whether the synthetic data simulations are close to the observations.

3.6 Model structure effect on high flow discharges

3.6.1 Hydrograph analysis

In order to determine which section of the model structure mostly influence the high flow discharges. Five different flood waves have been selected. The three largest flood waves, a floodwave during the summer and a floodwave were snow played an important role in generating the floodwave. For multiple upstream sub-basins hydrographs will be presented (Chiers, Semois, Lesse, Ourthe. Mehaigne) These hydrographs contain additional information such as daily precipitation, snowfall according to the HBV model, and total volume of the discharge wave. The additional information can only be acquired from upstream basins simulations. This is because only the discharge from upstream basin simulations is used to determine downstream simulations. Additionally, using upstream simulations prevents any influences from other sub-basins on the hydrographs. Using the model structure descriptions stated in the previous paragraphs it is assessed whether the model structures can explain the hydrographs of the simulations.

3.6.2 Floodwave contribution

In order to also consider the effect of the model structure on downstream simulations the five selected discharge waves are used again. In this case it is calculated how large the contribution of each sub-basin is to the total volume of the discharges waves at Monsin for each hydrological model. By comparing this to the “observed” contribution it can be determined if the hydrological models are correctly mimicking the discharge contribution from each sub-basin. The contributions of each sub-basin are presented for the hydrological models and observations per sub-basins in the form of 20 Pie-charts. The lag that is mentioned in table 3-3 is used to only take the discharge from the sub-basins into account that contributed to the discharge wave at Monsin. For example only the discharge volume from Lorraine sud 2.7 days prior and 2.7 days before the end of the discharge wave at Monsin are considered.

4. Results

This chapter consists of three different sections. The first section will assess the performance of the hydrological models during the calibration and validation period. The performance is assessed using the historical data. Following the performance, the statistical analysis of the synthetic data is presented for 5 important sub-basins. The data is mainly compared between the observations. Unlike the performance assessment, the statistical analysis focusses on annual maximum discharge values alone. Finally, the switch is made back to the simulations with historical data. In this final section it is determined which hydrological model structure component can be important when simulating high value discharges. Furthermore, this section presents the sub-basin contribution to high flow discharges waves at Monsin. This is done in order to find if the hydrological models simulate the floodwave contribution percentages correctly.

4.1 Hydrological model discharge simulation performance (Historical)

The calibration results are presented in four separate graphs below. Each graph is presented in a similar manner. The colour theme for each hydrological model is mostly retained throughout this thesis. Calibration and validation results are presented for each sub-basin, which are denoted on the x-axis. In the first graph the results of the aggregated function values are given, where three objective functions are combined. Following the first graph, the values for the individual objective functions are given.

Aggregated objective function

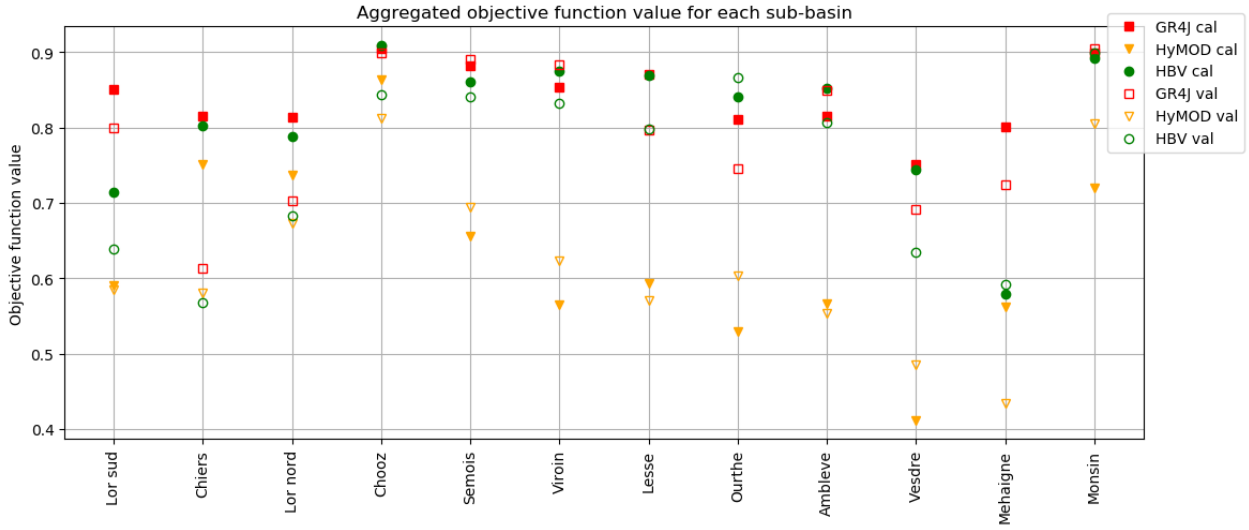

figure 4-1, Values of the aggregated objective function for each Meuse sub-basin. The values close to 1 are an indication that the simulations are closely mimicking the observations The different colours are representing the hydrological models, red represents the GR4J model, orange the HyMOD model and green the HBV model. The results for the calibration and validation are represented by filled and unfilled symbols respectively

In figure 4-1 the objective function values reveal that the HyMOD model is performing worse compared to GR4J model and the HBV model for every sub-basin. This is the case for both the calibration and validation period. The GR4J model shows similar results for the objective functions compared to the HBV model, although the GR4J model mostly has slightly better results than the HBV model. The discharges of six sub-basins are accumulating at Chooz and the discharges of all sub-basins are accumulating at Monsin. According to figure 4-1 the performance at Chooz and Monsin for all hydrological models is better compared to the upstream sub-basins. Downstream sub-basins cannot be calibrated separately since these sub-basins require discharge input from upstream catchments. Therefore it is possible that during the calibration process the model parameters for these downstream sub-basins are calibrated such that the faults of the upstream discharge simulations are compensated. These compensations could increase the value of the objective functions for downstream catchments compared to the objective function values of the upstream sub-basins.

Nash-Sutcliffe efficiency (NS)

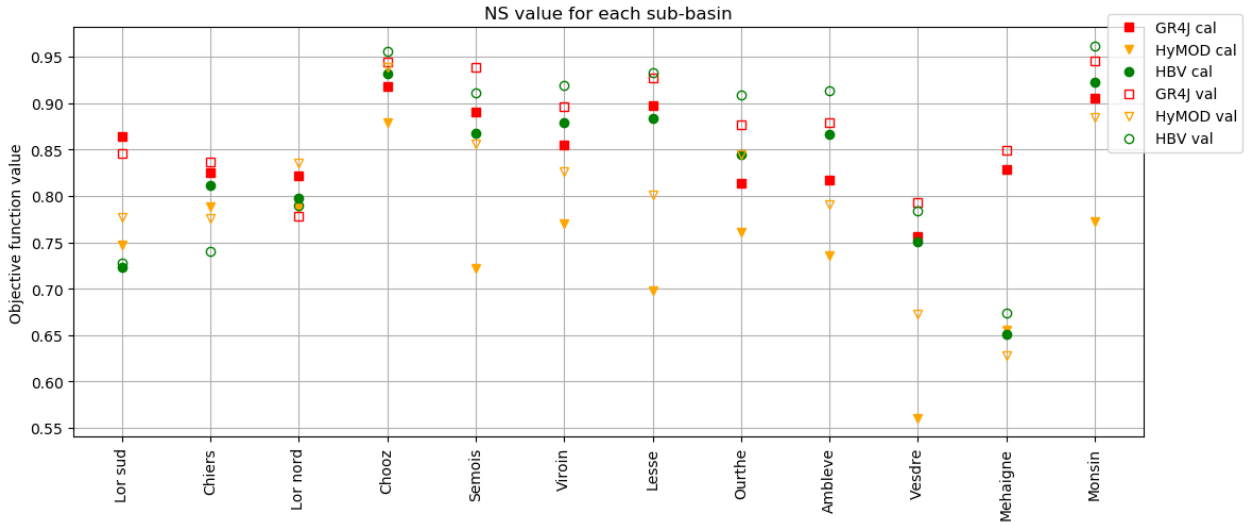

figure 4-2, Values of the Nash-Sutcliffe efficiency for each Meuse sub-basin. The values close to 1 are an indication that the simulations are closely mimicking the observations The different colors are representing the hydrological models, red represents the GR4J model, orange the HyMOD model and green the HBV model. The results for the calibration and validation are represented by filled and unfilled symbols respectively

Observing figure 4-2 shows that the difference between the objective function values of the HyMOD model compared to the objective function values of the other hydrological models is less than the difference in figure 4-1. This is especially the case for the first three sub-basins, where the HyMOD model no longer has the lowest objective function value. This is an indication that the objective functions other than the NS-value are responsible for the low aggregated objective function values for the HyMOD model. Another interesting aspect of figure 4-2 is the better NS-values for the validation period in most of the sub-basins. Usually the objective function has a better value during the calibration period since the value is optimized for this period. The NS-value emphasises on higher discharges. Therefore a possible explanation for the higher objective function value during the validation period could be the wetter conditions in the validation period. Another explanation could be an increase in observed data quality in the validation period.

Combination REVE objective functions: RMERV (return periods 10 and 25 years)

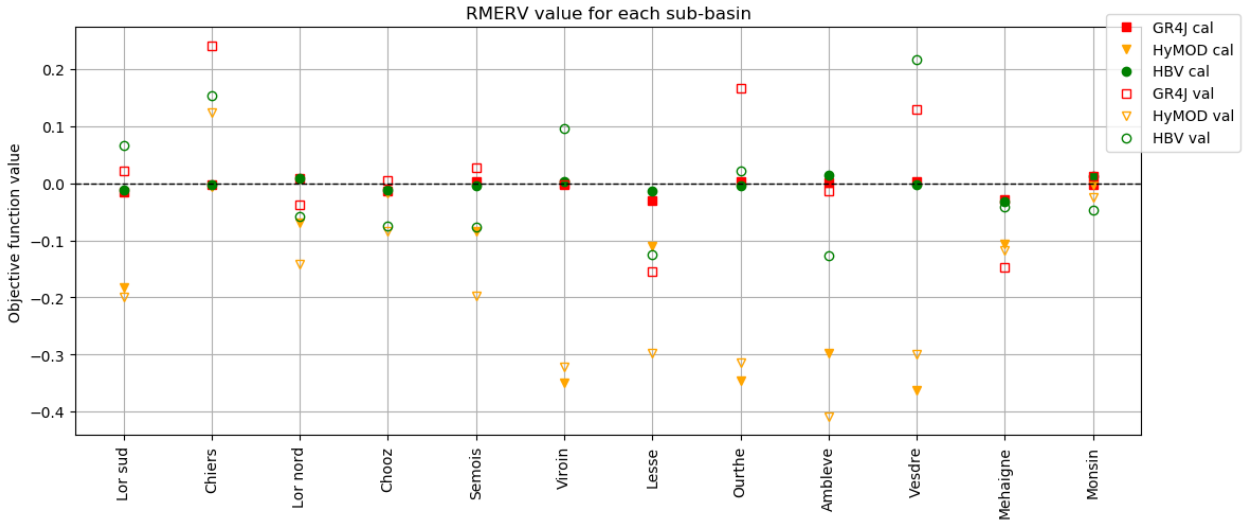

figure 4-3, Values of the combined REVE objective functions with a 10 year and 25 year return period for each Meuse sub-basin. The values close to 0 are an indication that the simulations are closely mimicking the observations. The different colours are representing the hydrological models, red represents the GR4J model, orange the HyMOD model and green the HBV model. The results for the calibration and validation are represented by filled and unfilled symbols respectively

figure 4-3 presents the value of the combined Relative extreme value errors, which is used to assess whether the hydrological models are able to simulate high flow discharges. During the calibration period the GR4J model and HBV model are showing a good performance for every sub-basin, since these objective function values are very close to zero. As opposed to what was seen for the Nash-Sutcliffe efficiency, the performance of these models worsens in the validation period for the combined REVE objective functions. The HyMOD has, again, the worst performance of the hydrological models. The negative objective function scores indicate that high flow discharge simulations are lower compared to the observations. This means that the HyMOD model is not able to simulate high discharges that are observed in most of the sub-basins. The values of the objective function at Chooz and especially Monsin are good, even for the HyMOD model. This further encourages the notion that the hydrological model parameters of the downstream basins are calibrated such that some of the simulation errors of the upstream basins are corrected.

Relative Volume Error (RVE)

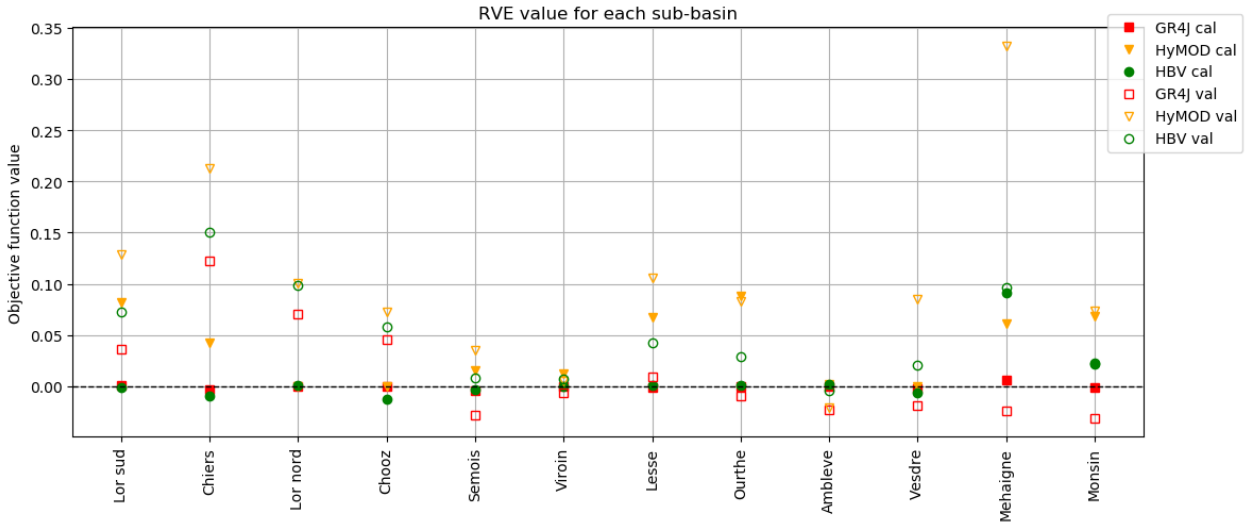

figure 4-4, Values of the Relative Volume Error (RVE) objective function for each Meuse sub-basin. The values close to 0 are an indication that the simulations are closely mimicking the observations. The different colours are representing the hydrological models, red represents the GR4J model, orange the HyMOD model and green the HBV model. The results for the calibration and validation are represented by filled and unfilled symbols respectively

figure 4-4 present the objective function values for the RVE. This figure shows good scores for the GR4J model and HBV model during the calibration period and become worse in the validation period. These results are similar compared to the results of the objective functions in figure 4-3. The HyMOD model still under performs compared to the other models. In this case the RVE values for the HyMOD model are positive instead of the negative results for the combined REVE objective function. This indicates that the HyMOD model is overestimating the discharge volume in the simulations.

4.2 Synthetic data analysis

In this paragraph the results of the statistical tests are presented. The used significance for every test in this study is 95%. This means that when a p-value lower than 0.05 is found the test is significant and the null hypothesis is rejected. The cells in the table that are marked red will indicate that the null-hypothesis can be rejected. This will be the case for every table in this chapter. Only a couple of upstream sub-basins are selected for this analysis. The selected upstream sub-basins are Chiers, Semois, Lesse, Ourthe, and the Mehaigne. The Mehaigne is added to the selection because of the calibration/validation results. First of all the calibration and validation results show that the performance of the GR4J is superior to the performance of the HBV and HyMOD model (figure 4-1). The good performance of the GR4J model might be explained by the additional term of the GR4J model structure that allows water to leave the sub-basin via groundwater. This makes the Mehaigne an ideal sub-basin for further analysis.

First of all the results of the equality of means test is presented. The results of the test is presented in a table. The table represents the results of the equality of means test of the annual maximum discharges that are from the following sources: observed, simulated using historical data, and simulated using synthetic. This will be done for all every hydrological model and for each selected sub-basin. The results of the equality of variance test is shown next. The lay-out of this table is the same as the table of the equality of means test results. After the results of the equality of variance/mean are presented, the Gumbel plots of the synthetic data annual maximum discharge simulations are given. These Gumbel plots show the results of the synthetic data simulations at Chooz, Monsin and each selected upstream sub-basin. Finally the results are presented for the scatter plots, which are used to analyse the synthetic data simulations and observations in more detail. Like the Gumbel plots, the results of the scatter plots are presented at Chooz, Monsin and each selected upstream sub-basin.

4.2.1 Equality of mean test

The statistical test that was used to test whether the population means are equal is the Two-independent samples T-test. The green cells are an indication that the null-hypothesis cannot be rejected. In this case it can be assumed that the population means of the annual maximum discharges are the same. If the means of the annual maximum discharge simulations are different compared to the annual maximum discharge observations the overall annual maximum discharges might be over or underestimated. table 4-1 shows that again the HyMOD model has difficulty properly simulating the annual maximum discharges. Thus the simulated annual maximum discharges are over or underestimated resulting in a higher or lower mean compared to the observations. The tests comparing the population means of the observations and synthetic simulations indicate that the means are unequal. Whereas the population means of the observations and historical data simulations appear to be equal.

table 4-1, Two-independent samples T-test results comparing annual maximum discharge means of different sources (downstream indicates that multiple sub-basins are linked together to simulate the discharge: 6 for Chooz, 14 for Monsin)

Equality of mean: historical simulations - observations							
	upstream		**downstream**				
	Chooz	**Monsin**	**Chiers**	**Semois**	**Lesse**	**Ourthe**	**Mehaigne**
GR4J	0.6263	0.5733	0.7801	0.9665	0.3314	0.7587	0.2829
HyMOD	0.4967	0.6033	0.6744	0.1961	0.0858	0.0139	0.5416
HBV	0.5791	0.4447	0.8417	0.7773	0.5018	0.9929	0.1865
Equality of means: synthetic data simulations - historical data simulations							
	upstream		**downstream**				
	Chooz	**Monsin**	**Chiers**	**Semois**	**Lesse**	**Ourthe**	**Mehaigne**
GR4J	0.5661	0.8490	0.6641	0.3594	0.7660	0.8487	0.7530
HyMOD	0.6274	0.5071	0.7749	0.8017	0.1760	0.4603	0.2733
HBV	0.4881	0.9588	0.6985	0.3604	0.9248	0.6832	0.9846
Equality of means: synthetic data simulations - observations							
	upstream		**downstream**				
	Chooz	**Monsin**	**Chiers**	**Semois**	**Lesse**	**Ourthe**	**Mehaigne**
GR4J	0.1681	0.1410	0.3993	0.4066	0.1730	0.7871	0.0636
HyMOD	0.0704	0.9954	0.2924	0.0015	0.0106	0.0000	0.9821
HBV	0.0986	0.1472	0.4736	0.1615	0.2801	0.6986	0.0322

4.2.2 Equality of variance test

The table below presents the p-values of the equality of variance test results. The statistical test that was used to acquire the p-values is the Brown-Forsythe test. If the test does not show a significant results (green cells) then it can said that the population variances of the distributions are the same. The simulations should be close to the observations. Thus when the population variances are significantly different (red cells) the simulations are not correctly showing the variability in the annual maximum discharge simulations. From table 4-2 it is clear that during the synthetic data simulations the HyMOD model has difficulty simulating the variability of the annual maximum discharges for most of the upstream basins. The equality of the population variances for the historical data simulations and observations can be explained by the smaller number of annual maximum discharges that are compared (30/30 instead of 49998/30). The larger sample size increases the precision of the test. This increases the chance that the test show significant results when even small variance differences are found (This is also the case for the HBV and GR4J model but these models seem to simulate annual maximum discharge variances that are close to the observations).

table 4-2, Brown-Forsythe test results comparing annual maximum discharge variances of different sources (downstream indicates that multiple sub-basins are linked together to simulate the discharge: 6 for Chooz, 14 for Monsin)

Equality of variance: historical simulations - observations							
	downstream		upstream				
	Chooz	Monsin	Chiers	Semois	Lesse	Ourthe	Mehaigne
GR4J	0.9065	0.2998	0.0607	0.8367	0.7635	0.6241	0.6350
HyMOD	0.6711	0.3817	0.3781	0.2853	0.3074	0.0075	0.2848
HBV	0.8825	0.4179	0.2265	0.7658	0.7636	0.7796	0.3460
Equality of variance: synthetic data simulations – historical data simulations							
	downstream		upstream				
	Chooz	Monsin	Chiers	Semois	Lesse	Ourthe	Mehaigne
GR4J	0.3949	0.5879	0.0993	0.2864	0.7810	0.5059	0.4617
HyMOD	0.1384	0.1315	0.0168	0.0812	0.1838	0.2947	0.1782
HBV	0.2853	0.6522	0.0483	0.3858	0.5947	0.2150	0.0140
Equality of variance: synthetic data simulations - observations							
	downstream		upstream				
	Chooz	Monsin	Chiers	Semois	Lesse	Ourthe	Mehaigne
GR4J	0.5274	0.2745	0.2887	0.4949	0.4113	0.9712	0.2207
HyMOD	0.0186	0.5245	0.5228	0.0000	0.0001	0.0000	0.0023
HBV	0.1877	0.4136	0.8720	0.1601	0.2789	0.4143	0.2129

4.2.3 Gumbel plots

figure 4-5 shows the annual maximum discharges of the observations and the synthetic data simulations. The graph shows sorted annual maximum discharge values. The synthetic data simulations for each hydrological model are presented using the same colours as was shown previously in this chapter. The largest discharge values have a low chance of occurrence. The chance of occurrence increases when the discharge values decrease. In order indicate return periods that are associated with the discharge values several red lines are given which present the return periods.

GR4J and HBV

Comparing the synthetic data simulations from the GR4J and HBV model shows that the simulations are similar in most plots (figure 4-5). This is especially the case for discharge simulations that have a higher chance of occurrence (before the T = 10 year line). However, when looking at larger discharge values the gap between the GR4J and HBV model discharge simulations increases. In most cases this means that the GR4J model discharge simulations are higher compared to the HBV discharge simulations. Thus, when the precipitation becomes more extreme the GR4J model simulates higher discharges compared to the HBV mode for most upstream sub-basins (Chiers, Semois, Ourthe, Mehaigne). This is also the case for the discharges at Chooz, showing increasing differences between the GR4J and the HBV when annual maximum simulations become larger. However, when all the discharges are combined for the simulation of the total Meuse discharge at Monsin the simulations are very similar.

HyMOD

From these graphs it becomes clear that the HyMOD annual maximum discharge simulations are lower compared to the simulations of the other hydrological models. This is supported by the low RMERV values for found during the calibration process. In the calibration process the RMERV value is underestimated for the HyMOD model in most of the selected sub-basins. The lowest HyMOD simulations (Semois, Lesse and Ourthe) are also supported by of the statistical analysis, showing that the population means/variance of the simulations and observations are unequal.

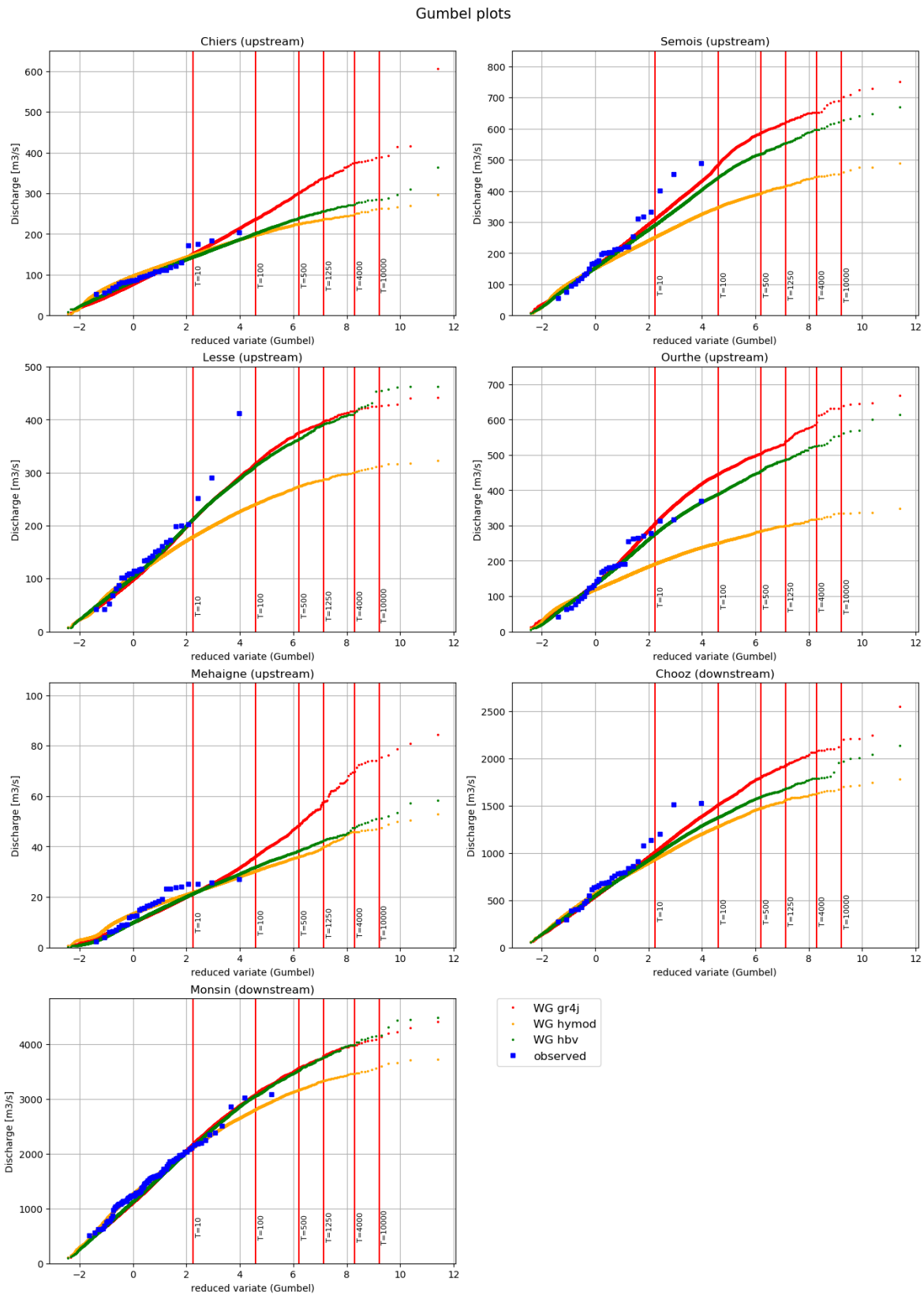

figure 4-5, Graphs, presenting the annual maximum discharge simulations for each hydrological model using synthetic data using a Gumbel scale

4.2.4 Scatter plots

The scatter plots present a more detailed comparison between the synthetic data simulations and the observations. Per selected sub-basin the discharge simulations are plotted against the observed discharges for each hydrological model separately. Using linear correlation techniques a line for the scatter plot is determined in order to clarify the graph. The black dashed line indicates when the observations are equal to the simulations. When the points are under the dashed black line the annual maximum discharge values are underestimated, while they are overestimated when located above said line. The scatterplots are presented in (figure 4-6).

Since the scatterplots are based on the Gumbel plots, the scatterplots reveal similar things as the Gumbel plots. The GR4J and HBV model simulations have similar lines when they are compared to each other. Although the simulations of the two models are similar in most cases the discharges are underestimated. An explanation for this is that the length of the observed series is limited. During this short period outliers could have occurred. This would have increased the steepness of the observation points in the Gumbel plots. For instance the highest discharge in the Lesse might be considered as an outlier since its approximately 33% larger compared to the second largest discharge.

HyMOD discharge simulations are in most cases larger underestimated compared to the discharge simulations of the GR4J and HBV model. However what the scatterplot also reveals is the overestimation of the lower annual maximum discharges by the HyMOD model. The overestimation of the lower annual maximum discharge and underestimation of the higher annual maximum discharges causes the fitted line to shift. This creates a gentle slope compared to the scatter plots of the other models. The gentle slope is an indication that the HyMOD model is unable to simulate the variability of the discharge that is required for the Meuse basin.

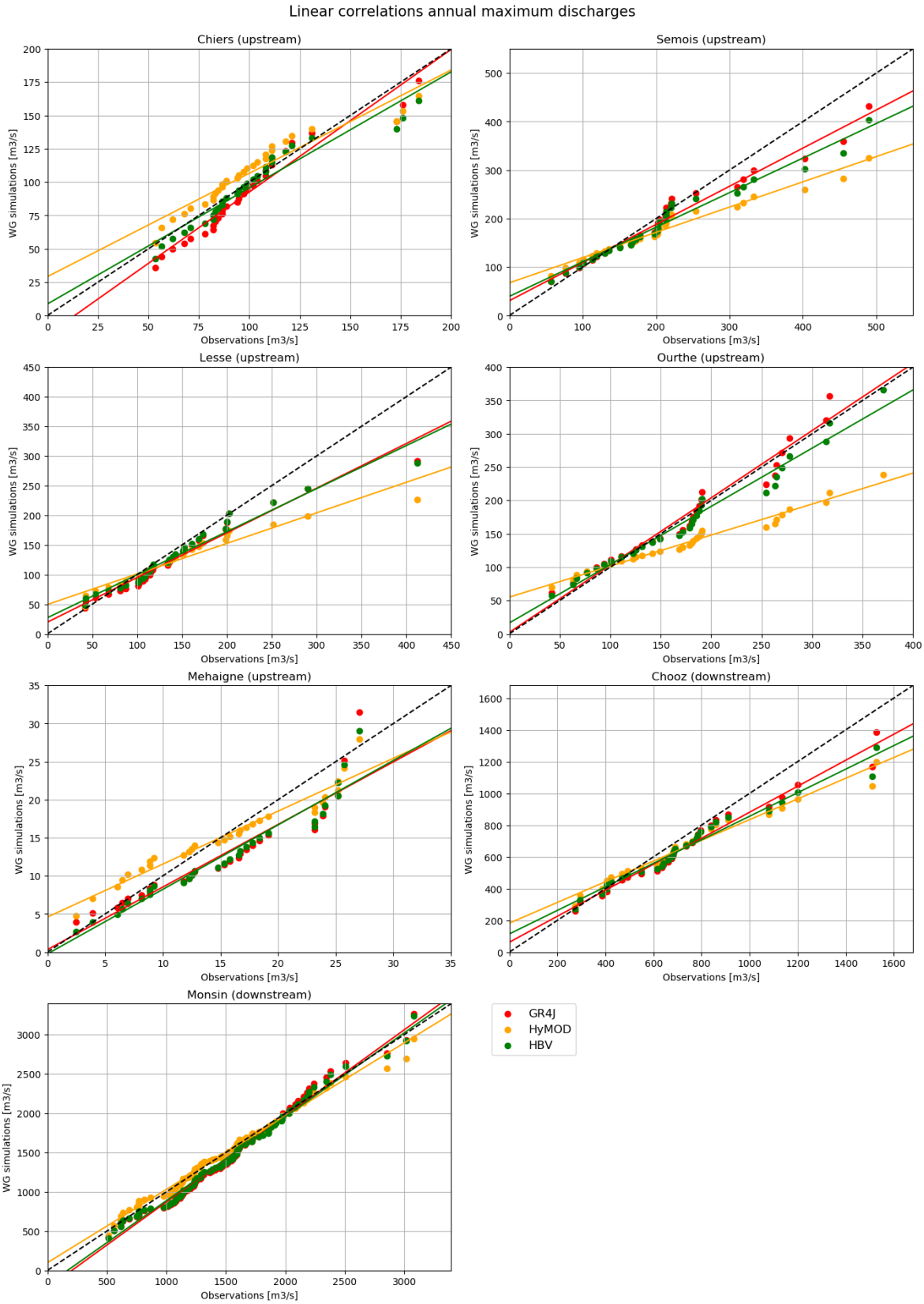

figure 4-6, Scatterplots using the observed annual maximum discharge data alongside the synthetic data annual maximum discharge simulations of the different hydrological models with similar reduced variate values.

4.3 Model structure analysis (historical)

The most important differences between the hydrological model structures are described in the method. Based on these differences, this paragraph will discuss which hydrological model structure components have the most influence on the high flow discharge simulations of the models. By analysing the influence of the model structure on the peak discharge the modeller gains a better understanding of the used hydrological models.

4.3.1 Linear storages

In Appendix C different hydrographs of five flood events are presented of multiple upstream sub-basins, figure 4-7 is presented as an example. What these hydrographs reveal is that peak discharge simulations of the HyMOD model are consistently underestimated. However the overall simulated discharge volume of the HyMOD model during that period is in most cases larger compared to the observations and other hydrological model simulations. This was also found for upstream basin calibration and validation results.

So some part of the HyMOD model structure is causing to underestimate peak discharges but also overestimates more average flows. The most likely cause is that the discharge is solely generated with the use of linear containers. Based on two model parameters a percentage of the containers water volume is transformed into discharge. This percentage does not increase with the water volume of the container. Whereas, for the GR4J and HBV model the percentage increases with the water volume of the container. Thus the HyMOD model is not capable of simulating the rapid response of the Meuse basin towards large volumes of precipitation. In an attempt to simulate the high discharge peaks and lower the RMERV value the discharge volume is overestimated and still the hydrological model fails to reach the highest discharge peaks.

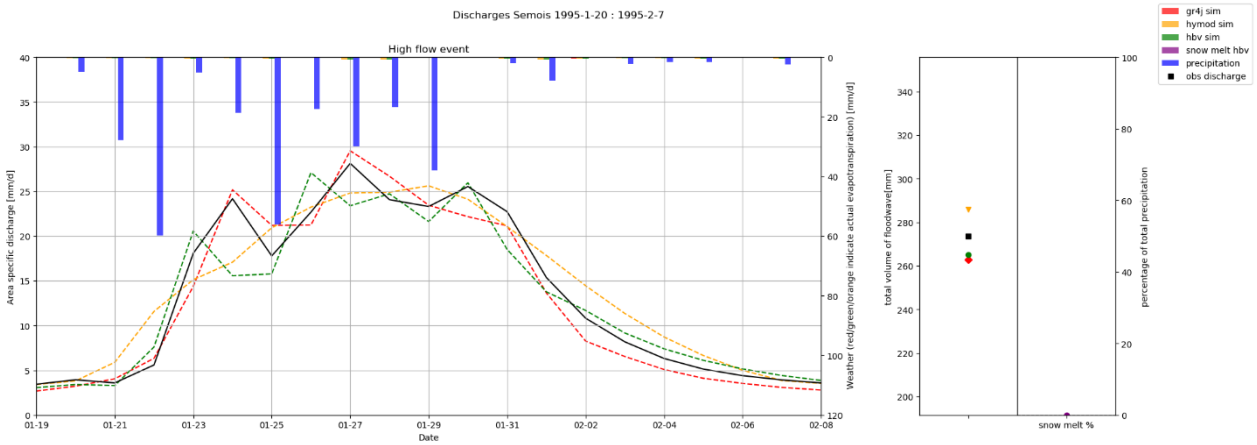

figure 4-7, Discharge flood wave for the Semois 1995, above the precipitation (all models) is presented, on the left the total volume of the discharge wave is presented. For this discharge wave actual evapotranspiration and snow melt does almost not occur.

4.3.2 Unit hydrographs

The GR4J in this study can control the discharge more precisely compared to the HBV model. With the use of unit hydrographs the time that it takes for precipitation to transition into discharge can be simulated. Since the MAXBAS parameter is not included in this version of the HBV model the reaction of the HBV model to precipitation is always one day. For a lot of sub-basins the parameter (x4) that controls the unit hydrographs in the GR4J model also uses a reaction time of one day. This occurs when x4 has a value close to two (Lesse, Ourthe. Appendix E). Indeed for most of the sub-basins the HBV and GR4J peak timing is similar for the Ourthe and Lesse. An interesting case is the Semois were the parameter value for x4 is higher than three. This implies that the reaction time of the Semois to precipitation is larger than one day. From the hydrographs it becomes apparent that the GR4J model is better at correctly timing the peak discharges in the Semois compared to the HBV model (figure 4-7, Appendix E).

4.3.3 Snow module

Another component that could have an influence on the high discharge peaks is the snow module. This module assumes whether precipitation falls as snow or rain based on the temperature. Precipitation could come down as snow and accumulates when the temperature is low enough. When the temperature increases, the combination of melt water and rain could induce large discharge peak. This large discharge peak would have been missed by hydrological models without a snow module since precipitation would always come down as rain. The precipitation would be transformed into discharge much earlier, thus resulting in a more evenly spread discharge wave. HBV contains a snow module , unlike the GR4J and HyMOD model. In order to illustrate the situation that is described above the hydrographs of the discharge wave of March 1988 Is presented for sub-basin the Ourthe (figure 4-8) (HBV does not generate discharges due to snowmodule, whereas GR4J and HyMOD simulate discharges). The hydrographs of other sub-basins in the same period have similar results.

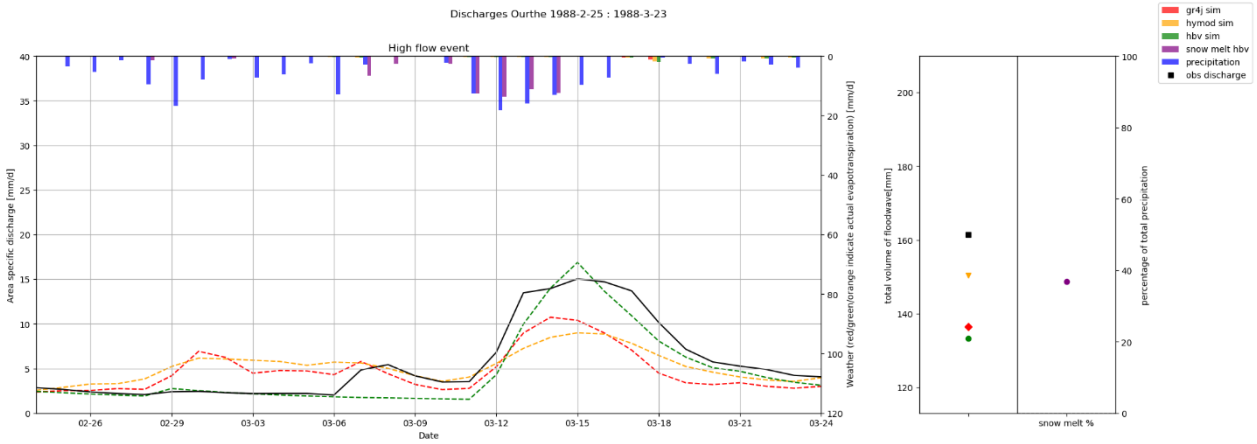

figure 4-8, Discharge flood wave with large snowmelt contribution for the Ourthe 1988, above the precipitation, and snowmelt (HBV) on the left the total volume of the discharge wave is presented alongside the precipitation percentage that contributed to the discharge wave as snow melt (HBV).

4.3.4 Upstream basin contribution

In previous chapters it was already mentioned that during the calibration process the values of the parameters that were found for downstream sub-basins might not correctly represent the hydrological behaviour of the sub-basin. Instead the values for the parameters that were found for downstream basins compensate for the lower simulations of upstream sub-basins. In order to assess this for the high flow discharge simulations the contribution to the total water volume of a discharge wave at Monsin is presented. This is done for the observations and each hydrological model for five discharge waves (same as in Appendix C), resulting in 20 different pie charts. In order to determine the percentage for each sub-basin only the discharge that contributed to the discharge wave are used. Although this might not be entirely true for the observations, it should illustrate how accurate the contributions are according to the different hydrological models figure 4-9.

From this graph it becomes clear that the HyMOD model is not capable of correctly simulating the contribution to the discharge wave. Compared to the observations the HyMOD model overestimates the upstream basin contribution. This shows that although the objective function values for the HyMOD model are decent at Monsin the model is producing decent simulations for the wrong reasons. When looking at the parameter set of the HyMOD model for the most downstream basins and the Sambre the value for parameter five implies that the sub-basins react faster to precipitation that the sub-basins in the Ardennes (Appendix E). This is unlikely since the slopes in the Ardennes are much steeper compared to the downstream sub-basins.

For most discharge waves the GR4J model and HBV model seem to approach the contribution suggested by the observed discharge waves (figure 4-9). However for the discharge wave in 1988 only the HBV model is approaching the contribution suggested by the observations. This can be explained by the snow module in the HBV model. The GR4J and HyMOD model are probably underestimating the volume of the discharge wave since a portion of the precipitation is already transitioned into discharge instead of being stored as snow. Still it is not entirely clear if the GR4J and HBV model correctly simulate the most downstream sub-basins when looking at the parameter sets. The GR4J model parameter set implies that water is leaking to other sub-basins via the groundwater. Whereas the parameter values of FC and BETA are very close to the maximum values set in the range.

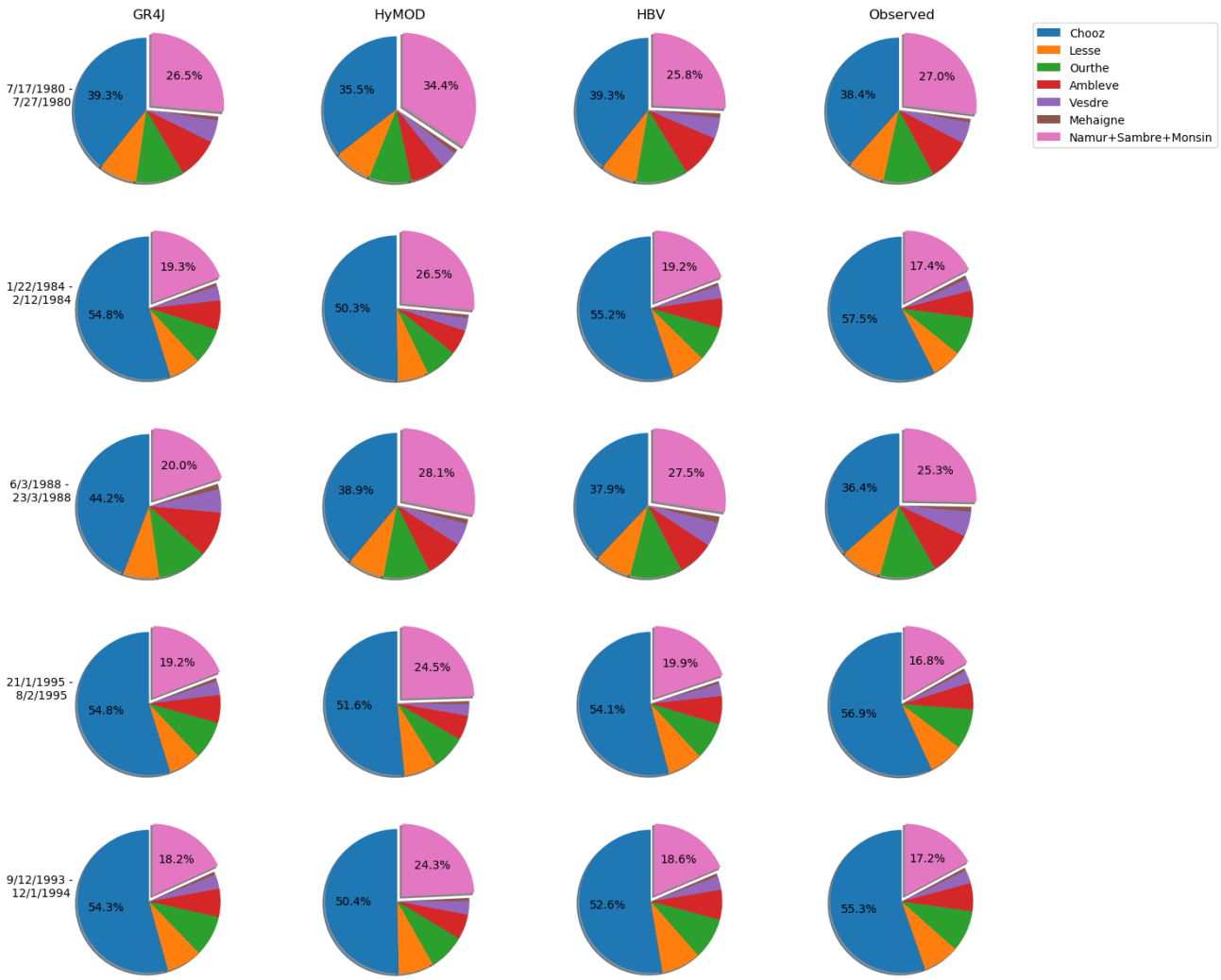

figure 4-9, sub-basin contribution to five different floodwaves according to the different hydrological models. Discharge contributions from Chooz contain the six sub-basins that are located upstream of Chooz.

5. Discussion

Potential

This study has been an attempt at assessing the hydrological model structure influence on synthetic data simulations. Exploring how different hydrological models, which are prepared using the same methods, and use the same input data, can influence annual maximum discharge simulations. It is shown that it is worth taking model structures into account when performing synthetic data simulations. The usage of another hydrological model could result in different synthetic data simulations (on a sub-basin level), which could lead to completely different conclusions.

Limitations

One of the most important limitations of this study is that there is no way of telling which hydrological model simulates the annual maximum discharges with the largest return periods more correctly. This large uncertainty about the synthetic data simulations makes it difficult to use for legislation purposes. Furthermore, the sudden similarity of the annual maximum discharge simulations at Monsin cannot be explained. There are some ideas why this happens for instance the HBV model could simulate larger discharges in the most downstream sub-basins (Chooz-Namur, Sambre, Namur-Monsin) under extreme precipitation conditions compared to the GR4J model. This is certainly possible since the parameter values suggests that when the storage that is mainly responsible for generating discharge contains a lot of water, large amount of run-off is generated by the HBV model (Large ALPHA and Kf value, Appendix E).

Aside from the uncertainty about the annual maximum discharge simulations using synthetic data, there are other uncertainties as well. Mainly because the aim of this thesis was to analyse the influence of model structures, the assessment of parameter uncertainty has been neglected. Whereas other studies focus more on parameter uncertainty assessment (Blazkova & Beven, 2002; Blazkova & Beven, 2004; Hegnauer et al., 2014) The optimization algorithm only provided a single optimal performing parameter set. Assessing the parameter uncertainty could have helped determine which hydrological processes are more important in the Meuse sub-basins according the hydrological models. Also the constant routing between the sub-basins does not correctly represents reality. The routing should be variable, however for the purpose of this thesis the constant routing is justified.

Generalisations

Although no studies have been found were multiple hydrological models use synthetic data for the simulations, the literature states that there is no reason not to do this. Blazkova & Beven (2002), suggested that other models (weather and hydrological) could generate discharges by using synthetic data that are just as “correct”. Furthermore the outcome of synthetic data simulations are extremely dependent on which hydrological model and synthetic data is used (Blazkova & Beven, 2002). Even with the large uncertainties considering the synthetic data simulations, there is no reason why the extrapolation of observed data provides results for large annual maximum discharge values that are more “correct” (Blazkova & Beven, 2004). The approach of using synthetic data and hydrological models provides a more physical basis for large discharge estimations (Hegnauer et al., 2014) , which takes basin characteristics and rainfall statistics into account (Blazkova & Beven, 2004).

Implications

When comparing the results of the of the annual maximum discharge synthetic data simulations at Monsin with the discharges found in the original study the results are very similar (Hegnauer et al., 2014, appendix A.2.3). The discharges found in the original paper are higher but this might be explained by the use of the hydrodynamic SOBEK model. This would probably increase the flow velocity during high flow discharges, resulting in larger annual maximum simulations. This study shows that with a relative simple routing method similar annual maximum discharges can be generated.

Many studies for the GRADE instrument have already been performed in perfecting the discharge simulations (Hegnauer & Verseveld, 2013; Kramer et al., 2008; Kramer & Schroevers, 2008; Leander & Buishand, 2011; Leander & Buishand, 2004; Winsemius et al., 2013). These studies have not yet included another hydrological model in their analysis. In this study the GR4J model clearly had the best performance in simulating discharges of the Mehaigne. Suggesting that components of this hydrological model are better capable of mimicking the hydrological behaviour of the Mehaigne. Instead of trying to optimize a hydrological model that is missing a certain process that is important for a sub-basin it might be worth it to consider another hydrological model for the synthetic data simulations.

The amount of uncertainty outlined in the limitations imply that it will be difficult to make a strong conclusion about the results. Even so, this research is still valuable, showing that model structure can have large influences for synthetic data simulations on a sub-basin level. This further increases the notion that it is always important to determine if the hydrological model structure is correctly representing hydrological processes in a sub-basin, especially when using synthetic data that create conditions that have not yet been observed.

6. Conclusion and Recommendations

6.1 Performance of the hydrological models

When comparing the objective functions it shows that the GR4J and HBV model have similar performances in simulating discharge for most sub-basins. These two hydrological models are generating objective function values that are approaching their optimum value for all separate objective functions. This is the case for the calibration and validation period, indicating robust performances for both hydrological models. The differences between the GR4J and HBV models are to small too conclude which of the hydrological has the best performance. While two hydrological models have good performances, the HyMOD model shows worse performances in almost all sub-basins. This is especially the case for the objective function value which represents the peak discharges (RMERV) indicating that the HyMOD model is not capable of simulating the peak discharges correctly. Although the downstream simulations generate better objective function values, floodwave contribution analysis reveal that the downstream sub-basins overestimate the discharge. Indicating that the downstream sub-basin simulation is compensating for the upstream sub-basin performance.

Conclusion:
The GR4J and HBV model show similar robust performances for the calibration and validation periods. Both the hydrological models are capable of simulating discharges that are similar to the observed discharges. Due to the small differences it is unclear which of these two hydrological models have the best performance. The HyMOD model cannot is not able to reach the required peak discharge values, resulting in a worse performance compared to the other hydrological models.

6.2 Annual maximum discharge simulations using synthetic data

The results of the statistical tests, gumbel plots, and scatter plots support each other. Showing that for higher occurrence rates the GR4J and HBV model simulate similar annual maximum discharges when using synthetic data. However when looking at most upstream sub-basin simulations the annual maximum discharge simulations of the GR4J model starts to increase faster compared to the annual maximum discharge simulations of the HBV model. This shows that the model structure selection for upstream sub-basin simulation can have an effect on the annual maximum discharge simulations with larger associated return periods. When analysing the synthetic data simulations at Monsin the GR4J and HBV simulations are over the whole range of annual maximum discharge values. Thus, something is flatting the effect in the upstream sub-basin simulation. The HyMOD is not able to reproduce the peak discharges of the Meuse basin. This effect translates to lower annual maximum discharge simulations for all sub-basins.

Conclusion:
While the synthetic data discharge simulations of the GR4J and HBV model are similar for the lower return periods (< T=10), they start to differentiate when the return period increases. This suggests that the selection of a model structure has a large influence on the most annual maximum discharge simulations with a small chance of occurrence. However, the similar simulations at Monsin indicates that the differences caused by the upstream sub-basin simulation can be reduced when the discharges of multiple sub-basins are combined.

6.3 Final conclusion

When looking at both the conclusions for the research questions some interesting aspects can be found. First of all similar performances seem to indicate similar synthetic data simulations. Furthermore higher values for the objective function responsible for peak discharge simulations (RMERV) also lead to higher synthetic annual maximum discharge simulations. However the upstream sub-basin synthetic data simulations, which are only influenced by the model structures, show that hydrological models with similar performances can diverge when the associated return periods of the discharges increase. This suggests that similar performances of hydrological models do not automatically lead to similar annual maximum discharge with a small occurrence chance. Although, there are differences for the synthetic data upstream sub-basin simulations, the results for the discharge simulations at Monsin are encouraging. Even with the combination of all the different sub-basins the GR4J and HBV still manage to simulate discharges over a 50000 year period that are very similar.

Conclusion:
Similar performance does not automatically result in similar synthetic data simulations in upstream sub-basins when considering the annual maximum discharge values associated with large return periods. Different model structures can result for similar synthetic data simulations for the whole Meuse basin. Although, the paths of the hydrological model to reach these similar results might be different.

6.4 Recommendations

Policy recommendations
The similar results of the synthetic data simulations and historical data simulations for the GR4J and HBV model near Monsin are encouraging. The contribution of sub-basins to high discharge wave simulations are very similar (except when snow is involved) and more importantly close to the observed values. This indicates that both hydrological model seem to correctly reproduce the hydrological behaviour of a sub-basin. Although it is impossible to say which of the synthetic data simulations are more “correct” the similarity of both these hydrological models seem to suggest that the GR4J and HBV simulations are in the right direction. Therefore, the synthetic data annual discharge simulations of the GR4J and HBV should be considered over the synthetic data of the HyMOD model.

Scientific recommendations
This study showed that when the model structure is almost completely isolated (single upstream sub-basin simulations) large differences in the synthetic data simulations occur for discharge associated with large return periods. Whereas this is not the case for simulated discharges that are more common (< T=10). This might indicate that the influence of the differences between hydrological model structures are more apparent for larger discharges. Further research could determine whether this is case. Aside from the annual maximum discharges, the influence of hydrological model structures on the simulation of low flow discharges using synthetic data could be investigated as well.

References

Akhtar, M., Ahmad, N., & Booij, M. J. (2009). Use of regional climate model simulations as input for hydrological models for the Hindukush-Karakorum-Himalaya region. *Hydrology and Earth System Sciences*, *13*(7), 1075–1089. https://doi.org/10.5194/hess-13-1075-2009

Apel, H., Thieken, a. H., Merz, B., & Blöschl, G. (2004). Flood risk assessment and associated uncertainty. *Natural Hazards and Earth System Science*, *4*(2), 295–308. https://doi.org/10.5194/nhess-4-295-2004

Arnaud, P., & Lavabre, J. (2002). Coupled rainfall model and discharge model for flood frequency estimation. *Water Resources Research*, *38*(6), 11. https://doi.org/10.1029/2001wr000474

Berger, H. E. J., & Mugie, A. L. (1994). *Hydrologische Systeembeschrijving Maas*.

Blazkova, S., & Beven, K. (2002). Flood frequency estimation by continuous simulation for a catchment treated as ungauged (with uncertainty). *Water Resources Research*, *38*(8), 141–1414. https://doi.org/10.1029/2001WR000500

Blazkova, S., & Beven, K. (2004). Flood frequency estimation by continuous simulation of subcatchment rainfalls and discharges with the aim of improving dam safety assessment in a large basin in the Czech Republic. *Journal of Hydrology*, *292*(1–4), 153–172. https://doi.org/10.1016/j.jhydrol.2003.12.025

Booij, M. J., & Krol, M. S. (2010). Balance between calibration objectives in a conceptual hydrological model. *Hydrological Sciences Journal*, *55*(6), 1017–1032. https://doi.org/10.1080/02626667.2010.505892

Brauer, C. C., Teuling, A. J., F. Torfs, P. J. J., & Uijlenhoet, R. (2014). The Wageningen Lowland Runoff Simulator (WALRUS): A lumped rainfall-runoff model for catchments with shallow groundwater. *Geoscientific Model Development*, *7*(5), 2313–2332. https://doi.org/10.5194/gmd-7-2313-2014

Davis, J. C. (2002). *Statistics and Data Analysis in Geology* (Third). New York: John Wiley & Sons.

de Boer-Euser, T., Bouaziz, L., De Niel, J., Brauer, C., Dewals, B., Drogue, G., … Willems, P. (2016). Looking beyond general metrics for model evaluation : lessons from an international model intercomparison study. *Egu 2016*, (April), 2–3. https://doi.org/10.5194/hess-2016-339

de Wit, M. J. M., Peeters, H. A., Gastaud, P. H., Dewil, P., Maeghe, K., & Baumgart, J. (2007). Floods in the Meuse basin: Event descriptions and an international view on ongoing measures. *International Journal of River Basin Management*, *5*(4), 279–292. https://doi.org/10.1080/15715124.2007.9635327

Duan, Q., Schaake, J., Andréassian, V., Franks, S., Goteti, G., Gupta, H. V., … Wood, E. F. (2006). Model Parameter Estimation Experiment (MOPEX): An overview of science strategy and major results from the second and third workshops. *Journal of Hydrology*, *320*(1–2), 3–17. https://doi.org/10.1016/j.jhydrol.2005.07.031

Duan, Q., Sorooshian, S., & Gupta, V. (1992). Effective and Efficient Global Optimization for Conceptual Rainfall-Runoff Models, *28*(4), 1015–1031.

Duan, Q., Sorooshian, S., & Gupta, V. K. (1994). Optimal use of the SCE-UA global optimization method for calibrating watershed models. *Journal of Hydrology*, *158*(3–4), 265–284. https://doi.org/10.1016/0022-1694(94)90057-4

Equipe Hydrologie Irstea Antony. (2017). GR4J model source. Retrieved August 10, 2017, from https://webgr.irstea.fr/en/modeles/journalier-gr4j-2/

Falter, D., Schröter, K., Dung, N. V., Vorogushyn, S., Kreibich, H., Hundecha, Y., … Merz, B. (2015). Spatially coherent flood risk assessment based on long-term continuous simulation with a coupled model chain. *Journal of Hydrology*, *524*, 182–193. https://doi.org/10.1016/j.jhydrol.2015.02.021

Harlin, J., & Liden, R. (2000). Analysis of conceptual rainfall ± runoff modelling performance in different climates, *238*, 231–247.

Hegnauer, M., Beersma, J. J., van den Boogaard, H. F. P., Buishand, T. A., & Passchier, R. H. (2014). Generator of Rainfall and Discharge Extremes (GRADE) for the Rhine and Meuse basins. Final report of GRADE 2.0, 84.

Hegnauer, M., & Verseveld, W. van. (2013). *Generalised Likelihood Uncertainty Estimation for the daily HBV model in the Rhine Basin, Part B: Switzerland*. Delft, Netherlands.

Herman, J. D., Reed, P. M., & Wagener, T. (2013). Time-varying sensitivity analysis clarifies the effects of watershed model formulation on model behavior. *Water Resources Research*, *49*(3), 1400–1414. https://doi.org/10.1002/wrcr.20124

Houska, T., Kraft, P., Chamorro-Chavez, A., & Breuer, L. (2015). SPOTting model parameters using a ready-made python package. *PLoS ONE*, *10*(12), 1–22. https://doi.org/10.1371/journal.pone.0145180

Kramer, N., Beckers, J., & Weerts, A. (2008). *Generator of Rainfall and Discharge Extremes (GRADE) Part D & E*. Delft, Netherlands.

Kramer, N., & Schroevers, R. (2008). *Generator of Rainfall and Discharge Extremes (GRADE): Part F*. Delft, Netherlands.

Kuchment, L. S., & Gelfan, A. N. (2011). Assessment of extreme flood characteristics based on a dynamic-stochastic model of runoff generation and the probable maximum discharge. *Journal of Flood Risk Management*, *4*(2), 115–127. https://doi.org/10.1111/j.1753-318X.2011.01096.x

Kundzewicz, Z. W., Kanae, S., Seneviratne, S. I., Handmer, J., Nicholls, N., Peduzzi, P., … Sherstyukov, B. (2014). Flood risk and climate change: global and regional perspectives. *Hydrological Sciences Journal*, *59*(1), 1–28. https://doi.org/10.1080/02626667.2013.857411

Leander, R., Buishand, A., Aalders, P., & Wit, M. De. (2005). Estimation of extreme floods of the River Meuse using a stochastic weather generator and a rainfall-runoff model. *Hydrological Sciences Journal*, *50*(6), 37–41. https://doi.org/10.1623/hysj.2005.50.6.1089

Leander, R., & Buishand, T. a. (2011). *Rainfall Generator for the Meuse Basin: Extension of the base period with the years 1999-2008*. De Bilt, Netherlands.

Leander, R., & Buishand, T. A. (2004). *Rainfall generator for the Meuse Basin, Development of a multi-site extension of the entire drainage area*. De Bilt, Netherlands.

Lindström, G., Johansson, B., Persson, M., Gardelin, M., & Bergström, S. (1997). Development and test of the distributed HBV-96 hydrological model. *Journal of Hydrology*, *201*(1–4), 272–288. https://doi.org/10.1016/S0022-1694(97)00041-3

Madsen, H. (2000). Automatic calibration of a conceptual rainfall–runoff model using multiple objectives. *Journal of Hydrology*, *235*(3), 276–288. https://doi.org/10.1016/S0022-1694(00)00279-1

Pechlivanidis, I. G., Jackson, B. M., Mcintyre, N. R., & Wheater, H. S. (2011). Catchment Scale Hydrological Modelling: A Review Of Model Types, Calibration Approaches And Uncertainty Analysis Methods In The Context Of Recent Developments In Technology And Applications. *Global NEST Journal*, *13*(3), 193–214.

Perrin, C., Michel, C., & Andréassian, V. (2003). Improvement of a parsimonious model for streamflow simulation. *Journal of Hydrology*, *279*(1–4), 275–289. https://doi.org/10.1016/S0022-1694(03)00225-7

Tian, Y., Booij, M. J., & Xu, Y. P. (2014). Uncertainty in high and low flows due to model structure and parameter errors. *Stochastic Environmental Research and Risk Assessment*, *28*(2), 319–332. https://doi.org/10.1007/s00477-013-0751-9

Verkade, J. S., Brown, J. D., Davids, F., Reggiani, P., & Weerts, A. H. (2017). Estimating predictive hydrological uncertainty by dressing deterministic and ensemble forecasts; a comparison, with application to Meuse and Rhine. *Journal of Hydrology*, *555*(October), 257–277. https://doi.org/10.1016/j.jhydrol.2017.10.024

Vrugt, J. A., Bouten, W., Gupta, H. V., & Sorooshian, S. (2002). Toward improved identifiability of

hydrologic model parameters: The information content of experimental data. *Water Resources Research*, *38*(12), 48-1-48–13. https://doi.org/10.1029/2001WR001118

Wagener, T., Boyle, D. P., Lees, M. J., Wheater, H. S., Gupta, H. V., & Sorooshian, S. (2001). A framework for development and application of hydrological models. *Hydrology and Earth System Sciences*, *5*(1), 13–26. https://doi.org/10.5194/hess-5-13-2001

Weerts, A. H., & van der Klis, H. (2006). *Reliability of the Generator of Rainfall and Discharge Extremes (GRADE)*. Delft, Netherlands. https://doi.org/Q4268

Winsemius, H. C. M., Verseveld, W. van, Weerts, A. H., & Hegnauer, M. (2013). *Generalised Likelihood Uncertainty Estimation for the daily HBV model in the Rhine Basin, Part A: Germany*. Delft, Netherlands.

Appendix A. The GRADE instrument

A.1 Stochastic weather generator

The weather generator in the GRADE instrument is generating daily weather for separate sub-basins of the Meuse. These generated daily weather series contain daily precipitation, daily temperature and daily potential evapotranspiration. This is done over a very long time period (50.000 years) (Hegnauer et al., 2014). The generated weather is based on historical precipitation and temperature series. The daily rainfall and temperature measurements are resampled using a nonparametric resampling technique. This creates different temporal patterns compared to the observed historical data (figure A-1). Since these different temporal patterns are simulated over a very long period, new extreme weather events are the result of this resampling (Hegnauer et al., 2014).

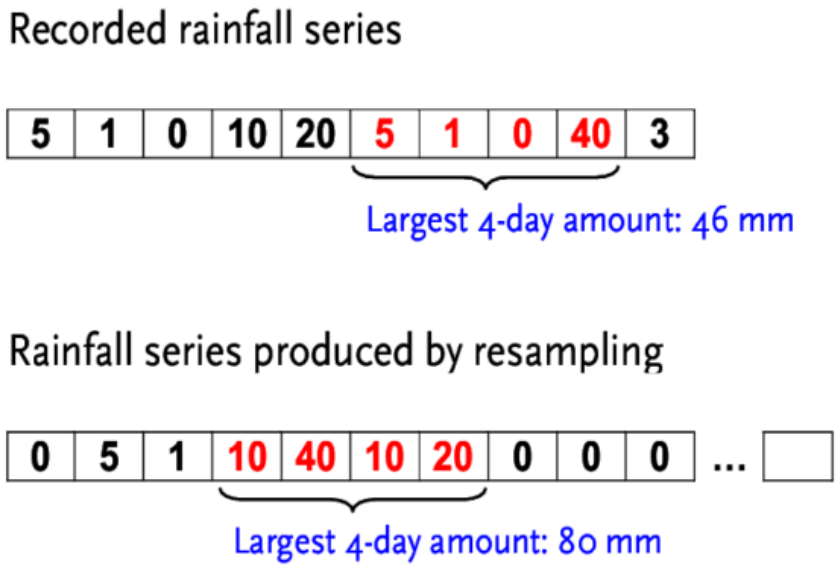

figure A-1, Resampling of the historical recorded rainfall series results in a different "largest 4 day amount" (Hegnauer et al., 2014).

A.1.1 Generating Potential evapotranspiration

Temperature and precipitation are generated directly with the resampling of historical temperature and precipitation series. This is not the case for the potential evapotranspiration, which is derived based on the resampled temperature and the averages of the observed potential evapotranspiration

The daily potential evapotranspiration for the weather generator is determined using the following equation (equation A-1).

equation A-1

$$PET_{wg} = \left(1 + etf \cdot (T_{re} - \bar{T})\right) \cdot \overline{PET}_m$$

Where PET_{wg} (mm·day^{-1}) the weather generator daily potential evapotranspiration, T_{re} (°C) is the daily temperature that was a result of the resampling, $\overline{T}$ (°C) observed long-term monthly average temperature, etf is the proportionality constant and $\overline{PET}_m$ (mm·day^{-1}) is the long-term monthly potential evapotranspiration. The value for etf varies from an average of 0.08 (°C)$^{-1}$ in winter and 0.13 (°C)$^{-1}$ in summer (Hegnauer et al., 2014).

A.2.1 Resampling process

Data sets

The resampling process uses two data sets. The first dataset is consists only of a few precipitation/temperature stations but is available for a longer time period and is used for the driving of the weather generator (step 3 and 4). The driving can be explained as the process of selecting a random day from which the data will be used. The second available dataset is for a shorter period but consists of more precipitation/temperature stations and also potential evapotranspiration stations, which results in a dataset with more spatial differential data. Therefore daily weather values are drafted from this dataset for each Meuse sub-basin (step 5) based on the day that was randomly selected in step 3 and 4. The details of these datasets will be described later in this chapter.

Feature vector

Each historical day from the long period observed weather series can be described using a feature vector. The feature vector consists of three different components:

1. The average daily value of the standardized temperature based on the only two temperature stations of the long period dataset, which is denoted by $\tilde{T}_t$.
2. The average daily value of the standardized precipitation based on seven precipitation stations, which is denoted by $\tilde{P}_t$.
3. The average of standardized rainfall of the four preceding days, i.e. ¼($\tilde{P}_{t-1} + \tilde{P}_{t-2} + \tilde{P}_{t-3} + \tilde{P}_{t-4}$), denoted by $\tilde{P}_{t-4\ avg}$.

This last component was added in order to improve the reproduction of the autocorrelation of daily rainfall and the standard deviation of monthly totals (Leander et al., 2005). The feature vector is used in the resampling process to find the nearest neighbours.

Resampling steps

This paragraph states the resampling steps in order to generate daily weather. These steps are based on the description given by Leander et al., (2005) with the extended datasets described in (Leander & Buishand, 2011). The resampling steps are schematized in the

1. Randomly select a historical day within the moving window centred on 1 January as the first simulated day.
2. Compose a feature vector consisting of the three following components: $\tilde{T}_t$, $\tilde{P}_t$ and the $\tilde{P}_{t-4\ avg}$
3. Find the k nearest neighbours of the latest sampled day within a window centred on the selected day (The number of nearest neighbours is denoted by k, the window is expressed in a number of days denoted by W)
4. Randomly select one of these nearest neighbours, using the decreasing (equation A-2). Denote the date of the selected nearest neighbour by $[i]$ and that of its historical successor by $[i+1]$.

5. For each of the simulated variables (areal rainfall or station temperature), check whether data for this variable exist for day $[i+1]$ in the short time period data set.

– If so, add the standardized historical data to the generated sequence for this variable.
– If not, use the feature vector of the standardized station data for day $i+1$, find the nearest neighbour of day $[i+1]$ among the days for which the data for the considered variable do exist and add the standardized data of this nearest neighbour to the generated sequence. The search is restricted to a W -day window centred on day $[i+1]$.

6. Repeat steps 2–5 for each simulated day.
7. Transform the resampled standardized variables back to their original scale.

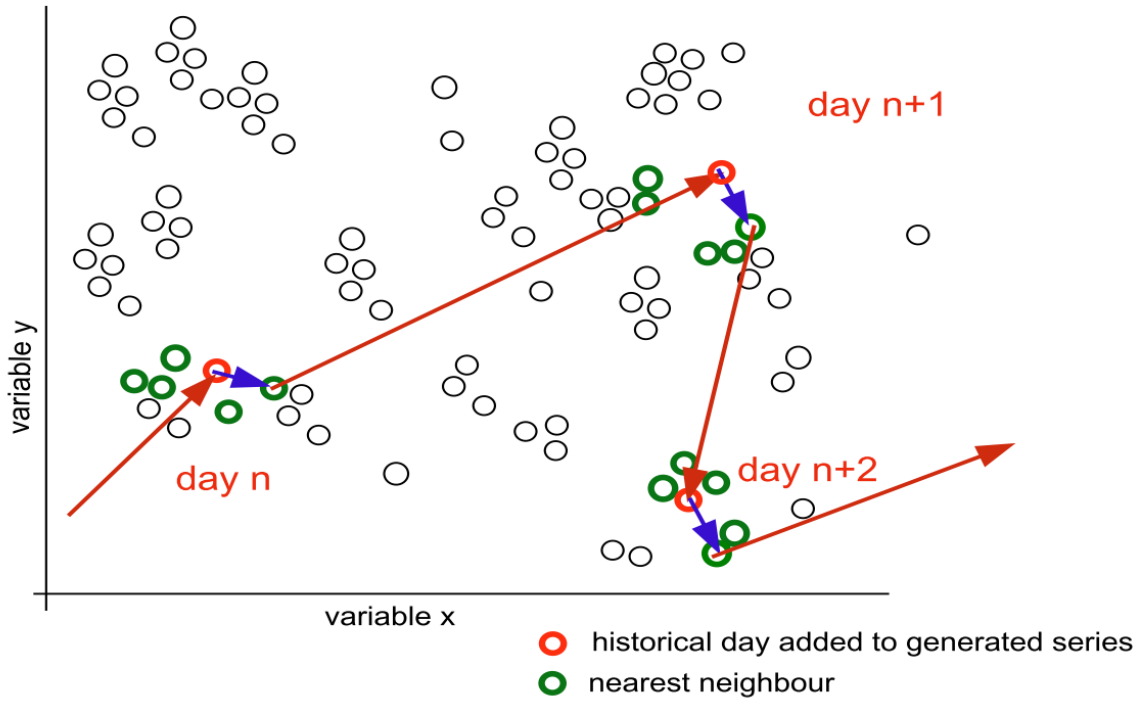

Figure A-2, Schematization of the resampling process (Leander & Buishand, 2004) *(One of the nearest neighbours (green, k=5) of the last sampled days (red) is randomly selected (blue arrow), with the use of a decreasing kernel* ***Fout! Verwijzingsbron niet gevonden.****)The next historical day (red arrow) provides the values for the new resampled day.*

equation A-2

$$p_j = \frac{\frac{1}{j}}{\sum_{i=1}^{k} \frac{1}{i}}$$

equation A-2 represents the decreasing kernel, where p_j is the selection chance, j gives the neighbour rank, i presents the selected day and k the number of neighbours. The decreasing kernel function gives a weight to closer neighbours increasing the likelihood of selecting the closer neighbours during the resampling process. Large values of k for number of nearest neighbours usually results in reproduction of autocorrelation coefficients that are worse compared to lower values of k. While small values of k could result in repetitive sampling of the same historical days. In order to preserve autocorrelation and prevent repetitive sampling the number for k was set to 10 (Hegnauer et al., 2014). A window which is centred on day i was incorporated in order to constraint the number of days that can be used for the nearest neighbour technique. This ensures that a summer day is never preceded or succeeded by a winter day (Leander & Buishand, 2004). The value for W was set to 121 days in order to prevent repetition of the same historical days during extreme multi-day weather events.

A.2 GRADE instrument discharge simulations at Borgharen

A.1.2 HBV and SOBEK model implementations

Discharges of the entire Meuse basin are generated using 15 smaller sub-basins. Daily precipitation, daily temperature and daily potential evapotranspiration for all of these sub-basins are used as input for the HBV model (Hegnauer et al., 2014) in order to simulate discharges for each sub-basin. Which is an semi-distributed hydrological model described in Lindström et al (1997). The sub-basins are located upstream of Borgharen and cover an area of approximately 21000 km^2. In order to calibrate the HBV model a GLUE analysis is applied. This calibration method also serves as an uncertainty analysis of the HBV model parameters.

A flood routing component is also included in the HBV model, however in order to incorporate the effect of upstream flooding a hydrodynamic model is required. The flood routing is performed with a hydrodynamic Sobek model. The hydrodynamic model starts at Chooz (France) and ends at Keizersveer (The Netherlands). Although the hydrodynamic model is incorporated simulations including upstream flooding have not yet been performed for the Meuse (Hegnauer et al., 2014)

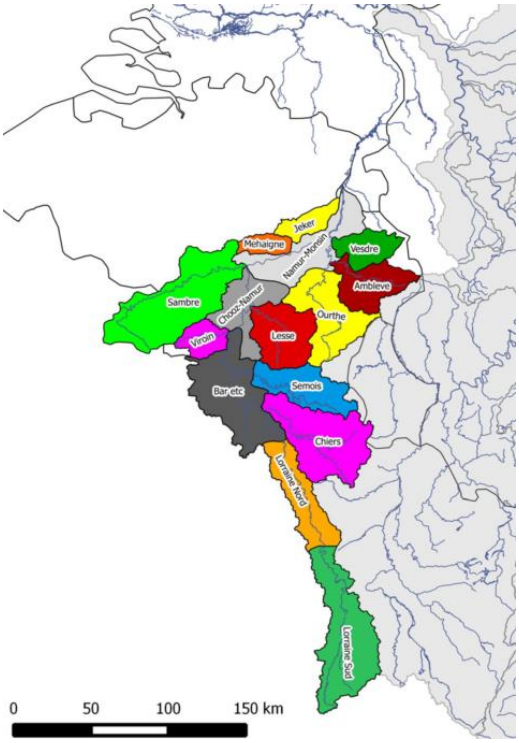

Figure A-3, Layout of the sub-basins of the Meuse HBV model
(Hegnauer et al., 2014)

A.3 GRADE instrument results

A.1.3 HBV model performance

As a result of the GLUE analysis calibration, multiple sets containing different parameter values are accepted. In order to reduce the calculation time, 500 parameter sets have been selected to perform simulations using the weather generator. After these simulations the yearly maximum discharge was found with a return period of 100 years was found for each simulation. From the yearly maximum discharge distribution five values are selected. Each of these represent different percentiles of the distribution. These are the mean 50%, the quadrants (25% and 75%), upper and lower (95% and 5%) boundaries. The five parameter sets that correspond to the percentiles are selected for the performance assessment. Each parameter set is used in the HBV model to simulate nine discharge events. In order to measure the performance the Nash-Sutcliffe (NS) efficiency is used The parameter sets are compared to the parameter sets that are used by Van Deursen who calibrated the HBV model for the entire Meuse basin without the focus on the high flow discharges. The results of the simulations are presented in table A-1. A value close to one indicate that the parameter set is performing well according to the NS efficiency.

table A-1, Nash-Sutcliffe (NS) efficiencies for the HBV simulations at Borgharen for 9 discharge events between 1993 and 2004.(Kramer & Schroevers, 2008) The bold numbers indicate the highest value for a high flow event

Start event End event	16-12-93 26-12-93	25-1-95 04-02-95	20-10-98 26-10-98	1-12-99 15-01-00	15-12-00 15-04-01	22-1-02 30-03-02	15-12-02 29-01-03	15-12-02 29-01-03	5-1-04 31-01-04	mean
Van Deursen	0.84	0.78	0.89	0.76	0.83	0.84	0.71	0.86	0.76	0.81
GRADE 5%	0.71	0.78	0.78	0.86	**0.89**	**0.91**	0.81	**0.97**	0.92	**0.85**
GRADE 25%	0.68	0.69	0.70	**0.89**	0.88	0.87	0.86	**0.97**	0.92	0.83
GRADE 50%	0.58	**0.83**	**0.91**	0.86	0.84	0.85	0.89	**0.97**	0.92	**0.85**
GRADE 75%	**0.95**	0.60	0.75	0.88	0.86	0.88	0.79	**0.97**	**0.94**	**0.85**
GRADE 95%	0.86	0.64	0.76	0.87	0.80	0.82	**0.90**	0.96	0.93	0.84

A.2.3 Final GRADE result

Frequency discharge curves are based on the long time series of daily discharges simulated by the HBV model in the GRADE instrument. In Hegnauer et al., (2014) the HBV model generates daily discharges for a period of 50000 years using the parameter set that is associated with the mean (50%) simulations. A 95% confidence band is constructed by performing additional simulations uncertainty simulations. The uncertainty of the weather generator is incorporated in the confidence band by generating multiple different 20000 year weather generator datasets that are using 69 year of daily weather data instead of 72 years. The historical daily weather dataset that is used by the weather generator shifts every 3 non overlapping years, which results in a total of 24 different 20000 year daily weather datasets. Each parameter set that represents different percentiles found in the previous paragraph (5%, 25%, 50%, 75%, 95%) uses the 24 weather generator datasets in order to simulate daily discharges. Thus the total amount of uncertainty simulations that are performed are 24x5 simulations (Hegnauer et al., 2014).

The frequency discharge curve with the confidence band is presented in figure A-4. By determining the standard deviations of the discharge that is associated with a return period using the uncertainty simulations the confidence band is constructed. The following equation is used in the process.

equation A-3

$$Q_T \pm z_y \cdot s = \text{upper / lower bound}$$

Where: Q_T is the discharge from the 50000 year reference simulation that is associated with return period T, z_y is 1.96 in the case of a 95% confidence interval, and s is the standard deviation. figure A-4 shows a shift in slope between the 100 and 500 year return period. Due to the shift in slope the design discharge with a return period between 4000 and 10000 years become lower compared to the design discharge of the HR2006 method with the same return period. Upstream flooding is not yet incorporated in the long time series simulations. Including upstream flooding will probably lower the most extreme discharges. Weissman devised a method to reduce the effect of random fluctuations in the upper tail of the distribution. This method makes use of the joint limiting distribution of these order statistics. The Weissman fit is also used to extrapolate to return periods of 100,000 years (Hegnauer et al., 2014).

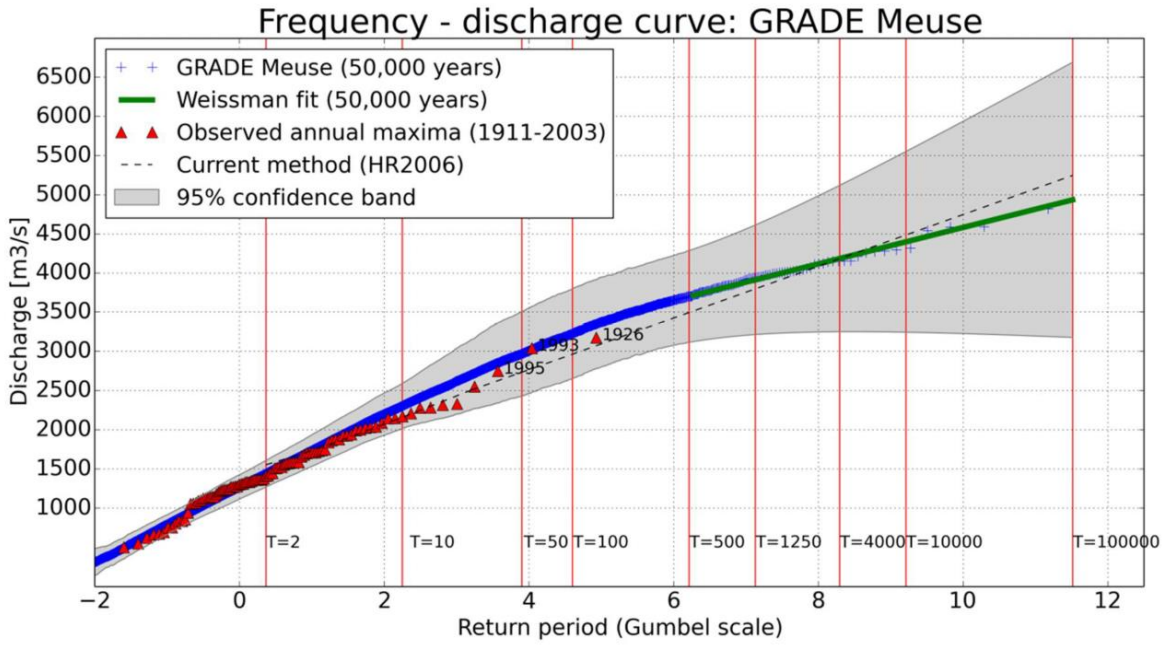

figure A-4, Frequency discharge curve for the river Meuse at Borgharen, together with the sorted observed annual maxima and the 95% confidence band

Appendix B.

The shorter more detailed daily weather series per sub-basin are consisting of precipitation: 1961-2007, temperature: 1968-2008 and potential evapotranspiration 1961-2007 (Not entirely clear but the potential evapotranspiration shares the source with the Belgian precipitation source). This dataset is resampled to create synthetic weather. A smaller part of this weather data set was actually available for this study (1967-1998)

B.1 Weather data

Driving data

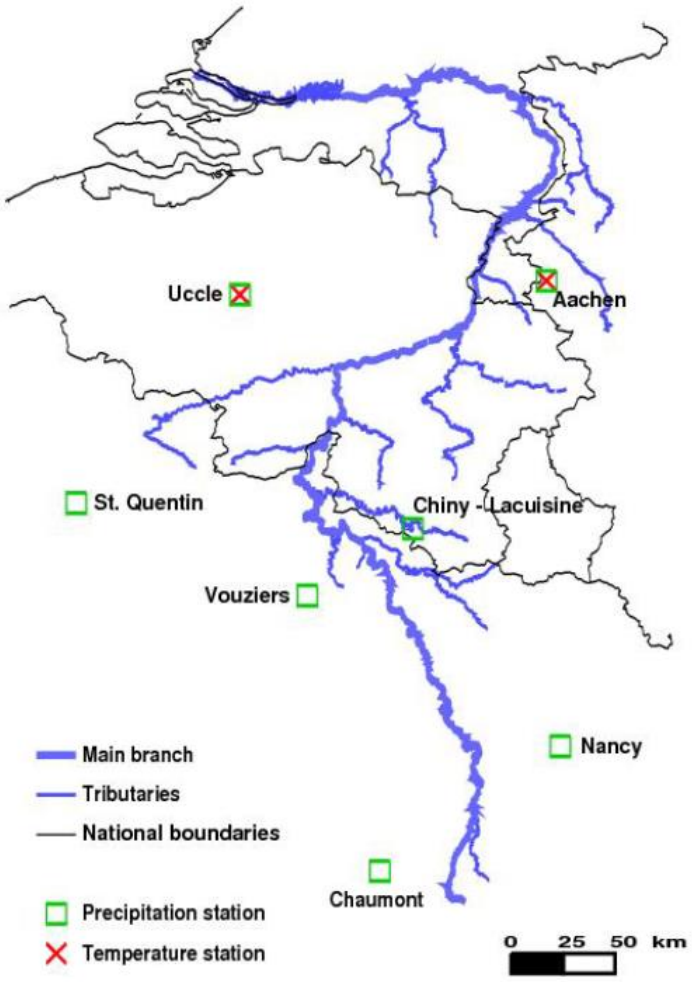

Figure B-1, Location of the observation stations for the long weather dataseries for the period 1930 – 2008 (except 1940-1945)

Long daily weather series

table B-1, Sources of the daily area-averaged precipitation for the period 1961 – 2007 per sub-basin. Interpolated station data is used for the French part. For the Belgian part the name of the (sometimes) smaller sub-basins with their associated observation location are mentioned

Sub-basin	Source of daily area-average precipitation
1. Lorraine Sud	Interpolated station data
2. Chiers	Interpolated station data (French part), and Ton (Harnoncourt)
3. Lorraine Nord	Interpolated station data
4. Stenay-Chooz	Interpolated station data
5. Semois	Semois (Membre)
6. Viroin	Viroin (Vierves)
7. Chooz-Namur	Meuse (Namur, ex. Sambre), excluding Lesse (Gendron), Viroin (Vierves), Semois (Membre) and Ton (Harnoncourt)
8. Lesse	Lesse (Gendron)
9. Sambre	Interpolated station data (French part), and Sambre (Namur Belgian part)
10. Ourthe	Ourthe (Hamoir,Tabreux)
11. Ambleve	Ambleve (Martinrive)
12. Vesdre	Vesdre (Chaudfontaine)
13. Mehaigne	Mehaigne (Moha)
14. Namur-Monsin	Meuse (Namur-Huy), Meuse (Huy-Liège), Berwinne (Dalhem) and Hoyoux (Marchin)
15. Jeker	Jeker (Kanne)

table B-2, Derivation of the area-averaged temperature for the period (1967-2008), The data of each sub-basins is corrected for the height before the data of the four sub-basin is averaged

Sub-basin	area-average temperature based on the following stations:
1. Lorrainde sud	Lacuisine, Langres, Loxeville, Reims
2. Chiers	Lacuisine, Loxeville, Reims, St Hubert
3. Lorraine Nord	Forges, Lacuisine, Loxeville, Reims
4. Stenay-Chooz	Dourbes, Forges, Lacuisine, St Hubert
5. Semois	Dourbes, Forges, Lacuisine, St Hubert
6. Viroin	Chimay, Dourbes, Forges, St Hubert
7. Chooz - Namur	Chimay, Dourbes, Ernage, Forges
8. Lesse	Dourbes, Forges, Lacuisine, St Hubert
9. Sambre	Chimay, Dourbes, Ernage, Forges
10. Ourthe	Dourbes, Forges, Lacuisine, St Hubert
11. Ambleve	Aachen, Ernage, Lacuisine, St Hubert
12. Vesdre	Aachen, Beek, Dourbes, Ernage
13. Mehaigne	Aachen, Beek, Dourbes, Ernage
14. Namur - Monsin	Aachen, Beek, Dourbes, Ernage
15. Jeker	Aachen, Beek, Dourbes, Ernage

table B–3, Sources of the daily area-averaged potential evapotranspiration for the period 1961 – 2007 per sub-basin.

Sub-basin	Source of daily area-average potential evapotranspiration
1. Lorraine Sud	Averaged potential evapotranspiration from all Belgian sub-basins
2. Chiers	Averaged potential evapotranspiration from all Belgian sub-basins
3. Lorraine Nord	Averaged potential evapotranspiration from all Belgian sub-basins
4. Stenay-Chooz	Averaged potential evapotranspiration from all Belgian sub-basins
5. Semois	Semois (Membre)
6. Viroin	Viroin (Vierves)
7. Chooz-Namur[1]	Meuse (Namur, ex. Sambre), excluding Lesse (Gendron), Viroin (Vierves), Semois (Membre) and Ton (Harnoncourt)
8. Lesse	Lesse (Gendron)
9. Sambre	Interpolated station data (French part), and Sambre (Namur Belgian part)
10. Ourthe	Ourthe (Hamoir,Tabreux)
11. Ambleve[2]	Ambleve (Martinrive)
12. Vesdre[3]	Vesdre (Chaudfontaine)
13. Mehaigne	Mehaigne (Moha)
14. Namur-Monsin[4]	Meuse (Namur-Huy), Meuse (Huy-Liège), Berwinne (Dalhem) and Hoyoux (Marchin)
15. Jeker	Jeker (Kanne)
1	*31-12-1988 onward coupled to sub-basin 6 with a transformation factor of 0.997 based on annual averages from 1968-1986*
2	*31-12-1987 till 01-01-1990 Coupled to sub-basin 10 with a transformation factor of 1,107 based on annual averages from 1968-1986*
3	*31-12-1987 till 01-01-1990 Coupled to sub-basin 10 with a transformation factor of 1,136 based on annual averages from 1968-1986*
4	*31-12-1987 till 01-01-1990 Coupled to sub-basin 9 with a transformation factor of 0.969 based on annual averages from 1968-1986*

B.2 Discharge

table B–4, Location, period and source of the observed discharges (1, http://www.hydro.eaufrance.fr/. 2, http://voies-hydrauliques.wallonie.be/opencms/opencms/fr/hydro/annuaires/index.html. 3, Direct source is not stated. 4, discharge data from 1969 – 1973 is based on Weerts & van der Klis, 2006.

sub-basin	river	discharge observation location	discharge period	Sources
1 Lorraine sud	Meuse	St-Mihiel	1968-1998	Banque Hydro[1]
2 Chiers	Chiers	Carigan	1968-1998	Banque Hydro[1]
3 Lorraine Nord	Meuse	Stenay	1968-1998	Banque Hydro[1]
4 Stenay-Chooz	Meuse	Chooz	1968-1998	Weerts & van der Klis, 2006[3]
5 Semois	Semois	Membre	1968-1998	Région Wallonne[2]
6 Viroin	Viroin	Treignes	1974-1998	Région Wallonne[2]
7 Chooz-Namur	Meuse	Monsin	-	
8 Lesse	Lesse	Gendron	1968-1998	Weerts & van der Klis, 2006[3]
9 Sambre	Flor./Salz.	Monsin	-	
10 Ourthe	Ourthe	Tabreux	1968-1998	Weerts & van der Klis, 2006[3]
11 Ambleve	Ambleve	Martinrive	1968-1998	Weerts & van der Klis, 2006[3]
12 Vesdre	Vesdre	Chaudfontaine	1968-1998	Weerts & van der Klis, 2006[3]
13 Mehaigne[4]	Mehaigne	Moha	1968-1998	Weerts & van der Klis, 2006[3] + Région Wallonne[2]
14 Namur-Monsin	Meuse	Sint Pieter + Kanne	1911 - 2015	Rijkswaterstaat

B.3 Calibration data

table B-3, Calibration data, Weather data includes precipitation, potential evapotranspiration and temperature. (Year 1967 – 1968 is used as a run up year)

Sub-basin	Daily Weather	Daily Observed Discharge
1. Lorraine Sud	01-01-1967 , 01-01-1983	01-01-1969 , 01-01-1983
2. Chiers	01-01-1967 , 01-01-1983	01-01-1968 , 01-01-1983
3. Lorraine Nord	01-01-1967 , 01-01-1983	01-01-1968 , 01-01-1983
4. Stenay-Chooz	01-01-1967 , 01-01-1983	01-01-1968 , 01-01-1983
5. Semois	01-01-1967 , 01-01-1983	01-01-1968 , 01-01-1983
6. Viroin	01-01-1967 , 01-01-1983	01-01-1974 , 01-01-1983
7. Chooz - Namur	01-01-1967 , 01-01-1983	-
8. Lesse	01-01-1967 , 01-01-1983	01-01-1968 , 01-01-1983
9. Sambre	01-01-1967 , 01-01-1983	-
10. Ourthe	01-01-1967 , 01-01-1983	01-01-1968 , 01-01-1983
11. Ambleve	01-01-1967 , 01-01-1983	01-01-1968 , 01-01-1983
12. Vesdre	01-01-1967 , 01-01-1983	01-01-1968 , 01-01-1983
13. Mehaigne	01-01-1967 , 01-01-1983	01-01-1969 , 01-01-1983
14. Namur - Monsin	01-01-1967 , 01-01-1983	01-01-1968 , 01-01-1983

B.4 Validation data

table B-4, Validation data, Weather data includes precipitation, potential evapotranspiration and temperature. (Year 1982 – 1983 is used as a run up year)

Sub-basin	Daily Weather	Daily Observed Discharge
1. Lorraine Sud	01-01-1982 , 01-01-1998	01-01-1983 , 01-01-1998
2. Chiers	01-01-1982 , 01-01-1998	01-01-1985 , 01-01-1998
3. Lorraine Nord	01-01-1982 , 01-01-1998	01-01-1983 , 01-01-1998
4. Stenay-Chooz	01-01-1982 , 01-01-1998	01-01-1983 , 01-01-1998
5. Semois	01-01-1982 , 01-01-1998	01-01-1983 , 01-01-1998
6. Viroin	01-01-1982 , 01-01-1998	01-01-1983 , 01-01-1998
7. Chooz - Namur	01-01-1982 , 01-01-1998	-
8. Lesse	01-01-1982 , 01-01-1998	01-01-1983 , 01-01-1998
9. Sambre	01-01-1982 , 01-01-1998	-
10. Ourthe	01-01-1982 , 01-01-1998	01-01-1983 , 01-01-1998
11. Ambleve	01-01-1982 , 01-01-1998	01-01-1983 , 01-01-1998
12. Vesdre	01-01-1982 , 01-01-1998	01-01-1983 , 01-01-1998
13. Mehaigne	01-01-1982 , 01-01-1998	01-01-1983 , 01-01-1998
14. Namur - Monsin	01-01-1982 , 01-01-1998	01-01-1983 , 01-01-1998

Appendix C. Floodwave hydrographs

In appendix C hydrographs are given for five different sub-basins during five flood waves. The 1980 floodwave occurred in the summer, whereas the 1988 hydrograph shows large snow melt contribution to the discharge waves. Each figure contains the observed discharges and the simulated discharges for each hydrological model these are presented on the bottom side of the left graphs. The top side of the left graphs contains precipitation, snow melt and actual evapotranspiration values. The right graph of each figure presents the discharge volume of the wave on the ride side and the snow melt on the left side. The snow melt is determined with the snow module of the HBV model

C.1 Summer Flood wave of 1980

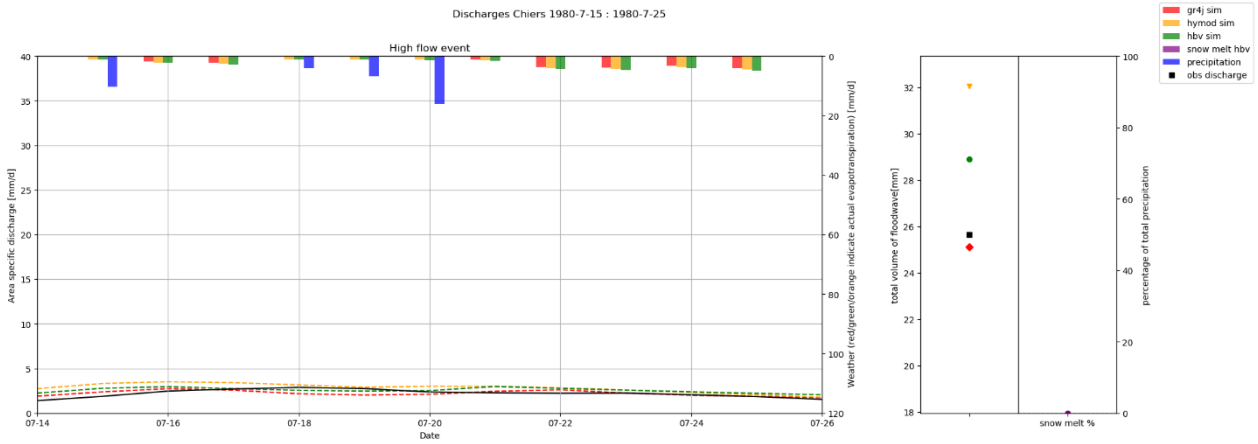

Figure C-1, Discharges Chiers 1980

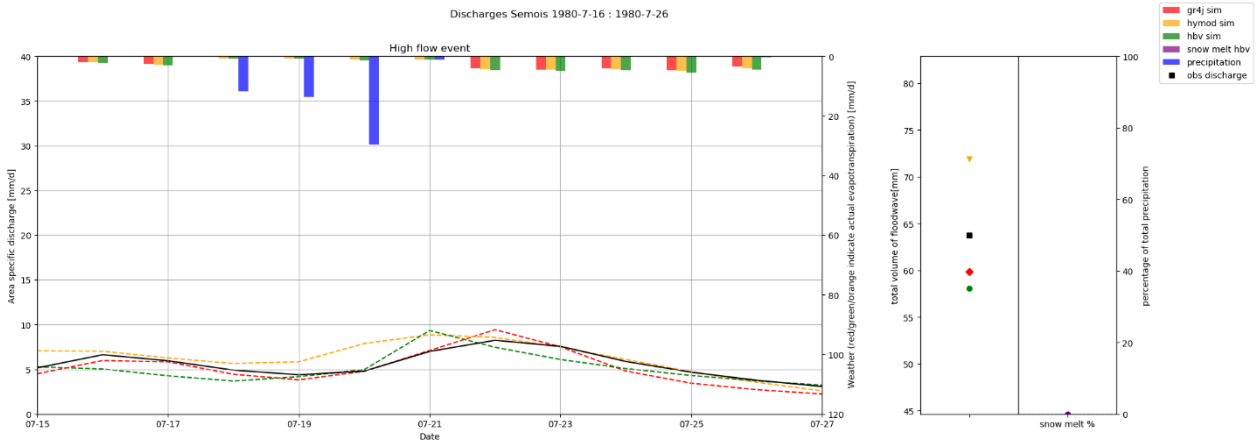

Figure C-2, Discharges Semois 1980

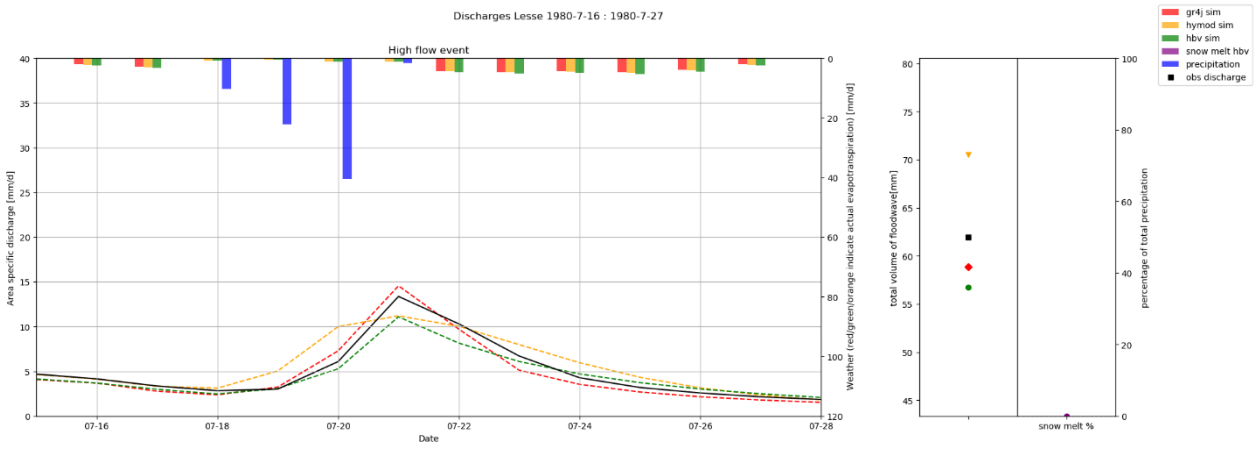

Figure C-3, Discharges Lesse 1980

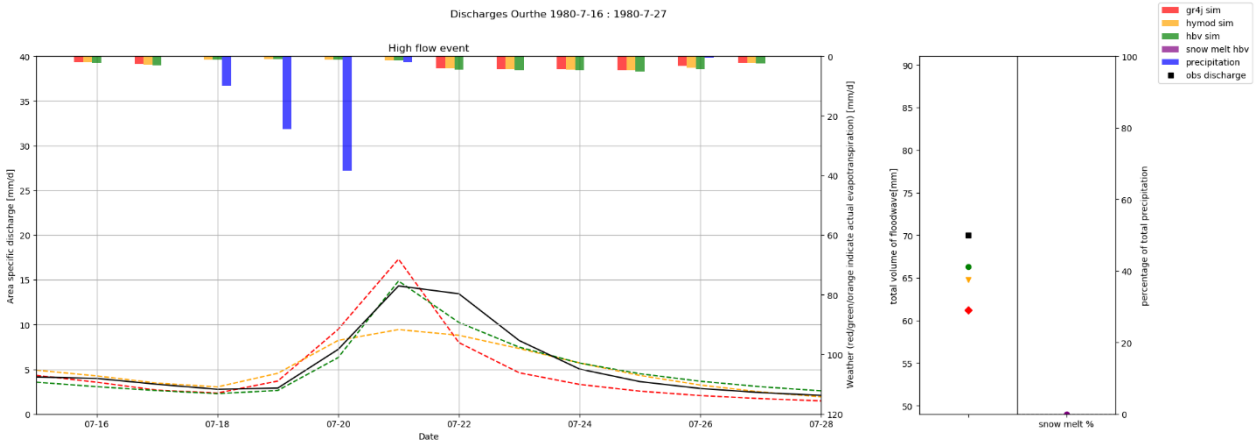

Figure C-4, Discharges Ourthe 1980

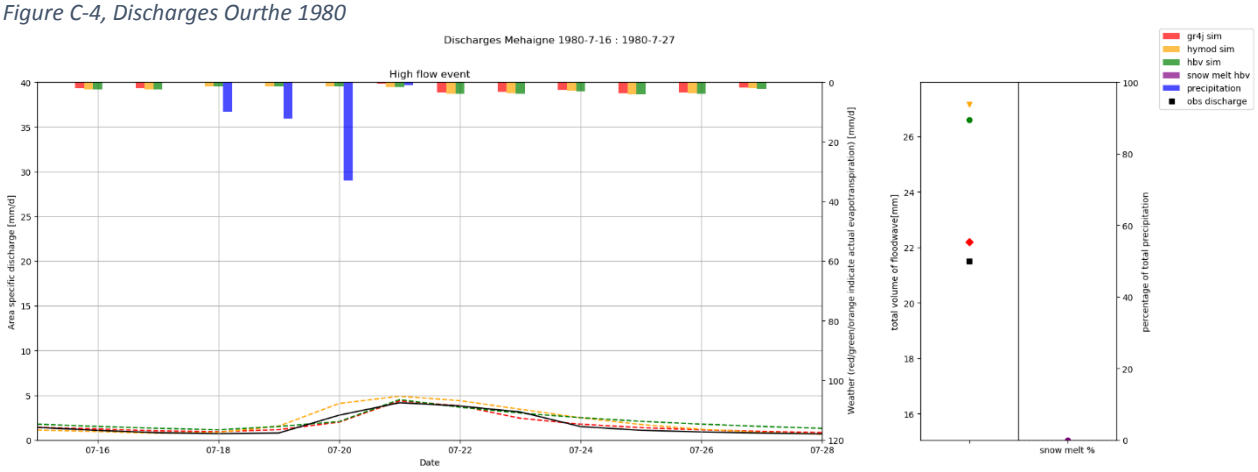

Figure C-5, Discharges Mehaigne 1980

C.2 Floodwave of 1984

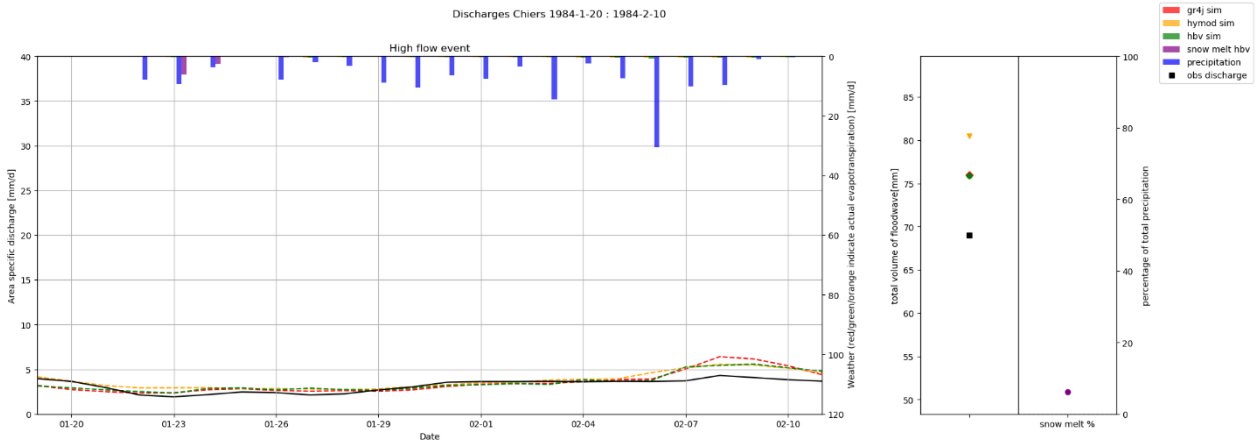

Figure C-6, Discharges Chiers 1984

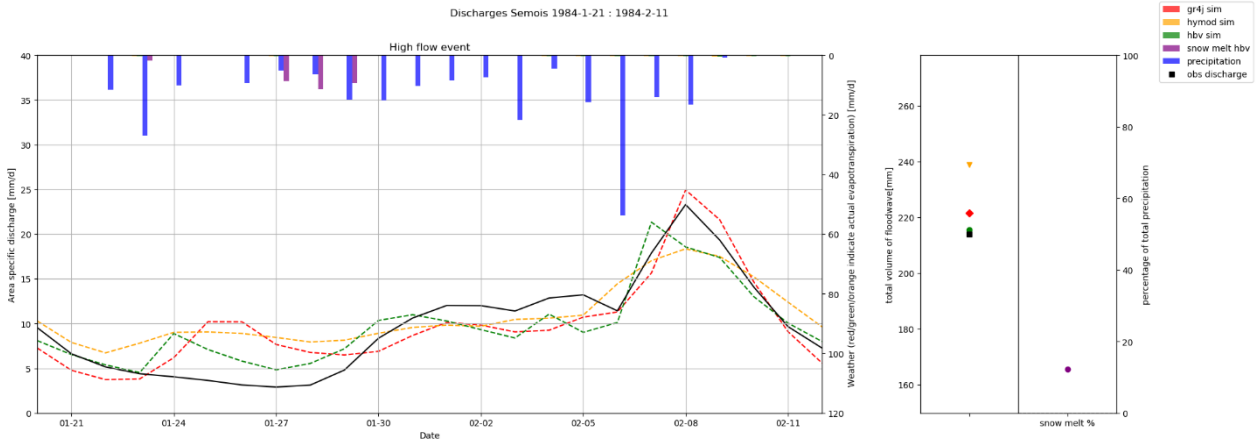

Figure C-7, Discharges Semois 1984

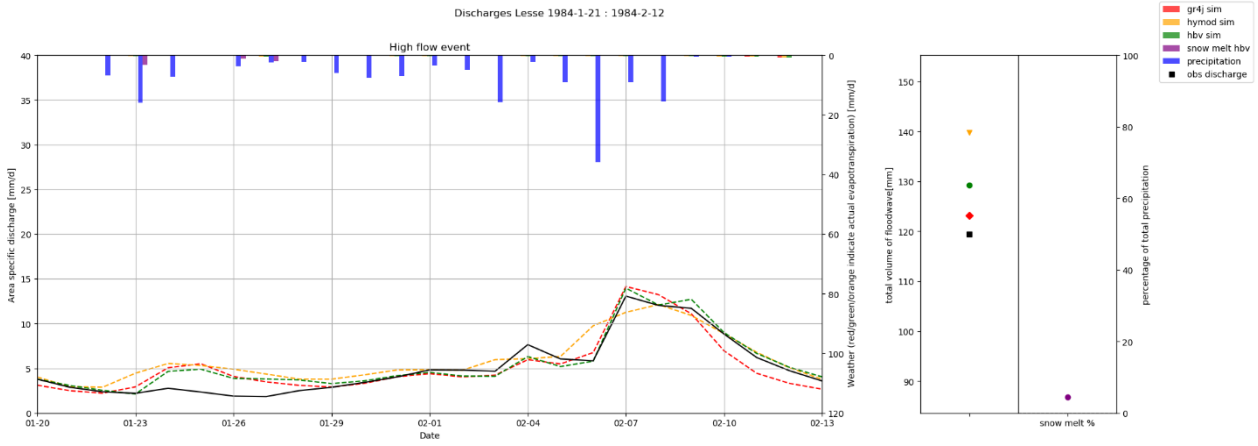

Figure C-8, Discharges Lesse 1984

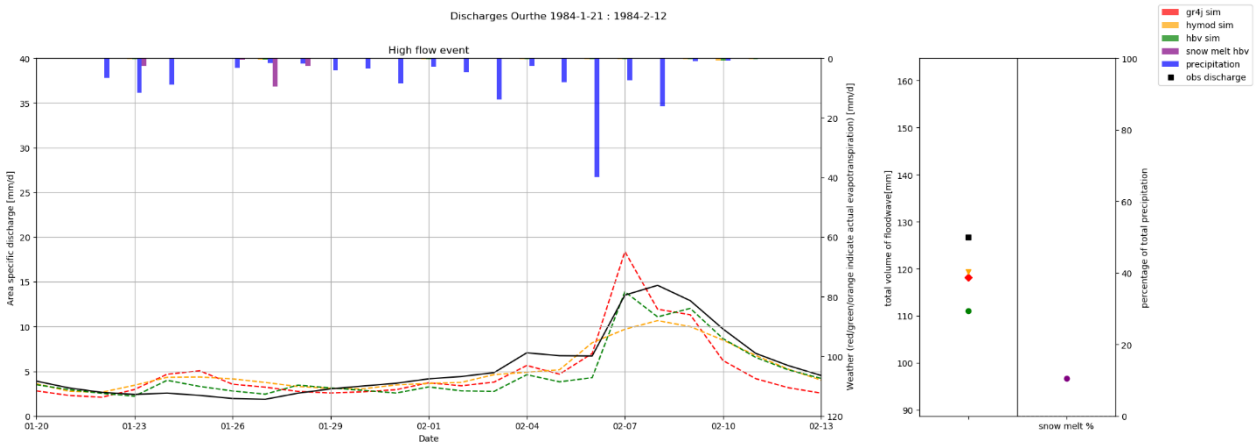

Figure C-9, Discharges Ourthe 1984

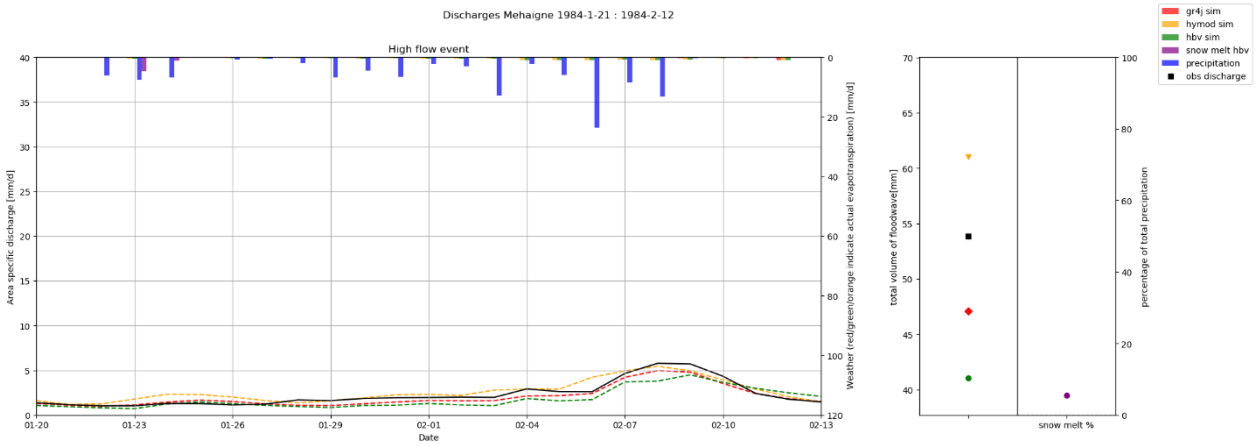

Figure C-10, Discharges Mehaigne 1984

C.3 Floodwave with large snowmelt contribution of 1988

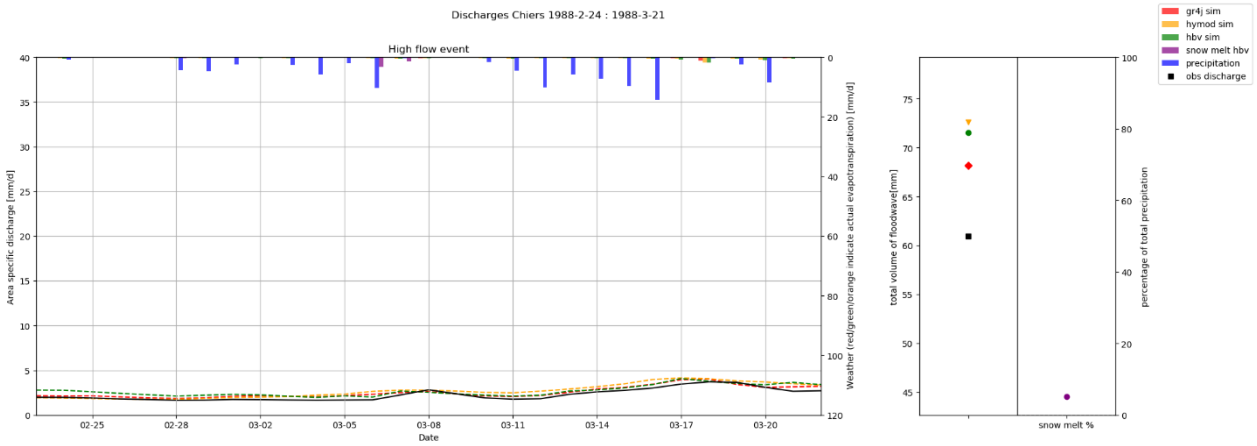

Figure C-11, Discharge Chiers 1988

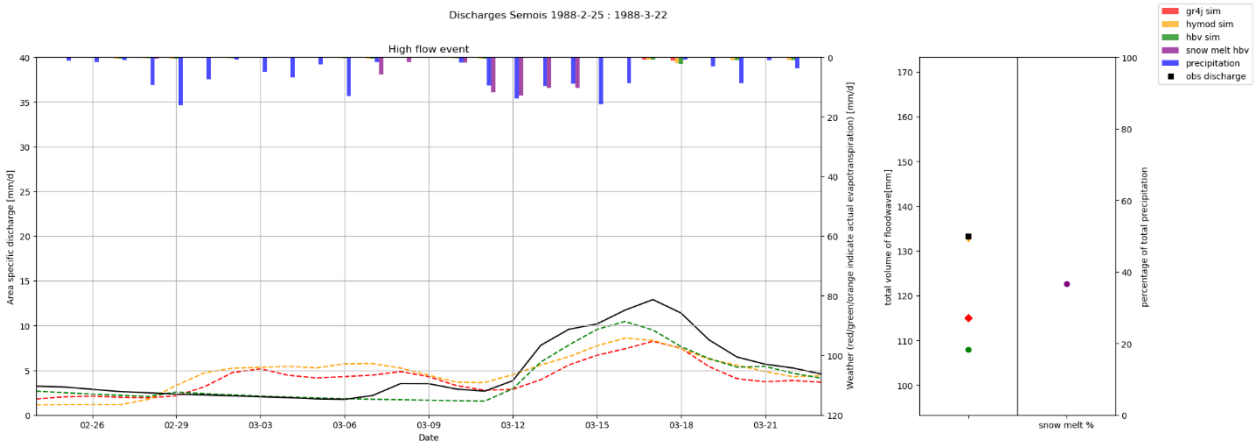

Figure C-12, Discharges Semois 1988

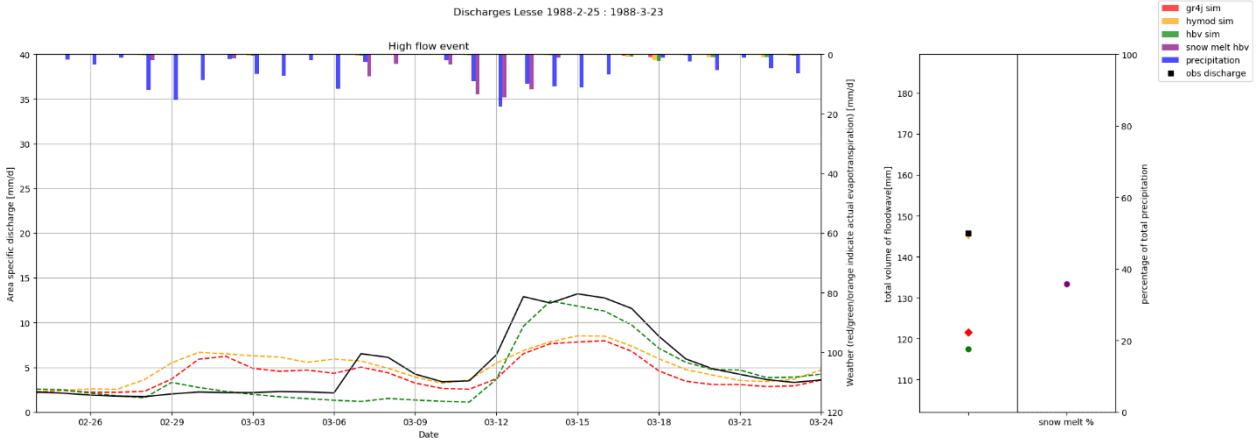

Figure C-13, Discharges Lesse 1988

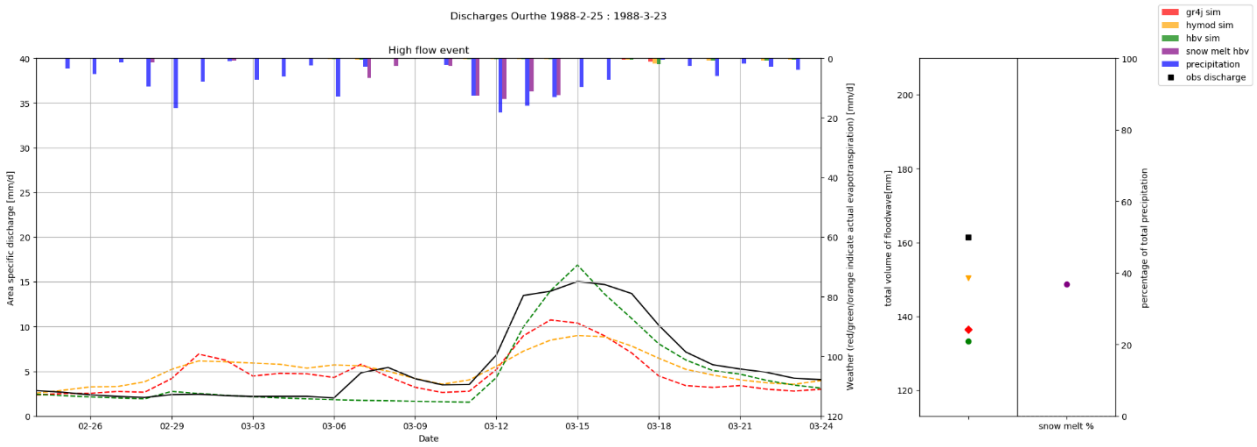

Figure C-14, Discharges Ourthe 1988

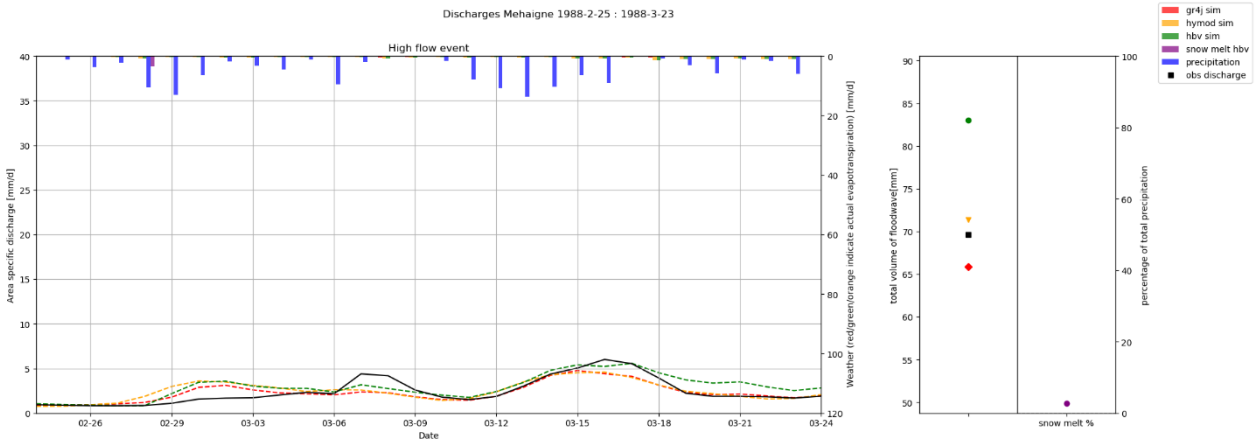

Figure C-15, Discharges Mehaigne 1988

C.4 Floodwave of 1993

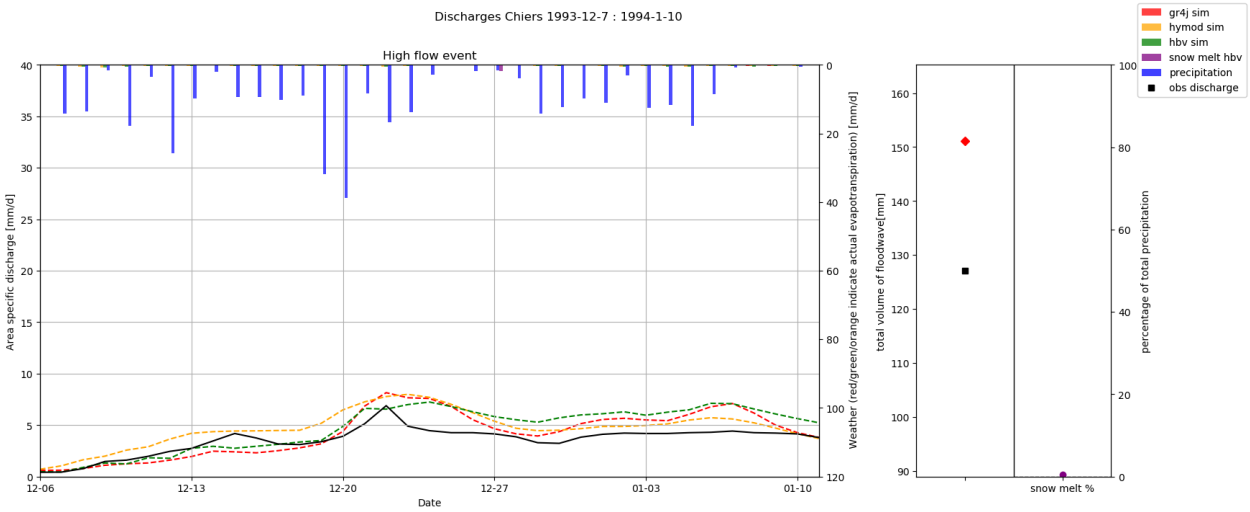

Figure C-16, Discharges Chiers 1993

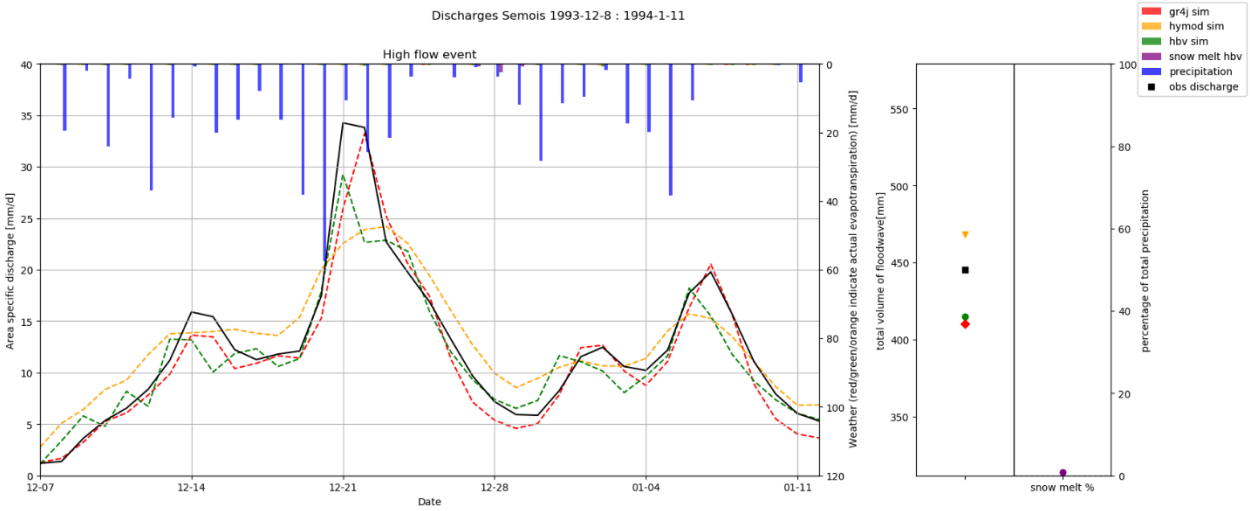

Figure C-17, Discharges Semois 1993

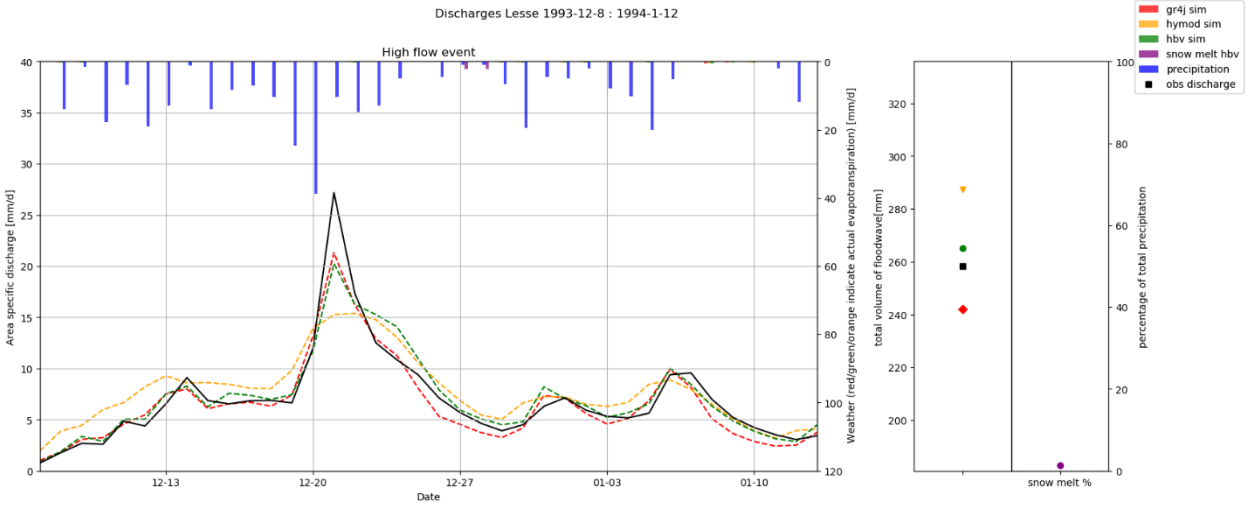

Figure C-18, Discharges Lesse 1993

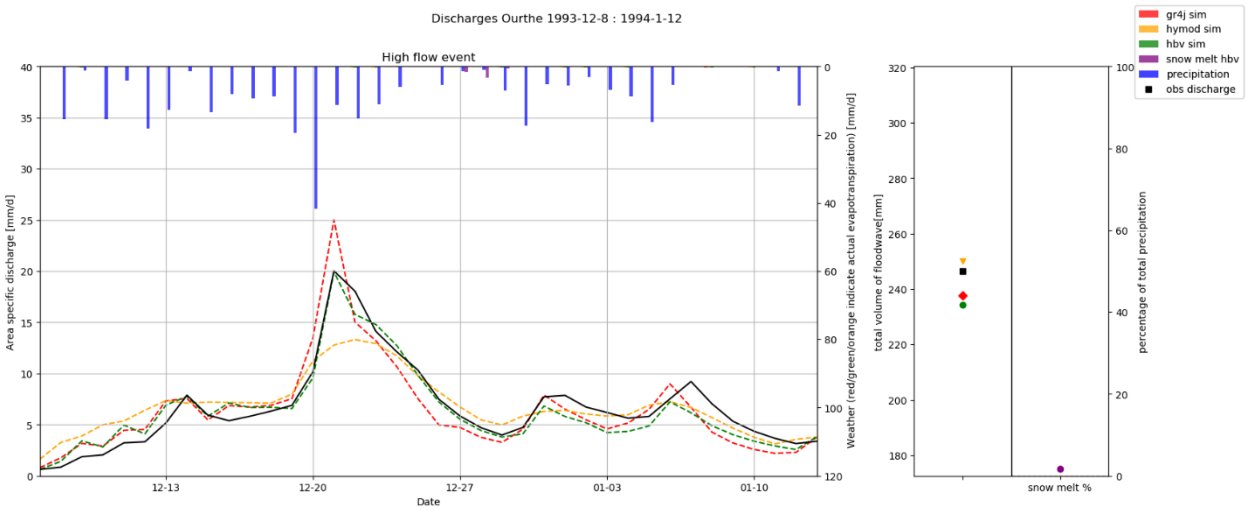

Figure C-19, Discharges Ourthe 1993

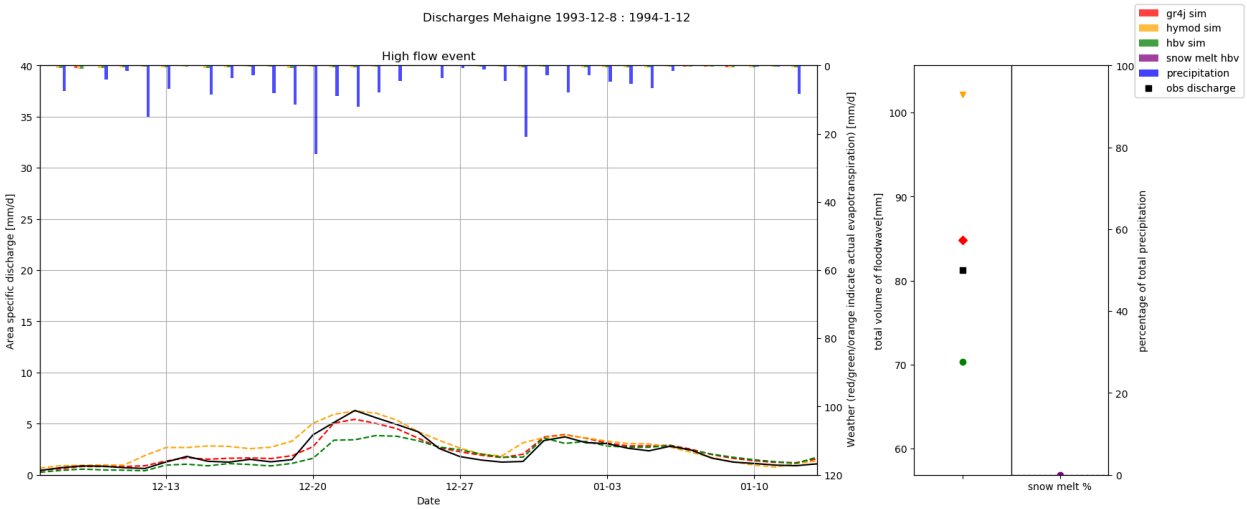

Figure C-20, Discharges Mehaigne 1993

C.5 Floodwave of 1995

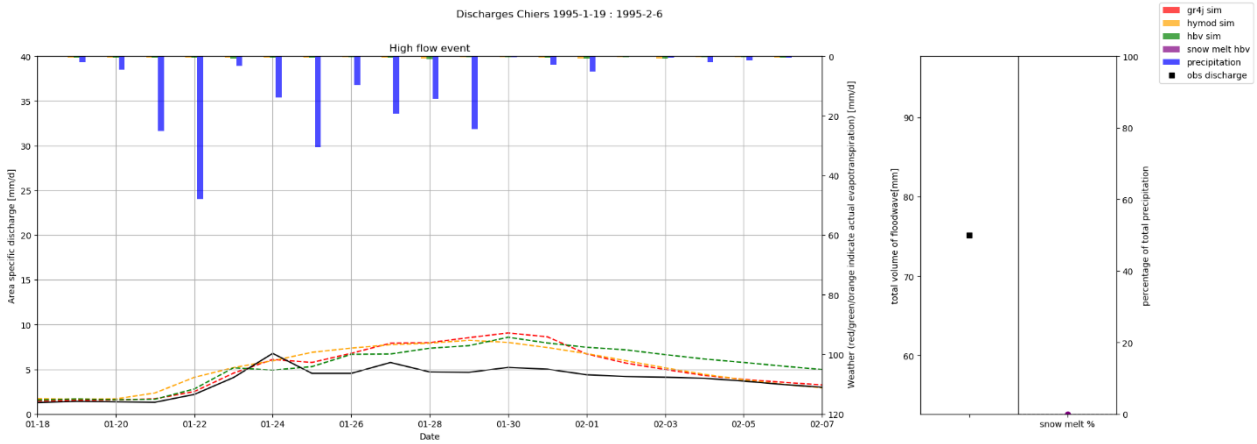

Figure C-21, Discharges Chiers 1995

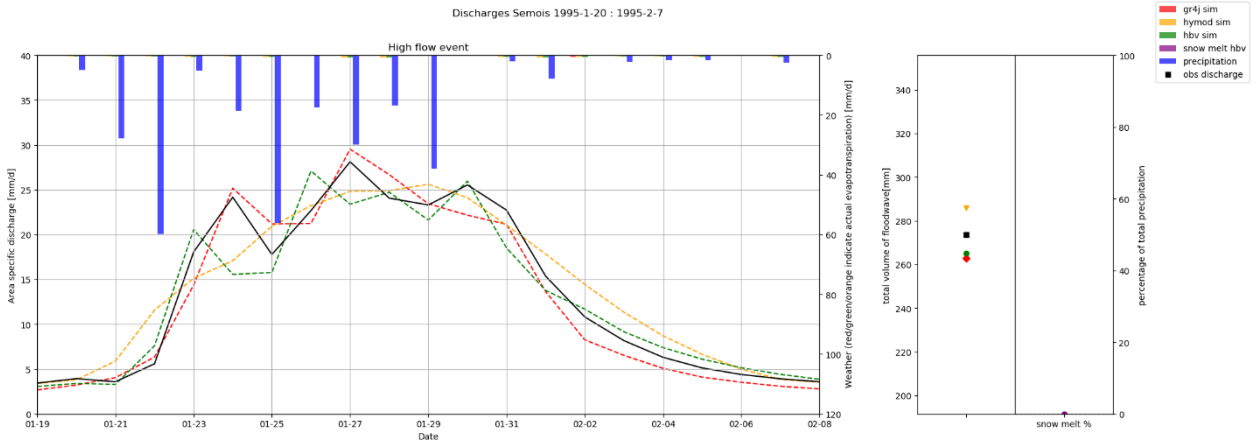

Figure C-22, Discharges Semois 1995

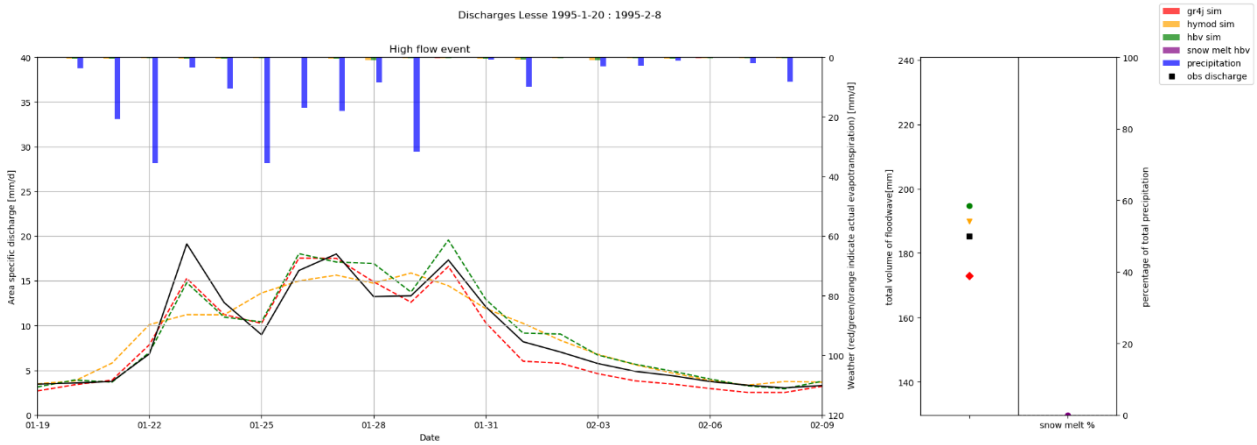

Figure C-23, Discharges Lesse 1995

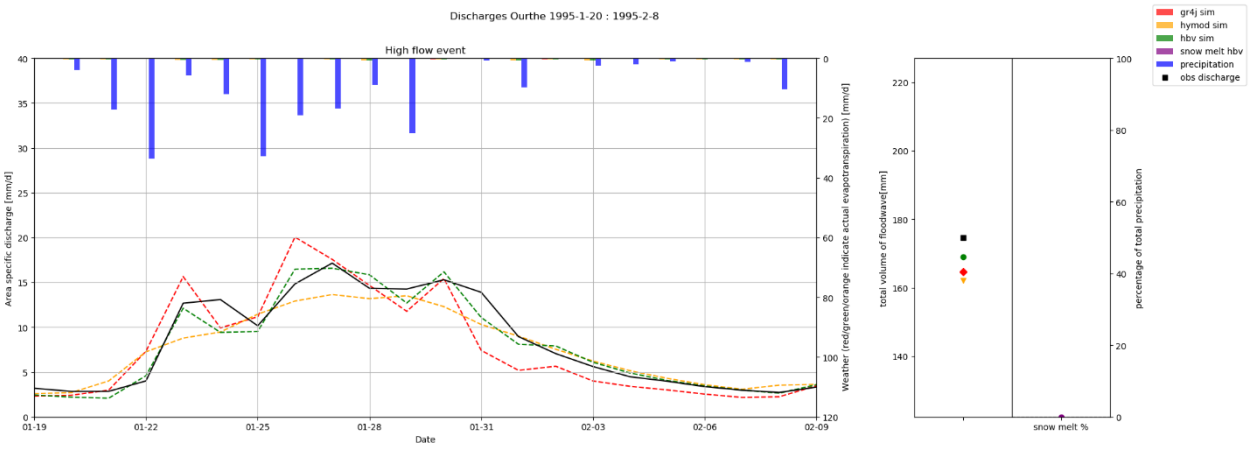

Figure C-24, Discharges Ourthe 1995

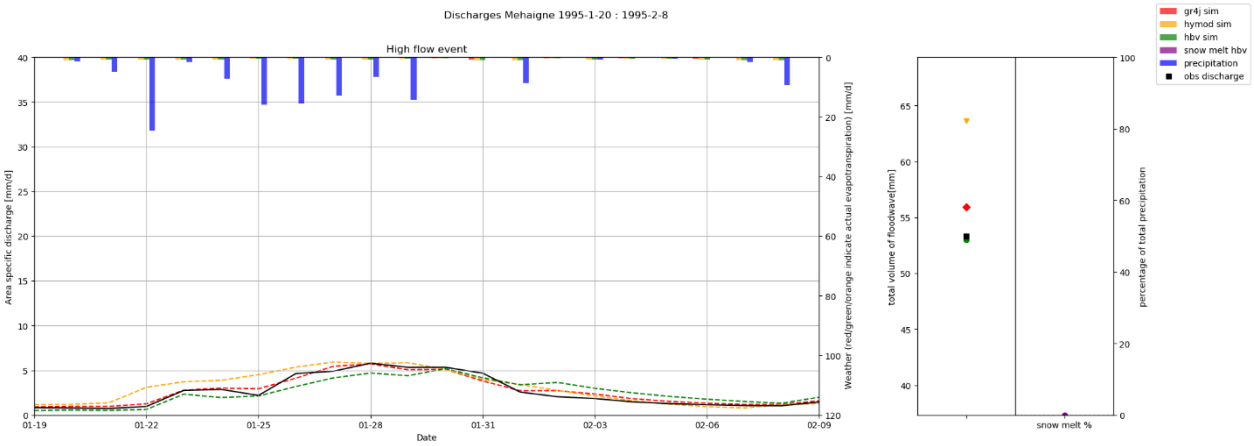

Figure C-25, Discharge Mehaigne 1995

Appendix D. Leaking catchments

This appendix present figures that indicate if sub-basins leak/gain water from other sub-basins. Values above the Blue line indicate that water is received from other sub-basins (figure D-1). Whereas values under the redline indicate that water is lost to other sub-basins via groundwater leakage (figure D-1). The analysis performed for Meuse sub-basins implicate that the Vesdre and the Mehaigne are losing water to other sub-basins. However all values are very close to critical line indicated by the purple dotted line (figure D-2).

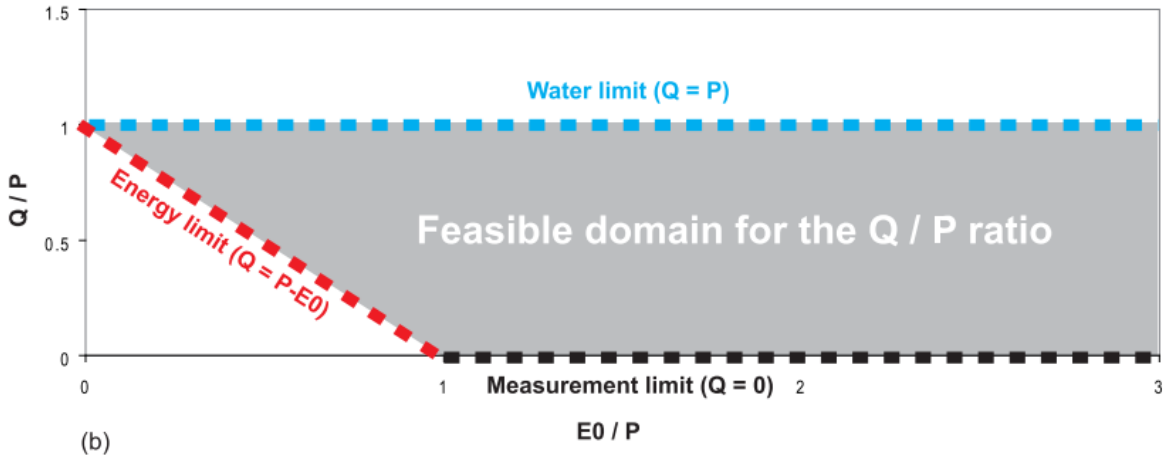

figure D-1, Leaking gaining sub-basin example graph, Q is the discharge, P is the precipitation, E0 is the potential evapotranspiration

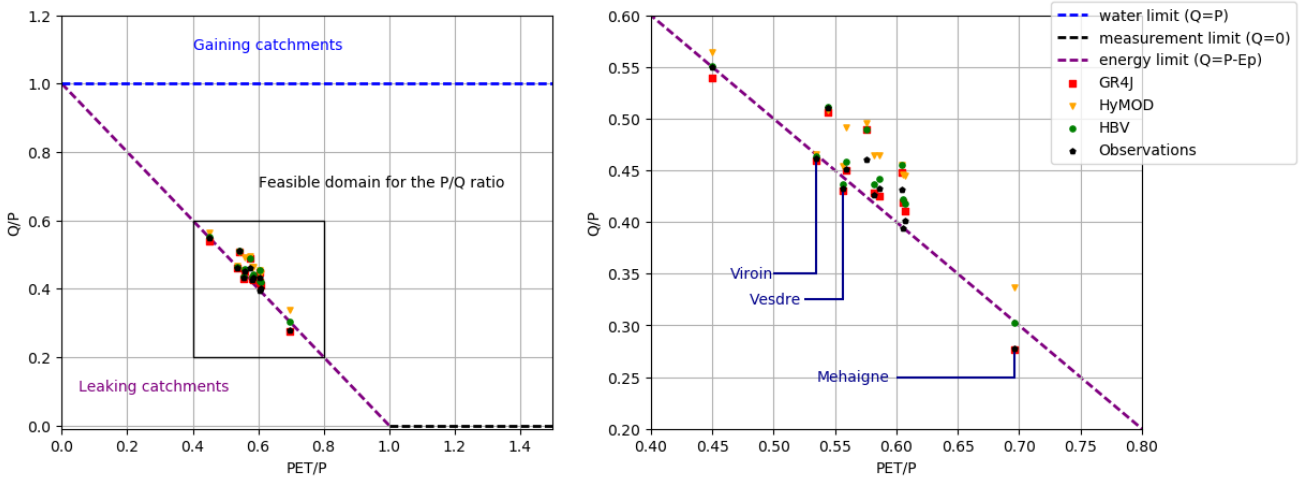

figure D-2, Graph indicating which sub-basins leak water. For these sub-basins, model structures (GR4J) that allow such a leak should be able to simulate the discharge better.

Appendix E. Parameter values

This appendix contains the parameter values that are generated via the calibration process. These parameter sets are the historical and weather generator simulations. Not all parameters have been calibrated for the HBV model. The cells that are yellow indicate that the values are kept constant in that certain sub-basin. Green cells indicate that the parameters are calibrated.

Table E-1, GR4J parameter sets for each sub-basin

Sub-basin	Parameters			
	x1	x2	x3	x4
Lorraine Sud	220	-1.21	67	4
Chiers	693	-1.46	182	2.57
Lorraine Nord	509	1.08	499	1.45
Stenay-Chooz	230	1.29	152	2.43
Semois	231	-1.06	84	3.31
Viroin	169	-1.07	49	2.02
Lesse	248	-1.21	71	2.19
Ourthe	179	-1.31	77	2
Ambleve	235	-0.5	88	2
Vesdre	290	-0.99	43	2
Mehaigne	448	-2.01	48	2.28
Chooz-Namur,Sambre, Namur-Monsin	147	-3.19	34	2

Table E-2, HyMOD parameter sets for each sub-basin

Sub-basin	Parameters				
	CMAX	Bexp	Alpha	Kq2	Ks
Lorraine Sud	1034	0.117	0.988	0.00017	0.34
Chiers	704	0.055	0.389	0.0092	0.39
Lorraine Nord	332	0.051	0.639	0.02451	0.15
Stenay-Chooz	349	0.569	0.675	0.03893	0.32
Semois	1482	0.11	0.962	0.0242	0.43
Viroin	539	0.187	0.85	0.00002	0.54
Lesse	1013	0.138	0.703	0.05482	0.52
Ourthe	703	0.084	0.65	0.02657	0.49
Ambleve	770	0.122	0.569	0.0439	0.56
Vesdre	1953	0.149	0.677	0.02568	0.6
Mehaigne	687	0.087	0.497	0.00042	0.53
Chooz-Namur,Sambre, Namur-Monsin	1428	0.081	0.999	0.114	0.65

Table E-3, HBV parameter sets for each sub-basin

Sub-basin	Parameters							
	FC	BETA	LP	ALFA	Kf	Ks	Cflux	PERC
Lorraine Sud	236	5.93	0.64	0.7419	0.008	0.01	1	2
Chiers	447	2	0.63	0.0033	0.077	0.01	1	1.05
Lorraine Nord	261	1.46	0.83	0.0011	0.02	0.01	1	1.08
Stenay-Chooz	100	3	1	0.0395	0.1	0.01	1	0.82
Semois	291	5.99	0.8	0.3779	0.039	0.01	1	3
Viroin	227	3	0.5	0.6658	0.027	0.01	1	0.88
Lesse	272	2	0.54	0.5118	0.026	0.01	1	0.57
Ourthe	188	5.99	0.61	0.4551	0.038	0.01	1	3
Ambleve	394	4.13	0.97	0.736	0.009	0.01	1	1
Vesdre	507	1.74	0.64	1.613	0.005	0.01	1	1
Mehaigne	546	3.53	0.5	0.1817	0.1	0.01	1	1.22
Chooz-Namur,Sambre, Namur-Monsin	799	5.99	0.6	0.643	0.05	0.01	1	0.34